TOHOKU
UNIVERSITY

# 博 士 学 位 論 文

論文題目　Multimodal Quantitative Gait Assessment Using Minimal Wearable Sensors (最小限のウェアラブルセンサーを用いたマルチモーダルな定量的歩行評価)

提 出 者　東北大学大学院医工学研究科
医工学専攻

氏　　名　**Yonatan Christian Hutabarat**

# Doctoral Thesis

Thesis Title

Multimodal Quantitative Gait Assessment

Using Minimal Wearable Sensors

Graduate School of Biomedical Engineering

TOHOKU UNIVERSITY

YONATAN HUTABARAT

| | |
|---|---|
| Advising Professor at Tohoku Univ. | Professor Mitsuhiro Hayashibe |
| Research Advisor at Tohoku Univ. | – |
| Dissertation Committee Members<br>Name marked with "○" is the Chief Examiner | ○ Prof. Mitsuhiro Hayashibe<br>1 Prof. Ryoichi Nagatomi 2 Prof. Takashi Watanabe<br>3 Prof. Dai Owaki<br>(*Graduate School of Engineering*) |

TOHOKU UNIVERSITY

Graduate School of Biomedical Engineering

# Multimodal Quantitative Gait Assessment Using Minimal Wearable Sensors

(最小限のウェアラブルセンサーを用いたマルチモーダルな定量的歩行評価)

A dissertation submitted for the degree of

Doctor of Philosophy (Biomedical Engineering)

by

Yonatan Hutabarat

January 7, 2022

# Multimodal Quantitative Gait Assessment Using Minimal Wearable Sensors

(最小限のウェアラブルセンサーを用いたマルチモーダルな定量的歩行評価)

**Yonatan Hutabarat**

## Abstract

Gait assessment is the study of a person's walking pattern. Walking is a primary function required to perform daily life activities. Although it may appear simple, walking requires precise coordination between several motor, sensory, and cognitive processes. Any alterations in motor, sensory, or cognitive functions induced by disease, trauma, or idiopathic nature may affect the gait pattern of a person. This highlights the importance of performing gait analysis to detect the presence of underlying conditions at an early stage. The current gold standard of gait analysis is performed in a laboratory environment based on gold standard measurements obtained using motion capture and force plate systems. However, the privilege of using specialized instruments is limited to a handful of clinics or research centers. Further, research facilities with space constraints may not be able to capture the natural gait of a person effectively. Recently, flexible, efficient, and inexpensive wearable sensors have been popularized as effective alternatives that can be used to perform gait analysis during daily activities. In this context, this thesis addresses the specific domain of multimodal quantitative gait analysis using wearable sensors.

Chapter 2 of this thesis details the identification and summarizing of the current advances in wearable sensors for gait analysis from various perspectives, such as the application of wearable sensor-based gait analysis, sensor systems and their attachment locations, and the algorithms used. The PRISMA guideline was adopted to find relevant studies from several scientific databases published between 2011 and 2020. In aggregate, 76 articles were selected based on the inclusion and exclusion criteria. The wearable inertial measurement unit (IMU) attached to the lower-limb region was found to be the most commonly utilized sensor–location pair. Temporal, spatial, and spatiotemporal features are the most common quantitative gait features extracted from wearable sensors. Varying performances were observed for each pro-

posed framework, where an increased number of sensors did not necessarily improve the estimation performance metrics. A few studies have integrated various machine learning techniques for classification problems, correction algorithms, cross-checking functions, and scoring functions.

Chapter 3 of the thesis describes the proposed framework for quantitative gait assessment using only two IMU sensors while extracting the maximum number of features. Decreasing the number of sensors negatively affects the gait assessment performance. Based on comparisons with a motion capture setup and previous studies, we verified the potential of the proposed framework to provide a compact sensing system with feature-rich diversity for gait assessment and identified its limitations. The results revealed that the temporal differences were 4.22 $\pm$ 15.48 ms (mean $\pm$ S.D.) and -8.31 $\pm$ 21.02 ms (mean $\pm$ S.D.) in the initial contact and toe-off events, respectively. Additionally, with respect to the spatial features, the stride length and heel vertical displacement were overestimated by 7.72 cm and 2.22 cm, respectively, on average. We successfully extracted 17 gait features from two IMUs located on the foot. We also demonstrated that the symmetry index feature can be used to distinguish healthy subjects from subjects with a recent history of lower-limb injury, which is a significant observation for clinical research.

Chapter 4 of the thesis further demonstrates the potential of the proposed framework, we present the following three case studies. The first case study demonstrates an application of the proposed framework to analyze a different type of gait. Detailed gait phases during walking and running were successfully extracted by employing finite state machine (FSM) transition rules. The second case study demonstrates the use of the proposed framework to distinguish cognitive dual-task gait from single-task gait. While visual observation may not objectively identify the differences between single-task and dual-task gait, the proposed framework facilitated the extraction of temporal gait patterns that were later derived into gait indices. Lower motion intensity, a slight increase in double support time, higher gait temporal variability, and worse gait symmetry were observed in the subjects performing dual-task gait in this study. The third case study demonstrates the utilization of the proposed framework in prolonged and outdoor gait experiments. The extraction of various gait index features enabled the objective comparison of the stages of walking as well as the derivation of inter-subject comparisons. In conclusion, all of the presented case studies revealed promising results and established the viability of using the proposed system in the respective applications.

Chapter 5 of this thesis details the integration of several machine learning algorithms to solve various gait-related problems, including gait phase classification, gait

activity prediction, and control of the swing phase for prosthetic knees. Three machine learning models, consisting of support vector machines (SVM), AdaBoost, and XGBoost, were trained for gait phase classification. The results indicate that the mean accuracy of XGBoost (84.54%) was higher than those of AdaBoost (82.26%) and SVM (78.31%) models, and the former also exhibited a notably faster processing time compared with SVM. On the other hand, temporal convolutional networks (TCN), recurrent neural networks, and long short-term memory networks were trained for gait activity prediction. The results demonstrate that TCN's predictions were the best corresponding to 50, 100, and 150-time steps, with an overall best performance of 4.94% mean absolute percentage error (MAPE) on the 100-time step prediction. To control the swing phase, we adopted a model-free reinforcement Q-learning control with a designed reward function as the controller of a semi-active prosthetic knee. The results indicate that the proposed control strategy converges within the desired performance index and is capable of adapting to several walking speeds. Further, the proposed control structure exhibited better overall performance compared to user-adaptive control, while at some walking speeds it outperformed the neural network-based predictive control method.

# Contents

# List of Figures

# List of Tables

# Chapter 1

# General Introduction

## 1.1 Background

Gait is often translated into how the person is walking. Quantitative gait analysis is an in-depth analysis of how a person walks as seen by various quantifiable parameters. A broad range of gait analysis applications is found from sport application to clinical application. In sports applications, gait analysis is often utilized to assess the performance of athletes, prevent injuries, and provide a training guide [1], [2]. Meanwhile, in clinical application gait analysis is performed to characterize certain gait pathology, track rehabilitation progresses, evaluate certain treatment effectiveness [3]–[5]. Other than those applications, gait analysis could also be used to predict the risk of falling in the elderly subject group [6], [7]. Therefore, by studying the way a person walks or runs, we can determine normal gait patterns, diagnose issues that cause pain, identify a person's unique movements, while also implementing and evaluating certain given treatments to correct abnormalities.

There are several approaches that can be used to perform gait analysis. In most clinical settings, a combination between observation and qualitative assessment is usually performed by means of clinicians observation and patient self-reported assessment [8], [9]. Observation performed by clinicians such as doctors or physical therapist may give some quantitative gait features such as distance covered, total time spent walking, gait speed, and cadence. Nevertheless, these are subjected to inter-observer variability and human error. Gait parameters or gait features such as walking speed has been considered as the sixth vital sign [10]. It can be used as a functional vital sign combined with other measures to determine health outcome from the subjects.

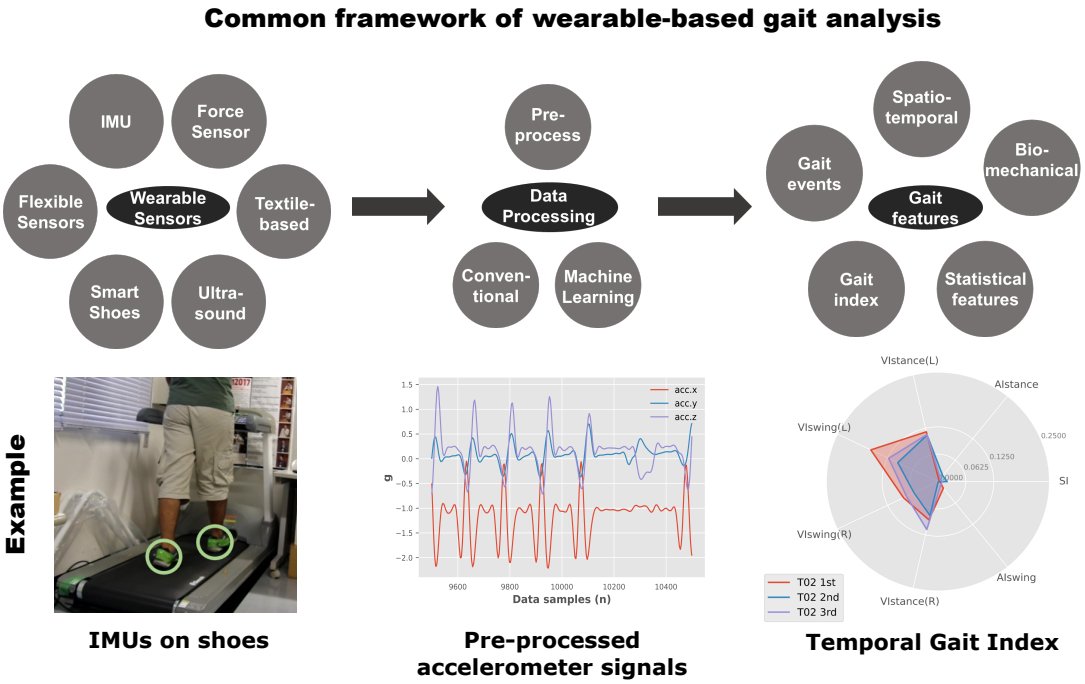


Figure 1.1: The concept of wearable-based quantitative gait analysis. Various kind of small and light weight wearable sensors such as IMU, force-sensitive sensors, flexible sensors, and others have been used to extract gait features by means of both conventional and machine-learning based algorithms. For example, data from IMU attached on the shoes is processed to give temporal gait index.

Presently, it is very common to perform quantitative gait analysis in a laboratory environment using a gold standard measurement such as the combination of motion capture and force plate systems. Motion capture enables a precise tracking of spatial information of human motion in 3D, while force plates gives the dynamic features such as ground reaction forces and moments. However, using those specialized instruments are limited to only a few clinics or research facilities with limited capture volume, thus may not necessarily capture the natural gait of the subject[11]. Another concern is the long time spent preparing for the experiment such as marker placements and anthropometric measurement that may not be convenient for participants such as patients.

On the other hand, a vast and recent development in both sensor systems and computational methods have made it possible to assess gait outside of laboratory by means of wearable sensor system. Other than gait analysis, wearable sensors have also been investigated to predict several clinical conditions [12], [13].The number of sensors used may be dependant on the subject of interest. For examples, in a highly impaired gait, sensors attached in both legs are preferred [14]. Wearable inertial sensors-based gait analysis has also become a supplementary assessment of the physical function of patients undergoing a total hip arthroplasty [15], and on

clinical analysis of idiopathic normal pressure hydrocephalus [16]. There have been several studies discussing the long-term assessment of gait by using wearable sensors [17]. On clinical application, it has been reported that there was a good correlation between accelerometer-based motor fluctuation measurement to the gait item in UPDRS-III (Unified Parkinson's Disease Rating Scale - Part III) [18], which suggest that accelerometer may be a useful tool to monitor PD patients. Wearable inertial sensors have also been used in a biofeedback system for gait and balance training in PD subjects [19], [20]. Gait quality metrics were found to be robust in assessing the gait of two matched groups of MS patients in two separate locations with different experiment protocols [21]. On assessing gait ataxia in people with spinocerebellar degeneration (SCD), accelerometer-based assessment is more responsive compared to the standard clinical scale for the assessment and rating of ataxia (SARA) [22].

A few existing applications of gait analysis using wearable sensors described in the previous paragraph were only a tip of the iceberg on the full scale of gait analysis application. For rehabilitation purposes alone, the use of gait analysis may aid the physical rehabilitation of stroke survivors, since 90 % of the cases show that stroke survivor suffers from motor impairment that is reflected by their gait pattern [23]. The broad applications of wearable-based gait analysis have made a positive trend in terms of the number of existing research and the quality of the study in this field. Therefore, this thesis firstly aimed to summarize the current state of the arts on gait analysis using wearable sensors as well as to find the current challenges. Further, this thesis aimed to construct a framework for performing quantitative gait analysis using a minimum number of wearable sensors and demonstrate it to various applications. Finally, this thesis is going to investigate the use of machine learning models and algorithms for wearable-based gait analysis.

## 1.2 Research Objectives

The objectives of this research are divided into general objectives and specific objectives, which are explained as the following.

### 1.2.1 General Objective

- To review and summarize the state of the art of quantitative gait analysis using wearable sensors,
- To construct a framework on extracting feature-rich diversity on quantitative gait analysis using minimum wearable sensors,

- To integrate machine-learning algorithms to the proposed framework for an extended quantitative gait analysis.

### 1.2.2 Specific Objectives

- Filter the relevant papers related to wearable sensors for gait analysis by following PRISMA guideline for reporting systematic review based on the formulated keywords.
- Summarize the eligible studies and discuss the current challenges on this research area.
- Develop experiment protocols for benchmark experiments on using wearable sensors for quantitative gait assessment.
- Develop a proper informed consent for subjects as well as the accompanied questionnaire about subject perception for later analysis.
- Propose a quantitative gait assessment framework using wearable sensors to extract feature-rich gait assessment.
- Perform benchmark experiments with able-bodied subjects in a laboratory environment.
- Compare the performance of the proposed framework to the gold-standard measurement of motion capture and force plates.
- Compare the performance of the proposed framework to various existing studies.
- Demonstrate that the proposed framework can also be used for running gait analysis.
- Demonstrate that the gait indices can distinguished single-task and cognitive dual-task gait.
- Demonstrate that the proposed framework is robust for a prolonged use in outdoor environment.
- Design and compare several machine-learning algorithms for gait phase classification.
- Design and compare several advanced machine-learning algorithms for gait activity prediction.

- Propose a reinforcement learning-based control for swing phase control of a prosthetic knee.

- Define conclusions, main contributions, as well as future works according to the results.

## 1.3 Outline

This thesis is divided into six chapters and described as follows.

**Chapter 1: Introduction**

This chapter presents the general introduction to this study. The background as to why this study was conducted is briefly explained in this chapter, followed by research objectives and outline of this thesis. The subsequent chapters can be summarized as follows.

**Chapter 2: Overview on wearable-based gait analysis**

This chapter presents an overview of the current state of the arts on quantitative gait analysis using wearable sensors. Types of wearable sensors, location attachment on the body, and algorithm used as well as the performance are extensively discussed in this chapter.

**Chapter 3: Proposed framework: Two IMUs approach for rich gait features**

This chapter addresses the proposed framework for feature-rich quantitative gait assessment. Two IMU sensors attached on foot as sensors and its location was benchmarked to gold standard measurement and various existing study. This chapter can be considered the basis contribution of this thesis.

**Chapter 4: Case studies using the proposed framework**

This chapter further demonstrates the potential application of the main proposed idea of this thesis. Three case studies are presented which incorporate mixed walking and running gait analysis, cognitive dual-task gait, and a prolonged outdoor gait experiment.

**Chapter 5: Machine learning for gait analysis**

This chapter further extends the developed framework to include machine learn-

ing (ML)-based algorithms for gait phase classification and gait activity prediction. Additionally, an advanced use of machine learning for control algorithm of a specific gait phase in prosthetic knee is presented in this chapter.

**Chapter 6: Concluding remarks**

This chapter summarizes the overall presented study, provides clear contributions, and gives research direction for future works related to the area of this study.

# Chapter 2

# Overview of wearable-based gait analysis

## 2.1 Introduction

This chapter discusses the recent state of the art of quantitative gait analysis using wearable sensors. A vast and recent development in both sensor systems and computational methods have made it possible to assess gait outside of laboratory by means of wearable sensor system. Nevertheless, the performance accuracy and the types of analysis are dependent on many factors such as types of sensors, number of sensors and its location attachment to the body, and methods and algorithms used. Therefore, this chapter aimed to address the recent advances on wearable-based gait analysis based on the above mentioned factors. The overall scientific contributions of this chapter are to:

- present an overview of the recent state of the arts of quantitative gait analysis using wearable sensors that have been validated to gold standard measurement or other measurement systems.
- provide key insights of the existing wearable-based gait analysis as seen from the number and types of sensors and gait features, location attachment of sensors to the body, as well as method and algorithms used on each literature.
- highlight the current applications of wearable-based gait analysis for both general purposes such as in sports, and clinical purposes on various pathological conditions.
- discuss the issues, challenges, and future research direction for researchers and

clinicians working in this field.

## 2.2 Methods

The method used for finding relevant references for making this state of the arts was following the Preferred Reporting Items for Systematic Reviews and Meta-Analyses (PRISMA) guideline [24], which is commonly used for reporting systematic reviews. The search was done in several databases including PubMed, IEEE Xplore, Scopus, and ISI Web of Science with a time constraint starting from 2011 until 2020, thus consisted of a ten year reported studies. The time constraint was added to account only the recent advances on this topic. Search keywords and combination were formulated as depicted in Fig. 2.1. We limit the search only on the title of the articles with a time constraint from 2011 to 2020. Gait is the must have term on the document title, followed by any combination of keywords as depicted in Fig. 2.1.

Database searching was done on February 8, 2021. A total of 1550 records from all of the databases were found as included for further selection process. These results were then imported to Mendeley® Desktop reference management software (version 1.19.4, Elsevier). Duplicate records were automatically removed by the software if an exact match was detected. A total of 860 duplicates were found, thus resulting in 690 records left to be screened.

The screening stage is the exclusion of certain study based on title and abstract which main field of study is depicted on Fig. 2.1. Assistive walking technologies were not included on this study as most of it were putting sensors on the walking device itself such as on the cane or the walker. Non wearable sensors such as camera-based analysis including Kinect or any combination to those system were excluded. Smartphone was excluded as it is not a fully dedicated system and mostly used for activity recognition or human authentication as opposed to a detailed gait analysis as this review aims. Other non related study such as sensors development, sensor to body alignment, gait underwater, and person/ gender recognition were also found on the screening stage and excluded. At the end of screening stage, a total of 344 records were excluded based on the set criterion and thus leaving 356 articles for the next stage.

On eligibility stage, full-text articles were accessed for finding relevant study to make this state of the arts. Inclusion criterion for full-text screening is also depicted in Fig. 2.1. We highly regard studies that show some sort of benchmark or validation

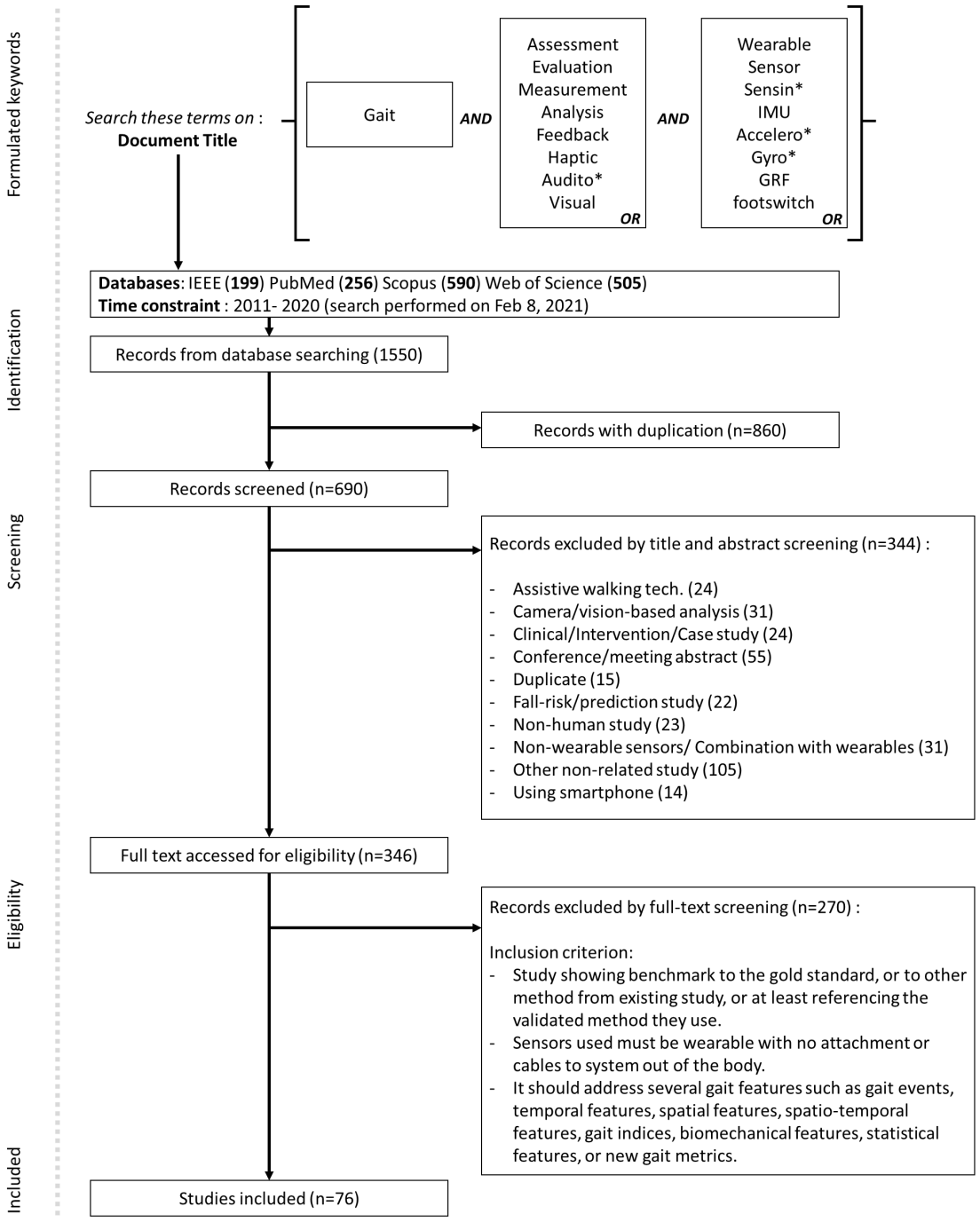


Figure 2.1: Formulated search keywords on several scientific databases with time constraint, followed by the PRISMA flowchart for inclusion process and exclusion criterion of the articles selected in this study. Asterisk (*) indicates wildcard for the search term.

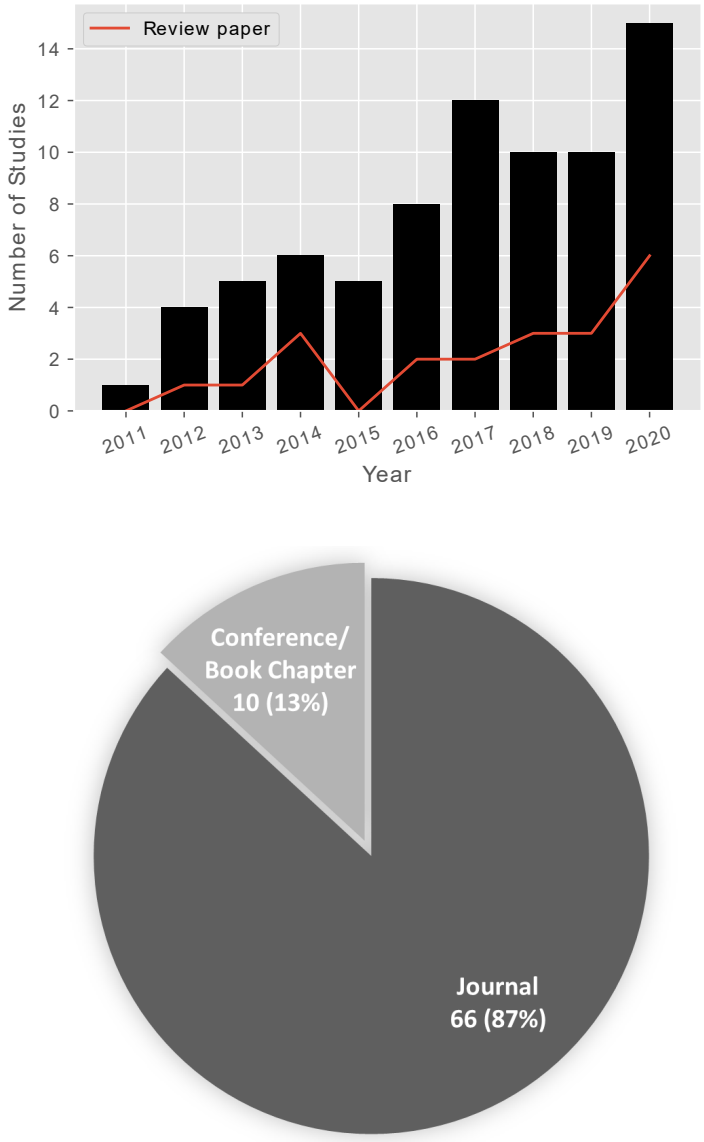


Figure 2.2: Distribution of the eligible articles based on year (bar chart) and publication types (pie chart).

of their proposed framework/ system to a gold standard system or other existing studies and only include studies that have those discussion. Moreover, each of the studies should address various gait features as depicted in Fig. 2.1. On the other hand, we still found some studies that use sensors with cables tethered to data processing unit such as computer. Another criteria is that the studies must address more than one gait feature in their study. At the very end of this stage, a total of 76 articles were eligible for making systematic review. The overall flowchart of article selection is depicted in Fig. 2.1, while distribution of eligible articles is depicted in Fig. 2.2.

### 2.2.1 Existing review

While doing these process, a total of 21 review papers were also identified regarding this topic. Among them, there are six review papers published in 2020, which are described briefly as the following. Kobsar et al. on [25] addressed a specific application of wearable inertial sensors for adults with osteoarthritis. Gondim et al. [26] discussed the use of portable accelerometer to evaluate gait of people with Parkinson's disease. Junior et al. [27] was focused on reviewing gait assessment in children. However, all of the above papers discussed a very specific subject and conditions. Díaz et al. [28] discussed a wider scope of gait that includes balance and range of motion analysis using wearable sensors. Dasgupta et al. [29] was focused on acceleration gait measure for motor skill assessment. Hence, it was specific on to motor skill instead of gait. Saboor et al. [30] discussed about the latest trend on gait analysis using wearable sensors combined with machine learning based methods. However, the study selected was constrained from 2015 onwards with limitation only to machine learning methods. Other notable review papers are from Weijun et al. [31] in 2012 that discussed basic human gait analysis and sensors system, Lopez-Nava et al. [32] in 2017 that focused on wearable inertial sensors for motion analysis, and Caldas et al. [33] that specifically discussed about inertial sensors and adaptive algorithms for gait analysis.

The differences of this review to the above works are this review aim to provide a comprehensive review of quantitative gait analysis using wearable sensors with no constraint on specific subject groups nor the method of analysis. Thus, it covers a wider range of gait analysis that includes various application such in general walking gait, running gait, and different kinds of pathological gait. In addition to that, this review is intended to summarize the last decade advancement of this topic, identify challenges in recent studies, and give future directions on research on this topic.

Table 2.1: State of the arts of quantitative gait assessment (QGA) using wearable sensors.

| Ref. | Subjects (n) | Sensors (Location) | Experiments/ Benchmark | Algorithms/ Data Processing | Gait features [Performances metrics] |
|---|---|---|---|---|---|
| [34] | Healthy (3) | 7 IMUs (lumbar, thighs, shanks, feet) | Overground indoor walk, variable-speed treadmill/ Motion capture | Non-ML/ Online (joint angles), Offline (stride length) | Stride length, joint angles (hip, knee, ankle) [RMSE $< 4$ deg] |
| [35] | Healthy (5) | 1 IMU (left heel) | 20 m corridor walk with various speed/ Camera | Non-ML (threshold based, sliding window)/ Real-time | Stride count, cadence, gait speed, ratio of swing/stance, stride regularity, stride length [err. $< 3\%$], walking distance [err. $< 2\%$] |
| [36] | Healthy (5) | 2 IMUs (shanks) | Treadmill walk at [2,4] kph and run [8,12] kph/ Motion capture | Non-ML (threshold based)/ Offline | Gait events (HS and TO [err. $< 1\%$], MSw) , stride time [err. $< 1.6\%$] , swing, stance time. |
| [37] | Healthy (22) | 1 acc. (L4-L5) | Level walk, 10m, barefoot/ Motion capture | Non-ML (peak detection, integration)/ Offline | Step length, stride length [$p > 0.05$], {stride, step, stance, swing, DS, SS} time, gait speed [$p > 0.05$], cadence, foot symmetry |

*continued on next page*

Table2.1 (continued) State of the arts of QGA using wearable sensors

| Ref. | Subjects (n) | Sensors (Location) | Experiments/ Benchmark | Algorithms/ Data Processing | Gait features [Performances metrics] |
|---|---|---|---|---|---|
| [38] | Healthy (10), OA(12) | 4 IMUs (shanks and foot) | 50 m corridor walk/ Motion capture | Non-ML/ Offline | Joint angles (multi-segment foot angles) [RMSE $<$ 2 deg, Mean RoM diff. $<$ 4 deg] |
| [39] | Healthy (10), pre-HD (10), HD (14) | 1 acc (thorax level) | 4.8 m level walk/ GAITRite® | Non-ML (Inverted pendulum)/ Offline | Gait speed [ICC(CI) 0.95(0.75,0.97)], cadence [ICC(CI) 0.95(0.75,0.97)], stride length [ICC(CI) 0.89(0.77,0.95)], step length, step time, step time asymmetry, step-stride regularity |
| [40] | Healthy (8) | Textile socks | 2 min walk on treadmill at 4 kph/ F-scan | Non-ML (direct use of sensors data)/ Offline | Gait events (HS [0.08 $\pm$ 0.08 s], TO), stride time [err. $<$ 3.5%], stance time |
| [41] | Children (1), Children with CP (6) | 7 IMUs (lumbar, thighs, shanks, feet) | 10m walk preferred speed/ Motion capture | Non-ML ('Outwalk' protocol)/ Offline | Joint angles [RMSE $<$ 4 deg] |
| [42] | Older (10), PD (10) | 2 IMUs (upper shoes) | 2x20 m and 4x50 m walk with 180 deg turn/ Motion capture | Non-ML/ Offline | Gait speed [2.8 $\pm$ 2.4 cm/s], stride length [1.3 $\pm$ 3.0 cm], swing width, path length |

*continued on next page*

Table2.1 (continued) State of the arts of QGA using wearable sensors

| Ref. | Subjects (n) | Sensors (Location) | Experiments/ Benchmark | Algorithms/ Data Processing | Gait features [Performances metrics] |
|---|---|---|---|---|---|
| [43] | Healthy (5) | 7 IMUs (pelvis, thighs, shanks, feet) | 5m indoor level walk/ Motion capture and force plates | Non-ML/ Offline | Joint angles [RMSE < 10.14 deg] and 2D joint trajectories |
| [44] | Healthy (10) | Instrumented insoles | 5m indoor level walk/ F-scan | Non-ML/ Real-time (Data streaming) | Step time, stance time, swing time |
| [45] | Healthy (10) | e-AR | Treadmill walk with variable speed and inclination/ Instrumented treadmill, High speed camera (250Hz) | Non-ML (recursive)/ Offline | Stride time [err. < 1.47%], stance time [err. < 4.84%], swing time [err. < 8.03%] |
| [46] | Children (15), Children with CP (14) | 2 IMUs (feet) | 6 m straight walk and figure 8 walk for benchmark; 200 m walk in clinical setting with self selected speed for testing/ Motion capture | Non-ML/ Offline | Gait speed [4.3 ± 4.2 cm/s], stride length [3.4 ± 4.6 cm] , % {stance, swing, DS}, cadence, heel-toe clearance, strike [0.5 ± 2.9 deg] and lift off [3.9 ± 5.8 deg] angles |

*continued on next page*

Table2.1 (continued) State of the arts of QGA using wearable sensors

| Ref. | Subjects (n) | Sensors (Location) | Experiments/ Benchmark | Algorithms/ Data Processing | Gait features [Performances metrics] |
|---|---|---|---|---|---|
| [47] | Healthy (12), Older (12) | 1 IMUs (L5) | 5x25 m route on preferred and fast speed/ GAITRite®, camera | Non-ML (continuous wavelet transform)/ Offline | Step time and count, stride time [ICC 0.994-0.999], step length [ICC 0.756-0.929], step velocity [ICC 0.853-0.942] |
| [48] | Healthy (4) | 3 IMUs (thigh [right], shank, foot) and force sensors | 3 m walking straight indoor/ Motion capture and force plates | Non-ML/ Offline | Joint moments [3.5 % < NRMSE < 21 %] |
| [49] | Healthy (3) | Soft sensing suit | Instrumented split-belt treadmill with 5 speeds (3 walk and 2 run)/ Motion capture | Non-ML/ Offline | Joint angles (hip, knee, ankle) [RMSE < 15 deg] |
| [50][c] | Healthy (10) | 2 acc. (L3-L4 and shank) and 1 gyro (shank) | Instrumented split-belt treadmill with 5 speeds (all walk)/ Motion capture | Non-ML/ Offline | Gait events (IC, TC), stride time [RMSE < 1.6%], step time [RMSE < 4.3%], DS time [RMSE < 25.7%], stance and swing time |

*continued on next page*

Table2.1 (continued) State of the arts of QGA using wearable sensors

| Ref. | Subjects (n) | Sensors (Location) | Experiments/ Benchmark | Algorithms/ Data Processing | Gait features [Performances metrics] |
|---|---|---|---|---|---|
| [51] | Young (9), Mid-age (5), Old (6) | 2 IMUs (ankles) | Self-selected speed walking with variation on stride velocity and stride length/ Motion capture | Non-ML/ Offline | Heel [3.22 ± 1.50 cm] and toe [1.69 ± 0.70 cm] clearances, foot angle [2.49 ± 1.21 deg] |
| [52][f] | Healthy (10) | Sensorized insoles | Treadmill walk at 2 km/h/ Not needed | Non-ML/ Real-time | Gait phases |
| [53] | Healthy (25), SCD (25), PD (25) | 2 IMUs (lower back, upper back) | 6 min walking/ Not needed | Non-ML/ Offline | Statistical (Mean amplitude and Coefficient of Variation) |
| [54] | Older (19), PD (13) | 3 IMUs (C7, L5, back of head) | 2 min walking on 25 m circuit/ GAITRite® | Non-ML/ Offline | Statistical (Magnitude, attenuation, harmonic ratio) |
| [55] | Healthy (15), PD (5), Stroke (4) | 2 IMUs (feet) | 10 m straight walk normal speed/ FSR sensors | Non-ML/ Online | Gait events (HS [0.125 ± 0.01 s], TO [0.089 ± 0.015 s]), {stride, stance, swing, walking} time, stride count, stride length, gait speed, cadence |

*continued on next page*

Table2.1 (continued) State of the arts of QGA using wearable sensors

| Ref. | Subjects (n) | Sensors (Location) | Experiments/ Benchmark | Algorithms/ Data Processing | Gait features [Performances metrics] |
|---|---|---|---|---|---|
| [56] | Older (82) | 1 acc. (L3-L4) | 2x40 m round walkway at comfortable walking speed/ GAITRite® | Non-ML/ Offline | (Cadence, gait speed, step length, step time) [ICC 0.91-0.96], variability and asymmetry indices |
| [57] | ACL (23), TKR (31) | e-AR | 6 min walking on the corridor/ Pressure insoles | Non-ML/ Offline | Asymmetry($\|acc\|$) [MSE=0.044] |
| [58] | Healthy (10), OA (14) | Smart shoes | 15 m walking straight/ Force plates | ML (SVM)/ Real-time | Gait phases (IC, FF, HO, TO, swing) [Accuracy 94.08 %] |
| [59] | Healthy (10), Older (21) | 1 acc. (waist) | 10 m walking/ Video camera | ML (K-means clustering)/ Offline | Gait event (IC), step detection [Sensitivity 99.33 %], frail classification |
| [60] | Older (24) | 2 IMUs (shoes lateral) | 5 min walking on treadmill with variable slope/ Instrumented treadmill | Non-ML/ Offline | Gait speed [RMSE $<$ 0.089 m/s], stride length [RMSE $<$ 0.336 m], stride time [RMSE $<$ 0.004 s], cadence [RMSE $<$ 0.098 steps/min] |
| [61][f] | PD (3) | Sensorized insoles, 6 IMUs (hips, shanks, feet) | 18 m walking straight with variable pace/ Motion capture | Non-ML/ Offline | Gait phases (IC, FF, TC, swing), step length [Mean diff. 0.9 cm] |

*continued on next page*

Table2.1 (continued) State of the arts of QGA using wearable sensors

| Ref. | Subjects (n) | Sensors (Location) | Experiments/ Benchmark | Algorithms/ Data Processing | Gait features [Performances metrics] |
|---|---|---|---|---|---|
| [62] | Healthy (10) | Smart shoes | Free walking and 4x5 m walk/ Motion capture | Non-ML/ Real-time (Data streaming) | Gait phases (HS, stance, HO, swing) [Error range between 0.036-0.110 s] |
| [63] | Healthy (16), Neurologic patients (6) | 2 IMUs (feet) | Walking with preferred pace/ Kinect | Non-ML/ Real-time (Data streaming) | Stride length [RMSE 0.05 m], step length, cadence, gait speed, {stride, stance, swing [RMSE 0.02 s]} time, foot clearance, turning rate |
| [64] | Healthy (12), Obese (10) | 7 IMUs (pelvis, thighs, shanks, feet) | 14 m walk straight/ STEP32 | Non-ML/ Offline | Cadence, % gait phases, ROM (ankle, knee, hip) [Range of ICC 0.43-0.72] |
| [65] | Healthy (16), PD with FoG (26) non FoG (16) | 2 IMUs (shins) | TUG (3 m walk)/ Motion capture and video camera (for FoG) | Non-ML/ Offline | Step velocity, stride length, stride time, cadence, FoG detection [Accuracy 98.51 %] |
| [66] | Healthy (6) | 1 IMU (foot) | Level ground walking, stairs climbing/ Motion capture | Non-ML/ Offline | Step count, walking distance [Err. 0.81 %], % gait phases, 3D trajectory [RMSE 0.28 m] |

*continued on next page*

Table2.1 (continued) State of the arts of QGA using wearable sensors

| Ref. | Subjects (n) | Sensors (Location) | Experiments/ Benchmark | Algorithms/ Data Processing | Gait features [Performances metrics] |
|---|---|---|---|---|---|
| [67] | Healthy (7) | 2 acc. (heels) | 12 m walk/ Motion capture and video camera | Non-ML/ Offline | Gait events (HS [7.2 ± 22.1 ms], TS [0.7 ± 19.0 ms], HO [3.4 ± 27.4 ms], TO [2.2 ± 15.7 ms]), {stride, stance, swing} time [Range of ICC 0.87-0.98], heel clearance |
| [68] | Healthy (15), MS (45) | 2 IMUs (shanks) | Various walking tasks/ Activity monitor, Inertial sensors | Non-ML/ Offline | Step count, {stride [6 ± 9 ms], step [6 ± 7 ms], swing [25 ± 19 ms]} time |
| [69] | Healthy (25) | 4 IMUs (ankles, mid of superior iliac spine, C2) | 15 m walk normal speed/ Motion capture, GAITRite® | Non-ML/ Offline | Cadence [SEM 5.24 steps/min], gait speed [SEM 0.14 m/s], stride length [SEM 0.21 m], {stride [SEM 0.04 s], stance [SEM 0.04 s], swing [SEM 0.02 s]} time, {strike [SEM 2.11 deg], lift-off [SEM 3.33 deg], pelvis, spine} angle |

*continued on next page*

Table2.1 (continued) State of the arts of QGA using wearable sensors

| Ref. | Subjects (n) | Sensors (Location) | Experiments/ Benchmark | Algorithms/ Data Processing | Gait features [Performances metrics] |
|---|---|---|---|---|---|
| [70] | Stroke (25) | 1 IMU (L5) | Laboratory and real-life longitudinal study/ GAITRite®, OPAL, video camera | Non-ML/ Offline | Step velocity [ICC 0.744 m/s], step length [ICC -0.411 m], {step [ICC 0.797 s], swing [ICC 0.431 s], stance [ICC 0.759 s]} time, step width, asymmetry and variability indices |
| [71] | Healthy (14), children (10), CP (22) | 3 IMUs (L2-L3, thighs) | 30 strides at various speed/ FSR sensors | Non-ML/ Offline | Statistical (Pearson's r, variance ratio, harmonic ratio), Gait segmentation [Sensitivity 83.34 % (CP), 96.67 % (Healthy)] |
| [72] | Older (23) | 2 IMUs (feet) | Combination of normal and fast speed with added cognitive task/ GAITRite® | Non-ML/ Offline | Cadence, gait speed [ICC 0.34-0.96], step time [ICC 0.22-0.27], step length [ICC 0.45-0.84] |
| [73] | Children (10) | 6 IMUs (sternum, wrists, L4-L5, shanks frontal) | 7 m walk straight at self-selected and fast speeds/ Motion capture | Non-ML/ Offline | Stride length [RMSE 6.43 % of subject's height], gait speed [RMSE 7.80 % of subject's height], {stride [RMSE 0.014 s], stance [RMSE 0.026 s]} time |

*continued on next page*

Table2.1 (continued) State of the arts of QGA using wearable sensors

| Ref. | Subjects (n) | Sensors (Location) | Experiments/ Benchmark | Algorithms/ Data Processing | Gait features [Performances metrics] |
|---|---|---|---|---|---|
| [74][c] | Healthy (20) | 4 acc. (left wrist, waist, ankles) | Indoor, Outdoor, Treadmill walk and run/ FSRs sensors | Non-ML/ Offline | Gait events: (HS,TO) [F1 Scores (0.98,0.94) indoor, (0.82,0.53) outdoor] |
| [75][c] | Healthy (35) | 5 IMUs (L5, shanks, dorsal shoes) | 2 min walk at 10 m path back and forth/ Force plates | Non-ML/ Offline | Gait events (HS, TO), {step, stance} time |
| [76] | AD (16) | 1 acc. (L5) | Lab-based and free-living/ Prev. paper [5] | Non-ML/ Offline | Step velocity, step length, {step, swing, stance} time, step width, asymmetry and variability indices |
| [77] | Knee arthoplasty patients (16) | 2 IMUs (below knees) | 6 m walk straight at self-selected/ Motion capture | Non-ML/ Offline | Gait events (IC, TO), {stride [RMSE 0.036 s], stance [RMSE 0.041 s], swing [RMSE 0.049 s]} time |
| [78][c] | Healthy (27), PD (27) | 8 IMUs (chest, lumbar, thighs, shanks, feet) | 15 m walk straight at self-selected and fast speeds/ Not needed | ML (SVM)/ Offline | Step length, gait speed, {step, stride} time, {hip, knee, ankle} ROM, Patient vs. control classification [Highest accuracy 79.96 %] |

*continued on next page*

Table2.1 (continued) State of the arts of QGA using wearable sensors

| Ref. | Subjects (n) | Sensors (Location) | Experiments/ Benchmark | Algorithms/ Data Processing | Gait features [Performances metrics] |
|---|---|---|---|---|---|
| [79] | Healthy (30), Stroke (20), Joint disease (20) | 7 IMUs (waist, thighs, shanks, feet) | Walk straight >15m on corridor/ Motion capture | Non-ML/ Offline | Stride length, gait speed, stride freq., {stride, stance, swing} time, foot clearance, knee ROM [Position err. <0.015 m] |
| [80] | Healthy (24) | 7 IMUs (waist, thighs, shanks, feet) | 6 min walk test/ Motion capture | Non-ML/ Real-time | Step [RMSE 0.04 m] and stride length, step and swing width [RMSE 0.03 m], cadence [RMSE 3.1 steps/min], {step, stride, stance, SS, DS, swing} time [RMSE 0.02 s], gait speed [RMSE 0.03 m/s] |
| [81] | Healthy (10) | 1 IMU (CoM) | Walking at self-selected speed/ Motion capture | Non-ML/ Offline | Step length [Abs. Err. 5.6 %], gait speed [Abs. Err. 13.5 %], walking time [Abs. Err. 14.9 %], walking distance |
| [82] | MS (4), HSP (9) | IMUs, FSRs | 10 m walk, may use walking aid/ GAITRite® | Non-ML/ Offline | Gait events (IC, TC), % DS [3.89 ± 2.61 %], DS time [0.064 ± 0.060 s] |
| [83] | Healthy (16) | Flexible sensors | 6 m walk at preferred speed/ Motion capture | Non-ML/ Real-time (Data streaming) | Knee angle [RMSE 1.2 ± 0.4 deg] |

*continued on next page*

Table2.1 (continued) State of the arts of QGA using wearable sensors

| Ref. | Subjects (n) | Sensors (Location) | Experiments/ Benchmark | Algorithms/ Data Processing | Gait features [Performances metrics] |
|---|---|---|---|---|---|
| [84][c] | Healthy (15) | 1 IMU (foot) | 50 strides walk/ Motion capture | Non-ML/ Real-time (Data streaming) | Walking distance [Accuracy 95.24 %], stride count [Accuracy 95.47 %], {stride, stance, swing} time |
| [85] | Older (20) | 1 acc. (waist) | Real-world setting/ Video camera | Non-ML/ Offline | Step detection, gait speed [Mean diff. -0.206 m/s (for speed $<$ 1 m/s), and -0.045 (for speed 1-1.5 m/s] |
| [86] | Healthy (20), Neurological (20) | 2 IMUs (ankles) | 10 m corridor walk at preferred speed/ Prev. paper | Non-ML/ Offline | Cadence, gait speed, stride length, stride time, % stance and swing, ankle ROM, gait symmetry and regularity [Position Error $<$ 1%] |
| [87] | Healthy (20), Stroke (20), Joint disease (20) | 6 IMUs (thighs, shanks, feet) | 15 m obstacle-free corridor walk/ Motion capture | Non-ML/ Real-time (Data streaming) | Cadence, gait speed, stride length, stride time, % stance and swing, foot clearance, knee ROM and dorsiflexion-plantar angles [Err. $<$ 3 deg] |

*continued on next page*

Table2.1 (continued) State of the arts of QGA using wearable sensors

| Ref. | Subjects (n) | Sensors (Location) | Experiments/ Benchmark | Algorithms/ Data Processing | Gait features [Performances metrics] |
|---|---|---|---|---|---|
| [88] | Healthy (5) | 2 IMUs (feet) | 11 m walk indoor/ Motion capture | Non-ML/ Offline | Gait events (HS, TO), gait speed [Rel. Err. $6.3 \pm 2.2$ %], stride length [Rel. Err. $5.9 \pm 3.3$ %], % DS phase [Rel. Err. $4.3 \pm 3.3$ %] |
| [89] | Healthy (49) | 2 IMUs (feet) | Treadmill run at comfortable speed/ High speed camera | Non-ML/ Real-time | Step length [ICC 0.968-0.975], step frequency, stance [ICC 0.813-0.896] and swing [ICC 0.807-0.857] time |
| [90][f] | Healthy (10) | 4 IMUs (shanks, feet) | Treadmill walk with variable speeds/ Motion capture | Non-ML/ Real-time | Gait events (HS, TO), Gait phases (stance [Accuracy 97.9 %], swing [Accuracy 96.3 %]), ankle angle [RMSE $3.24 \pm 0.67$ deg] |
| [91] | Stroke (25) | 2 IMUs (feet) | Walking with total distance of 120 m/ Motion capture | Non-ML/ Offline | Stride time [Err. 0.003(0.020) s], stride length, cadence [Err. -0.341(0.467) steps/min], gait speed [Err. 0.002(0.003) m/s], % gait phases ; *Note*=[Err.=Non-paretic(Paretic)] |

*continued on next page*

Table2.1 (continued) State of the arts of QGA using wearable sensors

| Ref. | Subjects (n) | Sensors (Location) | Experiments/ Benchmark | Algorithms/ Data Processing | Gait features [Performances metrics] |
|---|---|---|---|---|---|
| [92][f] | Healthy (17), hemiparetic (18) | Textile insoles | 20 m corridor walk back and forth at self-selected/ Not needed | Non-ML/ Real-time (Data streaming) | Plantar pressure, stride time, stride count |
| [93] | Healthy (30) | 1 IMU (L5) | 6 m indoor walk at preferred speed/ GAITRite® | Non-ML/ Offline | Gait speed [ICC 0.92], cadence [ICC 0.96], stride length [ICC 0.88], stride time [ICC 0.93], % gait phases (SS, DS, Swing, Stance) [ICC 0.18, 0.12, 0.47, 0.47] |
| [94] | Healthy (3) | 3 IMUs (waist, thigh, shank) | Walk and run on treadmill, up and down stairs walking/ Footswitch insoles | ML (Random Forest)/ Offline | Gait phases (SS, DS, swing) [Accuracy 98.94 % (walk), 98.45 % (run)] |
| [95] | Healthy (22), cerebellar ataxia (29) | 3 IMUs (chest, ankles) | 5 m walk back and forth/ Motion capture | ML (Random Forest)/ Offline | Gait speed, cadence, gait ataxia quantification. [RMSE 0.18] |
| [96] | Healthy (10) | 3 IMUs (chest, wrist, thigh), 4 FSRs | 7 min treadmill walk at various speed/ Instrumented treadmill | Non-ML/ Real-time (Data streaming) | Gait events (HS, TO), stride time [RMSE 5.027 ms], stride count [Accuracy 99.6 %] |

*continued on next page*

Table2.1 (continued) State of the arts of QGA using wearable sensors

| Ref. | Subjects (n) | Sensors (Location) | Experiments/ Benchmark | Algorithms/ Data Processing | Gait features [Performances metrics] |
|---|---|---|---|---|---|
| [97] | Healthy (9), PD (6) | 2 IMUs (feet) | Walk at self-preferred speed/ GAITRite® | Non-ML/ Offline | Step length [Mean Err. 4.50 ± 2.54 %] , step time [Mean Err. 2.97 ± 2.51 %] |
| [98] | Healthy (5) | 4 Ultrasonics sensors | 8.5 m walking back and forth at normal speed/ Video camera | Non-ML/ Offline | Gait events, ankle angle [Mean diff. 0.19 ± 1.19 deg], toe clearance [Mean diff. 0.02 ± 0.84 cm] |
| [99] | Healthy (30), stroke (30) | 8 IMUs (waist [left and right], knees, ankles, feet) | More than 15 m level ground corridor walk/ Motion capture | Non-ML/ Offline | Stride length, cadence, gait speed, ankle ROM, gait symmetry, stance/swing ratio, foot clearance [Position Err. 0.02 m] |
| [100] | Healthy (6) | 2 IMUs (shoes posterior) | 4.5 m and 11 m indoor walk back and forth at self-preferred speed/ Motion capture, force plates | Non-ML/ Offline | Gait events (IC [4.22 ± 15.48 ms], TO [-8.31 ± 21.02 ms], % gait phases, gait speed, stride length [Accuracy 93.23 %], heel clearance [2.22 ± 5.28 cm], {stride, stance, swing} time, variability and asymmetry indices |

*continued on next page*

Table2.1 (continued) State of the arts of QGA using wearable sensors

| Ref. | Subjects (n) | Sensors (Location) | Experiments/ Benchmark | Algorithms/ Data Processing | Gait features [Performances metrics] |
|---|---|---|---|---|---|
| [101] | Healthy (3) | E-textile socks | 11 m indoor walk at various speeds/ Motion capture | Non-ML/ Real-time (Data streaming) | % Gait phases, cadence, stride length [Pearson's r = 0.283], gait speed |
| [102] | Healthy (11) | 7 IMUs (CoM, thighs, shanks, feet) | Walking on various terrain (level ground, stairs, ramp)/ Inertial sensors | ML (Neural Network)/ Real-time | Joint angles [NRMSE < 0.092 (knee joint)] |
| [103] | Healthy (20), older (20) | 5 IMUs (chest, wrists, ankles) | Figure eight walk at normal speed on laboratory environment/ Motion capture | Non-ML/ Offline | Stide length [Abs. Err. 0.02 ± 0.03 m], gait speed [Abs. Err. -0.01 ± 0.02 m/s], step width, % gait phases, cadence, stride time, foot clearance, arm-related metrics |
| [104] | Healthy (5) | 2 IMUs (top of shoes) | 60 m total walking distance with variable stride length/ Optogait system | Non-ML/ Offline | Stride count, stride length [RMSE 5.0 cm], stride time [RMSE 0.04 s] |
| [105] | Healthy (8) | 6 IMUs (thighs, shanks, feet) | 4.5 m straight walk with variable speeds and tasks/ Motion capture | ML (kNN)/ Real-time | Stride time, stride length [RMSE 3.33 cm] |

*continued on next page*

Table2.1 (continued) State of the arts of QGA using wearable sensors

| Ref. | Subjects (n) | Sensors (Location) | Experiments/ Benchmark | Algorithms/ Data Processing | Gait features [Performances metrics] |
|---|---|---|---|---|---|
| [106] | Healthy (9) | 2 IMUs (lateral shoes) | 20 m straight walk at preferred speed/ Motion capture | ML (Neural Network)/ Offline | Gait phases classification [Accuracy 92.63 %] |
| [107] | Healthy (40), PD (24) | 1 IMU (L5) | 10 m indoor straight walk at preferred speed/ GAITRite® | Non-ML/ Offline | Cadence [MSE Healthy(PD) 4.78(15.28) steps/min], gait speed [MSE Healthy(PD) 0.02(<0.01) m/s], stride time, stride length, % gait phases [MSE 17.40 % (for double support on PD) |
| [108] | Healthy (40) | Pressure insoles | 10 m indoor walk with various speeds/ GAITRite® | Non-ML/ Offline | Cadence [ICC 0.99], {stride, step, swing, stance, SS [ICC 0.65-0.96], DS [ICC 0.55-0.79]} time |
| [109] | Healthy (20) | 1 IMU (ankle) | Walking on various terrain/ Not needed | ML (Random Forest)/ Offline | Gait activity classification [Accuracy 98.2 %] |

## 2.3 Synthesis of Search Results

We ensure that all the included papers have some sort of validation to the gold standard measurement of motion capture and/or force plate systems or other widely accepted measurement methods such as using an instrumented treadmill or GAITRite® system. There was some exceptions to this, such if the authors used

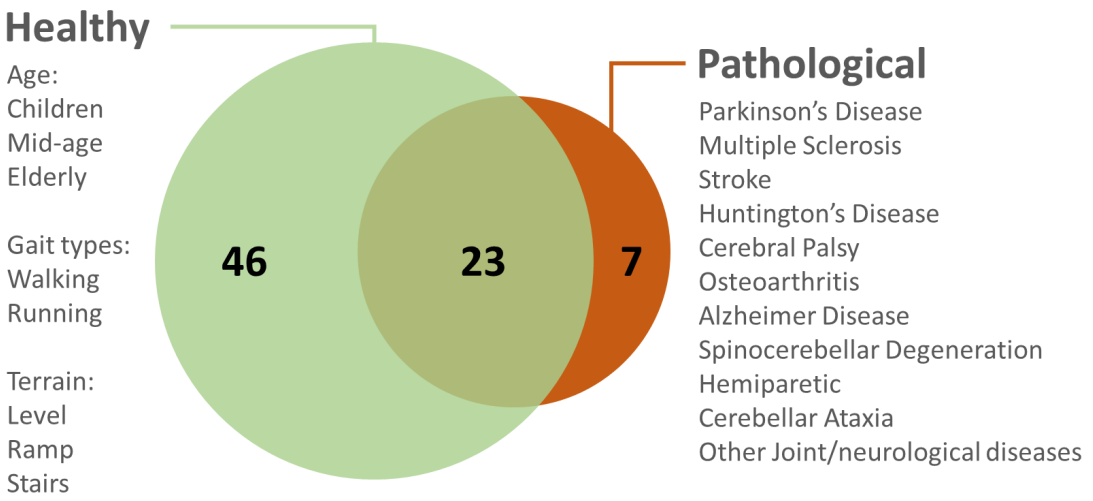


Figure 2.3: Identified application of wearable-based gait analysis. Twenty three studies discussed the application to both healthy control and patients with certain pathological conditions.

a force-based sensors [52], [92] on foot which directly estimate the initial/terminal contact of foot, analyzed only statistical features from raw data [53], or performed machine-learning based algorithm for classification [78], [109]. On other case, some authors may also cited their previous validated framework[76], [86].

We compiled all important information such as application and subject of gait analysis, number of sensors and locations, types of features extracted, experiment performed, algorithms used, data processing, and validation method on Table 3.1.

### 2.3.1 General Application of Wearable Gait Analysis

Based on the results of literature search, we identify that 46 (61%) of the eligible studies tested their framework only to general healthy control subjects, while 23 (30%) of the studies included both healthy control group and patients group. We did not discriminate the healthy subject group by age, thus children or elderly groups were also counted in this general application. Elderly specific analysis [56], [60], children [73], and comparison between age groups such as normal mid-age subject to elderly [47], [51], [59], [103] were the examples of general application by age differences.

On terms of assessing different gait types, we identified a few studies discussing about both walking and running gait [36], [49], [89], [94]. Analysis of walking on different terrain such as ramp walkway, up and down stairs, or outdoor were discussed on [66], [74], [94], [102], [109]. Temporal, spatial, and spatio-temporal gait

features were found to be the most included analysis within the studies. Those features could be further derived into a certain gait indices or gait metrics such as gait regularity and symmetry index [35], [100], which were mostly used in clinical-related application. Estimation of lower limb joint angles [43], [49], and joint moment [48] were also made available using wearable sensors.

### 2.3.2 Clinical Application of Wearable Gait Analysis

In addition to the general application of gait analysis, we identified several clinical applications such as on Parkinson's Disease (PD), Huntington's Disease (HD), Celebral Palsy (CP), Multiple Sclerosis (MS), Osteoarthritis (OA), post-stroke patients among many more clinical application within the literature. We found that most of the studies discussed the comparison from one disease group to healthy control group or other disease group. Other application for each disease group are discussed as the following.

#### 2.3.2.1 Parkinson's Disease

Parkinson's Disease (PD) is one of the brain disorder that leads to difficulty walking, balance, coordination as well as talking. Gait analysis performed in PD patients could give several insights such as the difference between OFF and ON state of medications [42] and detecting freezing of gait (FoG) [65]. Quantitative gait analysis could further give a clear quantifiable features that could track the progress of the patients.

We found nine studies [42], [53]–[55], [61], [65], [78], [97], [107] implemented wearable sensors approach for gait analysis in PD patients. All of the studies used IMU sensor with a combination between 2 to 8 IMU units. We found one study [61] proposed a combination between sensorized insoles and 6 IMUs to estimate gait phases and step length while also giving rhythmical auditory feedback to the user.

PD group has also been used as disease control group to distinguished another neurological condition such as spinocerebellar degeneration [53]. Other application such as analysis of upper body and postural control was discussed on [54], while comparison of several machine-learning based classification of PD patient was extensively discussed in [78].

#### 2.3.2.2 Stroke

Stroke is caused by an interruption of blood supply to the brain, usually in the form of blood clot. Stroke can be differentiated into two major categories, that are ischemic stroke and hemorrhagic stroke. On the case of stroke or post-stroke patients, gait analysis is usually performed to track the rehabilitation progress. We found a total of six studies discussing about the application of wearable gait analysis for stroke patients [55], [70], [79], [87], [91], [99]. A study using six IMUs on lower limb [87] provided a solution on tracking the rehabilitation progress of different group of patients including stroke, by estimating the knee ROM of patients pre- and post treatment.

All of the studies used IMU with a varying combination between 1 to 8 units. A study using two units of IMU on feet [55] showed a significant difference on several spatio-temporal features between stroke patients and healthy control groups. Another study [79], [99] also reported a clear differences on gait features between the compared subject groups.

An extensive reliability and validation study of a single trunk-attached (L5) IMU [70] showed a moderate to good agreement to a GAITRite® system on estimating stance time and several step-based features. Another validation study of using foot-worn IMU [91] showed a good to excellent agreement on various spatio-temporal gait features for both paretic and non-paretic sides, and moderate agreement for stance and swing phases.

#### 2.3.2.3 Huntington's Disease

Huntington's Disease (HD) is a neurodegenerative condition with a symptom of progressive movement disorder. We found one study [39] discussing about this application. This study [39] used one accelerometer on thorax level to extract various spatio-temporal features based on inverted pendulum model [110]. A comparison between three distinct group of healthy control, pre-manifest Huntington's disease (HD) and manifest HD were presented. Results show that there was a strong agreement between the sensor and GAITRite® system, and the gait features extracted from the accelerometer proved to be effective on differentiating between groups, especially the pre-manifest and manifest HD groups.

#### 2.3.2.4 Cerebral Palsy

Cerebral Palsy (CP) is the most common motor disability found in childhood. CP is classified into three types namely ataxia (poor balance and coordination), dyskinesia (uncontrollable movement), and spasticity (stiff muscles). Three studies [41], [46], [71] discussed the application of wearable sensors for gait analysis in CP.

This study [41] developed a specific protocol for children with CP called 'Outwalk' protocol to estimate joint angles using seven IMUs. This study [46] pointed out a significant differences between children with CP and typically developing children as seen by various spatio-temporal and kinematics features. On the other hand, another study [71] show that their unique statistical features analysis could distinguished the three sub-classes of CP subjects based on their motor function.

#### 2.3.2.5 Multiple Sclerosis

Multiple Sclerosis (MS) is a disease that affects the central nervous system (brain and spinal cord) that causes communication problems between the brain and other body functions. Two studies [68], [82] were found discussing wearable sensors for MS gait analysis and discussed as the following. Both of the studies employed IMU sensing units, where [68] used two units on shanks and [82] combined an IMU with three FSR sensors inside an insole as the wearable system.

This study [68] designed various walking protocols with variable walking speeds to assess the MS group. Gait event detection algorithm was adapted from [111] and further derived into temporal features. Their proposed framework was validated against an activity monitoring system (GT3X) and commercially available inertial sensor (MTx). Results show that there were $2 \pm 2$ steps, $6 \pm 9$ ms, and $25 \pm 19$ ms errors for step count, stride time, and swing time, respectively. On the comparison of MS group with healthy control group, it was found that using the system described could detect a significant ($p < 0.01$) distinct gait characteristics between the two compared groups. On the other hand, this study [82] proposed to use sensorized insoles consisted of three FSRs sensor and an IMU to extract temporal gait features on patient with gait disorders such as MS and hereditary spastic paraplegia (HSP). IC and TC events were labelled manually based on the heel FSR and lateral FSR, respectively. Results show that there was a mean error of $64 \pm 60$ $ms$ of DS time, or translated into $3.89 \pm 2.61\%$ of DS phase from 1321 analyzed strides from all participated subjects.

From both of the studies, we found that temporal features were the main gait

feature used to characterized MS patients. Several temporal features such as stride time and step time were found to be effective in differentiating between healthy and MS subject groups. Moreover, it was demonstrated that temporal features could also distinguish MS subjects by their severity level [68].

#### 2.3.2.6 Joint Diseases

Various joint-related diseases such as osteoarthritis were found within the search pool. Osteoarthritis is a degenerative joint disease that occurs when the protective cartilage on the ends of bones are worn down. On this case, gait analysis was performed to assess the effectiveness of treatment plan. We found six studies discussing about various joint-related diseases, such as osteoarthritis [38], [58], anterior cruciate ligament reconstruction [57], knee arthroplasty [77], and other joint diseases [79], [87]. A brief explanation of those studies are summarized in 3.1.

Kinematic features estimation such as foot angles was found to be effective in differentiating healthy control and ankle osteoarthritis groups [38]. A study using an ear-worn accelerometer [57] provided various asymmetry metrics to monitor the recovery gait of patients undergone ACL reconstruction or total knee replacement (TKR). An integrated FSRs and IMU sensors on smart shoes was used to extract gait phases on osteoarthritis patients using SVM algorithm in real-time with 94 % of accuracy [58]. Two IMUs below knees to extract temporal features were proposed by [77] for analysis of knee arthroplasty patients post knee replacement surgery. These studies [79], [87] used 7 and 6 IMUs respectively and extracted the most gait features comprised of temporal, spatial, spatio-temporal, and kinematics features. Knee ROM was chosen as one of the primary feature to track the prior and post-treatment gait of the patients.

### 2.3.3 Sensors and Location

In this review, we simplify sensor categorization to IMU-based, non IMU, and combination of IMU and other sensors (IMU+). IMU-based sensors was found to be the most common wearable sensors used on this topic. An IMU is generally consisted of accelerometer, gyroscope, and magnetometer. Using all three components could give orientation and relative position information by means of sensor fusion method. Nevertheless, in this review we found that those three components were not always used altogether. Some study only used the accelerometer part [37], [53], [54], while other may only use the gyroscope unit [36]. Other than that, we also found unique sensor systems such as textile-based [40], [101], ultrasonic-based [101], and flexible

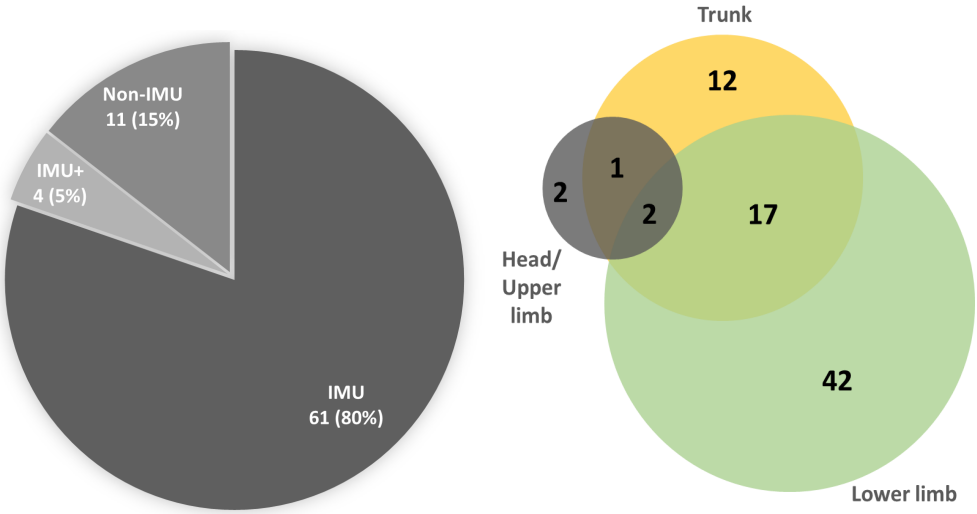


(a)

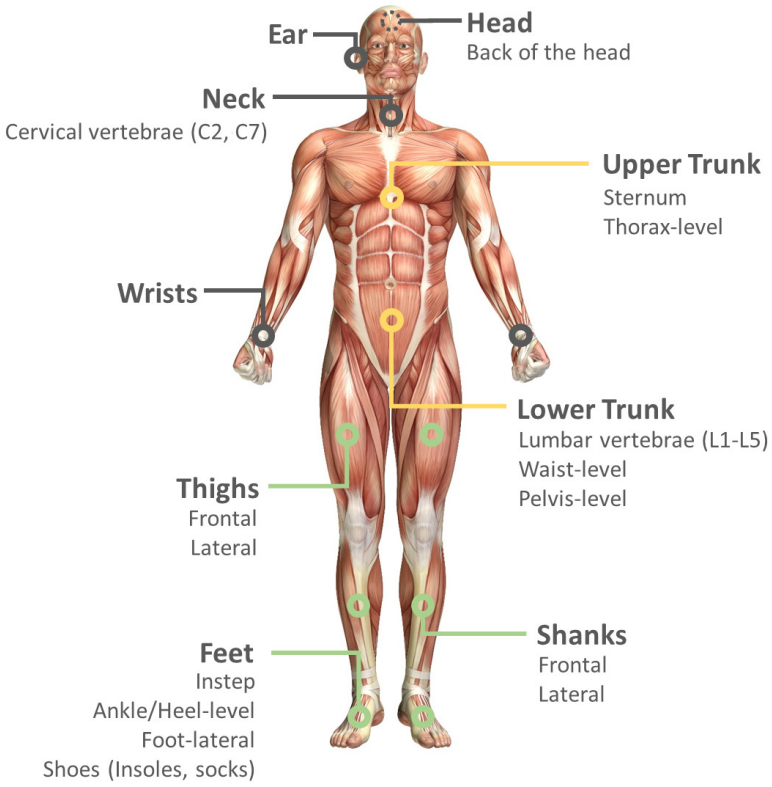


(b)

Figure 2.4: (a) Distribution of wearable sensors used, where IMU-based sensors account for 80%, and IMU+ which is combination of IMU and other sensors account for 5% of the total eligible studies [left]. Location of sensor attachment to the body, where the most was found at lower limbs (42 studies) followed by lower limbs and trunk attachment (17 studies) [right]. (b) The detailed view of attachment of sensors in different region of human body as summarized from the eligible papers.

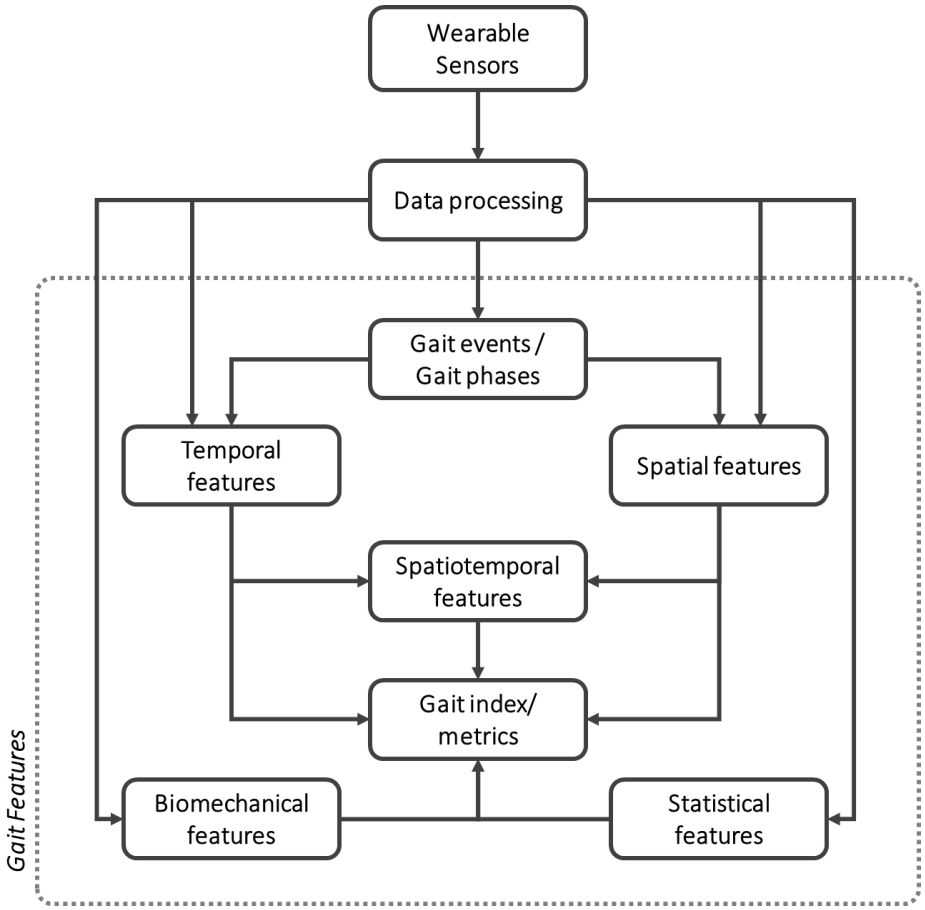


Figure 2.5: Classification of gait features that are extracted from wearable sensors, which comprised of gait event/gait phases, spatial, temporal, spatio-temporal, gait index/metrics, biomechanical features, statistical features. In this review, biomechanical features means any kinematic or kinetic-based gait features such as joint angles and joint moment.

[83] sensors.

Location-wise, we found that most of the studies proposed a lower limb sensor attachment which accounts for 42 papers, followed by both trunk and lower limb attachment which accounts for 17 papers and trunk-only attachment which totaled in 12 papers. Only two papers proposed a head-attached sensor which both of the papers were from the same authors which proposed an ear-attached sensor [45], [57]. Interestingly, two papers proposed upper limb, trunk, and lower limb sensor attachment, where [73] focused on gait assessment on children while [74] focused on the comparison of several algorithms and tested on various terrain/environments. One paper proposed a combination of trunk and head sensor attachment [54] for assessment of gait in elderly and PD patients.

### 2.3.4 Gait features

In this review, gait features are any quantifiable parameters or characteristics of gait that are measured directly from wearable sensors or estimated through sets of algorithms. We divide gait features into seven categories as depicted in Fig. 2.5. The first is gait events or gait phases. Gait events indicate the instantaneous any event occur based on the set detection algorithm, while gait phases marked the time of which the identified phase occurred from start to end of that phase. The most important gait events are initial contact (IC) and terminal contact (TC), where they represent the point where stance phase and swing phase is about to start, respectively. IC and TC may also be known as heel-strike (HS) and toe-off (TO). HS, TO, IC, TC, midswing (MSw), toe-strike (TS), heel-off (HO) were types of gait event identified on this review. On the other hand, the two primary phases of gait are stance phase and swing phase. Under the new terms of gait phase classification, we could further detailed it into eight distinct phases, i.e. initial contact, loading response, mid-stance, terminal stance, pre-swing, initial swing, mid-swing, and terminal swing. Other than stance and swing phase, we identified single support (SS), double support (DS), IC, foot-flat (FF), HO and TC phases in the eligible studies.

The second is temporal features which are any features containing time-based information. Stride time, step time, stance time, swing time, single support (SS) time, double support (DS), and cadence time are the widely known temporal gait features. Usually these features are computed with the information from gait event detection. For example, stride time which defined as time taken to complete a gait cycle, could either estimated from the consequent of HS or TO events. Stance time is estimated from the point of IC or HS to the point of TC or TO. SS and DS time are estimated from the information of both sides of the foot, where SS time is equivalent to time elapsed when only one foot contact with the ground. DS time is time elapsed when both of the feet are in contact with the ground. Cadence is the rate of how many steps does one walks per minute of time. Other than those features, some studies also computed total walking time which is the sum of stride time per walking trial.

The third is spatial features which are features containing length-based information such as stride length and step length. Other than that we also identified several other spatial features such as swing width, path length, walking distance, travelled arm distance, and clearance (heel, toe, foot).

The fourth is spatiotemporal features that are derived based on the both spatial

and temporal features. In this case, gait speed and step velocity are defined as the spatio-temporal gait features.

The fifth is the biomechanical features that are consisted of kinematic features and dynamic features. On kinematic features, joint angles such as hip, knee, and ankle angles are the most commonly derived kinematic gait features. In addition to that, we also identified strike and lift-off angles which are the angle of which the foot are about to contact the ground and lifted from the ground, respectively. In some clinical gait analysis, we found a study extracted and used pelvis and spine angles in all axes [69] for their analysis. In other study, we identified the use of turning rate feature to assess the turning movement performed by the subject. On dynamic features, we identified some studies estimate the joint moments and extracted plantar pressures from pressure-based insoles.

The sixth is statistical features that are derived from raw sensor data. We identified magnitude, RMS value, harmonic ratio, mean amplitude, coefficient of variation, Pearson coefficient, and variance ratio were extracted and classified as statistical features found within the eligible studies.

The seventh is gait index or gait metrics that are unique features derived from any major gait features mentioned previously. For example, we identified variability, symmetry, and asymmetry indices that are based on step length, stance time or swing time. Another gait metrics commonly reported are stride or step count which totals the number or stride or step in particular walking trial. Stride and step regularity, ratio of swing and stance, joint trajectory, stride frequency were also found within the eligible studies. For clinical gait metrics, we found a study discussed about frailty classification in elderly [59], and FoG metric in PD patients [65].

### 2.3.5 Data processing

Raw data from sensors can be processed in either offline, online, or real-time manner. We found that most of the studies in this review were adapting the offline data processing. This may be due to the need for proper experimental procedures that were designed carefully to validate the proposed framework to the gold standard system such as motion capture and force plates. Online data processing was presented in two studies [34], [55]. The first study [34] used 7 IMUs attached on the lumbar, thighs, shanks, and foot to estimate joint angles in an online manner. The integral differences between angular velocities between two sensors location coupled with Kalman filter was proposed to estimate joint angles. Results show that RMSE on joint angle estimation vary depending on walking speed, where slowest

walking speed leads to lowest RMSE. On the other hand, the second study [55] used a threshold-based algorithm to estimate HS and TO events from foot mounted IMU. Several spatio-temporal features were derived and compared between subject groups on the 10 m walking experiment, where data processing was done online. Their method was validated to FSR sensors and also compared to some of existing study. Results show that the presented method had good agreement with the FSR sensors and comparable to the existing method. Moreover, some of the extracted spatio-temporal features show a significant difference ($p < 0.05$) between the compared groups of stroke to healthy control and PD to healthy control.

Real-time data streaming has become more common on last few years [44], [62], [63], [83], [84], [87], [92], [96], [101], where it has contributed on preparation to processing time efficiency. On the other hand, real-time data processing was implemented on [35], [52], [58], [80], [89], [90], [102], [105], where on [102] it could accommodate up to 7 IMU units for lower limb joint angles estimation. The following briefly discuss each of the studies implementing real-time data processing. This study [35] used 1 IMU attached on the left heel to extract spatio-temporal gait features such as cadence, velocity, stride length and walking distance. A threshold-based algorithm and sliding window techniques enables a real-time implementation. A real-time data processing was employed to estimate gait phases from the insole equipped with 64 pressure sensitive elements, where GRF and CoP were simultaneously recorded [52].

Smart shoes equipped with 7 FSRs and 1 accelerometer on each of the shoe was proposed to estimate gait phases in real-time using machine-learning based algorithm [58]. Investigation of the validity and test-retest reliability of real-time event detection and further spatio-temporal gait features estimation using 7 IMUs was presented in [80]. Investigation of validity of two commercial wearables, i.e. Stryd™ and RunScribe™, for running gait analysis was presented in [89] and benchmarked to a high speed video analysis recorded at 1000 Hz. The use of 4 IMUs attached on shank and foot of both legs for gait phase recognition and ankle angle estimation in real time was studied in [90]. Another study [102] used 7 IMUs placed near CoM, and both of thighs, shanks, and feet to estimate joint angles in a real-time manner. Finally, this study [105] proposed an open-source application on Python for gait analysis using 6 IMUs attached on thighs, shanks, and feet. KNN followed by correction using foot acceleration were used as gait segmentation algorithm that estimate TO event. GUI was also developed for both commands and visualization tools.

### 2.3.6 Algorithms

Treatment of raw data or often called data pre-processing is usually consisted of applying some filtering techniques to remove unnecessary data or noise from the raw data. For example, Butterworth low-pass filter with various order and cut-off frequency was commonly applied within the studies. The sliding window technique was found implemented in studies proposing a real-time processing approach [35] or in data preparation for threshold-based algorithm [74], [106].

We identified a various sets of algorithms implemented to process the raw data from wearable sensors to provide quantitative gait analysis. To simplify, we classify the main algorithm into two classes, ML-based algorithm, and non-ML-based (conventional) algorithm. The majority of the eligible studies employed the conventional algorithm to extract gait features. On gait event/ gait phases detection, we identified several algorithms such as peak detection, threshold-based, state machines, heuristics rule-based, and finding local minima/ local maxima, which are more or less have the same principles. Fast Fourier transform (FFT) was implemented to extract gait frequency and cadence in few studies [55], [95]. Another method such as continuous wavelet transform (CWT) was found implemented to extract gait events [47], [70], [76], and for stride segmentation [67].

Since the majority of the eligible papers used IMU-based sensors, several sensor fusion algorithms were applied to estimate the orientation of the sensor position. Kalman filter (KF) and complementary filter (CF) were the two most adapted orientation estimation methods. This orientation position combined with the knowledge of gait events or gait phases could give the spatial features such as stride length and step length among many other spatial features. Double-integration combined with zero velocity update method was implemented in several studies to estimate stride length. A model based approach such as inverted pendulum [39], [47], [70], [76], [81], [101] was also found in a few studies to estimate gait features such as stride length.

Several studies have implemented ML-based algorithms to their proposed framework of quantitative gait analysis using wearable sensors. SVM [58], [78], [102], RF [94], [95], [109], NN [94], [102], [106], kNN [78], [105], k-means clustering [59], decision tree [78], [102], logistic regression [94], Naive-Bayes and LDA [78]. Most of the studies used ML-based algorithms for classification problems such as gait events/ gait phases classification [58], [78], [94], [106] and classification of gait in different terrains [109]. On the other hand, we identified four studies employed ML-based algorithm as a supporting algorithm such as cross-checking [59], correction [102],

and detecting false phase [105]. Lastly, only one study shows its usage as a scoring function in gait ataxia [95].

### 2.3.7 Experiments and validation

Experiments performed to capture gait could be done in various ways. Most of the time, experiment protocols were designed accordingly to be suited best for the objective of gait analysis. Therefore, there are no single experiment protocols that are better than the other. In this review, we found various experiment protocols developed in each study and summarized in Table 3.1. Indoor level ground walking was found to be the most adapted protocol. Other experiments such as treadmill at various speeds, outdoor walk, figure-eight walk, timed up and go (TUG), ramp and stairs walk were also identified with different distance covered or repetitions done. We found that the design of experiment protocols was highly dependent on the environment constraint, subjects in the study, and types of wearable sensors.

We found several validation systems that are considered gold-standard in assessing gait such as motion capture system, GAITRite®, instrumented treadmill, and force plates. Other than those systems, some studies validate their proposed wearable gait analysis framework to the camera-based system, pressure-sensor system, and other inertial sensors. Each of the studies has its own method on how to report the benchmark or validation results. We identified several validation metrics such as absolute error, relative error, accuracy and precision, root mean squared error (RMSE), mean differences, student t-test (p-values), intra-class correlation (ICC), confidence interval (CI), the limit of agreement (LoA), and Bland-Altman plot, sensitivity and specificity, F1 score, false-positive rate (FPR), and standard error of mean (SEM) among many other validation metrics. The range of choice of validation metrics has made reporting meta-analysis of benchmark studies impractical.

## 2.4 Discussion

**What types of assessment can be drawn from wearable-based gait analysis for general application ?**

As discussed previously in section 2.3, a total of 91 % of the eligible papers implemented their proposed approach to a healthy group or general application. We found that healthy group is mostly served as the control variable to be compared to some other pathological groups. Temporal, spatial, and spatiotemporal gait features

were found to be the most common assessment that can be done for general application. These features were not only reported as it was but could also be derived to give gait indices features such as gait regularity or gait symmetry [86]. A few papers discussed the difference between age groups, i.e. healthy adult subjects and elderly subjects [47], [59], [103]. On sport application, running studies were discussed in [36], [49], [89], [94]. Gyroscope-based temporal gait analysis with a peaked running speed of 12 km/h was validated in [36]. Commercial wearables such as RunScribe and Stryd were concluded valid wearables to measure spatiotemporal gait features on running at comfortable speed [89]. In another study, spatiotemporal features such as gait speed was associated with survival in older adults [112]. The importance of foot clearance assessment for the elderly subject has also been shown in [113].

**Types of features that give the most impact on clinical application and challenges on applying wearable-based gait analysis for clinical applications.**

There is no single gait features that are superior than the others in explaining certain gait conditions in a subject. Every gait condition have its own unique feature or markers that are distinguishable from other condition. On some occasion, visual inspection can be enough to assess certain pathological markers such as on hemiparesis where one side of the body is weakened. On the other hand, a quantifiable parameter is needed to report the factual condition of the subject. Temporal gait features such as stride time or step time were found to be effective in differentiating three types of MS patients based on their severity level [68]. Detection of FoG in as discussed in [65] was found to be helpful in the assessment of PD patients. Statistical features as described in [71] were found to be successful in detecting gait impairment in CP subject groups. Other studies show that the knee ROM feature can be used to track rehabilitation progress of both arthropathy and stroke patients [87]. Further, combining gait and other motion may give more comprehensive assessment on motor performance [114].

We have identified a variety of clinical applications such as Parkinson's Disease, Multiple Sclerosis, and post-stroke among other applications listed in Figure. 2.3. The performance, validity, and reliability of each proposed wearable approach have been extensively investigated. Since each of clinical conditions may produce a unique gait pattern disorder, we presume that it will affect the performance of any of the wearable-based approach in this review if applied to new clinical application. This issue highlighted the importance of benchmark experiments before adapting the proposed approach to a new applications.

**Challenges on wearable sensors and the importance of sensor placement**

We found that gyro-drift is a major concern of using IMU-based sensors. There are several methods on how to reduce or remove the drift such as using Kalman filter [34], [63], [66], [102] and zero velocity update [63], [79], [88], [99] as implemented widely on the studies in this review. Environmental interference that affect magnetometer was also one of the problem found in this review. A simple calibration procedure that are easy to implement was proposed by [79] to compensate the interference issue. Concern about secure attachment to the body was also raised in several studies. Soft-tissue artifacts have found to be one of the source of noise in data processing [41], [64]. Some studies that used multiple IMUs needed to perform sensor to segment alignment and calibration [43], [90] to achieve better performance. This may add more preparation time but comparatively still faster than preparation time if using marker-based systems.

In terms of location of sensor attachment, most of the studies placed the sensors on lower limbs, followed by lower trunk on lumbar vertebrae region. These positions was found to be well suited for wearable-based gait analysis in terms of number of features that can be extracted and also the accuracy of gait features estimation, where foot-based attachment performed better than the shank or trunk-based ones for gait events detection [75]. The number and location of sensors were found to be a higher factor than the algorithm used in the case of discriminating severity stages of PD patients [78]. On foot-based sensors, the search for optimum location was investigated in [84], where medial aspect of foot followed by the posterior side of foot were the optimal location for stride-related feature extractions.

**Contribution of machine learning algorithms in wearable sensor gait analysis and current challenges.**

Machine learning algorithms have been integrated into several studies. The overall contributions of machine learning algorithm were mostly for classification problem such as gait event or gait phase classifications [58], [78], [94], [106], and gait activity/terrain classification [109]. Other than those, we also identified a few other application such as cross checking frailty discrimination [59], joint angle correction [102], detecting false swing phase [105], and for scoring algorithm in gait ataxia [95]. Based on our search strategy, we did not found any paper discussing machine learning algorithms to extract gait features. However, outside of the eligible studies, we found a study [115] implementing deep learning approach to estimate spatio-temporal gait features. The dataset for deep learning and ground truth were

collected from seven IMUs and motion capture and force plate systems, respectively, with multiple 5 m walk protocols at various speeds. Another challenge related to machine learning is the availability of dataset.

**Online and real-time data processing for wearable-based quantitative gait analysis.** We found several studies that implemented online or real-time data processing as discussed in Section 2.3-E. The vast development in computing power has enabled an easier implementation of online and real-time data processing. This gives several advantages for both the general wearable users or for patients and clinicians if it is implemented in clinical settings. For example in sports applications, real-time data processing enables the user to directly reflect and possibly correct their action in real-time for motion improvement based on the provided real-time insights. In the clinical setting, a real-time visualization is favored as real-time insights for both patients and clinicians. Real-time data processing also enables real-time feedback to the user that may act as an intervention in the case of the occurrence of freezing of gait (FoG) in PD patients. Nevertheless, implementation of online or real-time data processing may face a problem such as data package loss while transmitting data to the processing unit and thus have to be validated first to ensure the accuracy of the extracted gait features.

**Slow walking speed and its effect to performance of algorithms**

In some of the studies, we observed that the performance of stride detection was decreased in a slow walking speed. For example this study reported a 97.8 % mean accuracy on 1.0 km/h speed, while 99.9 % detection was observed from speed 1.5 - 4.0 km/h [96]. Another example is shown by ICC metric, where slow walking speed produced the lowest ICC value compared to comfortable and maximum walking speed [108]. A further design and evaluation of algorithms are needed to accommodate slower walking speed for gait analysis in elderly group.

**Issues related to experiment protocols.**

Each of the studies proposed a variety of experimental protocols. Most of it can be simplified and referred to a 'level ground walking' either performed in a laboratory, long corridor, or outdoor setting. Pragmatically, a longer walkway is more suitable to capture the natural gait of a subject as it gives a proper time and distance for the subject to adjust their walking as they preferred. This study [116] has concluded that a minimum of 25 and 33 strides are needed to properly compute step symmetry and stride regularity in healthy control subjects. On different experiment protocols, a study on [117] suggested that curved walking instead of straight walking is more proper to assess people with gait disorder. On the other hand, the

treadmill-based experiment may affect the natural gait of the subject. However, this study [118], [119] suggested that self-paced instead of fixed-speed allows more natural stride variability.

**Integration of wearable sensor gait analysis and feedback system**

In this review, we identified several studies that utilized certain data analysis from wearable sensors as feedback to the user in various modalities such as audio, visual, and haptic feedback [52], [61], [90], [92]. Feedback strategies are needed for gait retraining or real-time assessment to correct certain parameters in rehabilitation or sports applications. Outside the studies in this review, several progress have been made in wearable-based gait feedback system. An auditory feedback investigated in [120] was found to be effective in short-term rehabilitation for stroke patients with hemiparesis. These studies [19], [20] proposed a biofeedback system for gait and balance training in PD subjects. Another study [121] proposed a sensing sock device with smartphone-based feedback with various modalities such as combined several feedback strategies such as auditory, visual, and haptic feedback. On the comparison of different feedback modalities, a study concluded that real-time haptic feedback was found to be effective and less expensive compared to visual feedback [122] for gait retraining in runners with high tibial load. Nevertheless, the effectiveness and correctness of feedback strategies needed to be investigated further.

## 2.5 Conclusion

This chapter investigates the use of wearable sensors for quantitative gait analysis. Each of the proposed framework of wearable gait analysis identified in this review must be validated to gold standard measurement or other established sensor system to ensure the performance of measurements taken. The links between number and types of sensors along with the attachment to the body, method and algorithms used, and number and types of quantitative gait features that can be extracted, are discussed comprehensively in this review. Future directions are to explore the integration between wearable-based gait assessment and feedback system to give a real-time feedback to the users/patients. Other area is to investigate the performance and validity of wearable-based gait analysis in other clinical applications. The use of machine learning algorithms to both quantify gait features and giving certain performance scores for clinical application is also a challenge and vital needs for researchers pursuing this research field.

# Chapter 3

# Proposed framework: Two IMUs for rich gait features

## 3.1 Introduction

This chapter discussed the thesis proposition of using two IMUs for quantitative gait analysis with rich gait features.

Several gait assessment studies have been conducted considering the use of wearable sensors. We identified several state of the art on this field as summarized in Table 3.1. The first study [123] extracted step length, stride length, and gait speed using four inertial measurement unit (IMU) attached on both shanks and thighs based on inverted pendulum model, as well as three gait events, i.e. initial contact (IC), toe-off (TO), and mid-stance (MSt). Using the same number of sensors and placement, the second study [124] estimated step length while also identified three gait events, i.e. IC, MSt, and leg straightening (LS), as well as gait asymmetry feature based on double pendulum model. Model based algorithm has a set of assumptions and all parameters/ inputs must be available to perform the algorithm. Comparison of using one IMU attached on waist and two IMUs on shanks were presented in [125]. It was concluded that using two IMUs on shanks leads to better accuracy in IC, stride time and step time features. The fourth paper [126] utilized only one IMU placed on foot and successfully detect heel-strike (HS), heel-off (HO) and TO events, and derived a number of spatial/temporal features (Table 3.1). However, the experiment was done in treadmill which may disturb natural gait of participants [118], [119]. Other study [5] also investigated the use of one IMU placed on the lower back/ fifth lumbar vertebrae (L5) and derived spatial/temporal features based on step activity instead of stride. Moreover, they also derived in-

Table 3.1: Comparison of several wearable-based gait assessment

| Ref. | Sensor and Location | Gait event/ Gait phase | Spatial/Temporal features | Other gait features | Benchmark |
|---|---|---|---|---|---|
| [123] | Four gyroscopes on shanks and thighs | IC, TO, MSt | Step length, Stride length, Gait speed | - | Instrumented mat |
| [124] | Four gyroscopes on shanks and thighs | IC, MSt, LS | Step length | Gait Asymmetry | Motion camera & tape measurement |
| [125] | One IMU on waist & Two IMUs on shanks | IC, FC | Step time, stance time, stride time | Coefficient of Variation | Pressure sensing insole |
| [126] | One IMU on foot | HS, HO, TO | Stride time, stance time, swing time, stride length, walking speed, incline | - | Footswitches and calibrated treadmill |
| [5] | One IMU on lower back | IC, FC | Step time, stance time, swing time, step length, step velocity | Asymmetry and Variability Indices | Instrumented walkway |
| Proposed framework | Two IMUs on feet | IC, TO, MSw, double support (DS) | Stride time, stance time, swing time, stride length, heel vertical displacement, gait speed, %gait phase, walking distance | Symmetry Index, Asymmetry Indices, Variability Indices, Activity class, Motion Intensity | Motion capture and force plates |

dices (asymmetry and variability) that can be used for clinical purpose such as in Parkinson's disease.

Research on gait assessment has widely been conducted. Nevertheless, many studies only focused on specific features rather than presenting a rich and diverse features that potentially could be extracted. In this study, we propose a framework to assess gait comprehensively with high-range of feature diversity using wearable sensors. Comprehensive here means extracting as many gait features as it possibly can, which includes gait event and/or phases detection, spatial and or temporal parameter extraction, and other related gait features. Table 3.1 represents the difference of feature diversity between our present study and the previous state-of-art works using portable sensors on gait assessment.

Table 3.2: Characteristics of participated subjects

| Subject | Age (years) | Height (cm) | Weight (kg) | Injury | Participation |
|---|---|---|---|---|---|
| S01 | 24 | 176 | 75 | No | benchmark, walkway |
| S02 | 23 | 178 | 70 | No | benchmark, walkway |
| S03 | 26 | 167 | 78 | No | benchmark, walkway |
| S04 | 23 | 166 | 57 | No | benchmark, walkway |
| S05 | 25 | 170 | 71 | No | benchmark |
| S06 | 42 | 177 | 78 | Yes | benchmark |

The rest of this chapter is organized as follows. Section 3.2 discussed about our proposed framework, experiments, and methods used in this study. Results and discussions are presented in Section 3.3, which covers agreement between our proposed framework and lab-based measurement, overall quantitative gait assessment results, and comparison to several related study. Finally, Section 3.4 concludes the study and provides direction of future research regarding this topic.

## 3.2 Methods

### 3.2.1 Subjects

Six subjects participated in the study with a mean age of 27.2±7.4 years and mean height of 172.3±5.3 cm and mean weight of 71.5±7.9 kg. Five of subjects reported that they have no severe lower limb related injuries in the past year, while one subject reported that he had injury on left foot and had performed a surgery regarding the injury five months prior to the experiment. Details of participated subjects are depicted in Table 3.2. All subjects had given informed consent prior to participation to this experiments.

### 3.2.2 Data collections

All subjects wore two IMU (Trigno Research+, Delsys, MA, USA) wireless systems on the back of the shoes as presented in Fig. 3.1. We selected this location

as it was found to be the second best position in terms of accuracy for detecting the stride number [84]. We picked this location mainly for the purpose of practicality and convenience for the subjects, while also considering the accuracy results from the reference study. On the preliminary experiment of the reference study, the second best position outperformed all of other locations with 100% accuracy on detecting stride number based on accelerometer (compared to 96% accuracy from the best position). When tested to larger datasets (15 subjects) the accuracy was comparable to the best position, i.e. 93.60% for the best position vs. 93.20% for the 2nd best. In terms of convenience and practical issue, we think that placing it on the back of the shoes is the best option because we could reduce relative movement of the sensors without sacrificing the convenience of the subject that could alter their gait. If we were attaching it on the best position, we would need to make sure we attached the sensors securely with a Velcro belt that could be inconvenience to the subject and may alter their gait. In this study, the 3-axis accelerometer and 3-axis gyroscope data alone from each foot were considered. Motion capture system (Optitrack, NaturalPoint, OR, USA) and force plates (AMTI, MA, USA) were also used for benchmark experiment to assess the performance of the proposed system. The sampling rate of the IMU sensors was set at 148 Hz, whereas the motion capture system and force plate were sampled at 100 Hz and 1,000 Hz, respectively. IMU and force plate were down-sampled to 100 Hz for consistency of data analysis. All the collected data were processed for analysis using MATLAB (Mathworks Inc., Natick, MA, USA).

### 3.2.3 Experiment protocols

We developed two experiment protocols to assess the performance of our proposed methods. Experiments were divided into two stages, namely, benchmark and walkway experiments. The protocols and objectives for each experiment are described as follows.

#### 3.2.3.1 Benchmark experiment

Subjects were instructed to walk back and forth in a confined space defined by the area of motion capture system for 10 repetitions. Subject were instructed to adjust their walking speed to their own convenience and were encouraged to step their foot onto the force plate. These instructions were chosen owing to the fact that the capture area of the motion capture system was small thus the longest straight walking could only be 4.5 m. For this reason, to perform slow, normal, and fast walking would be ineffective. Heel markers were attached on the lateral side of each

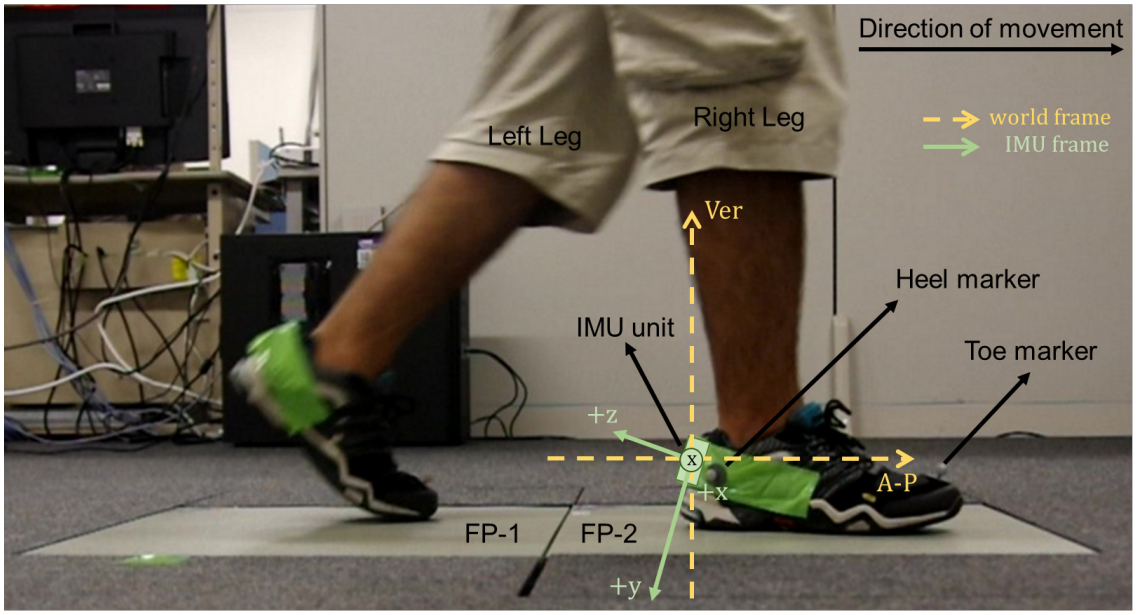


(a)

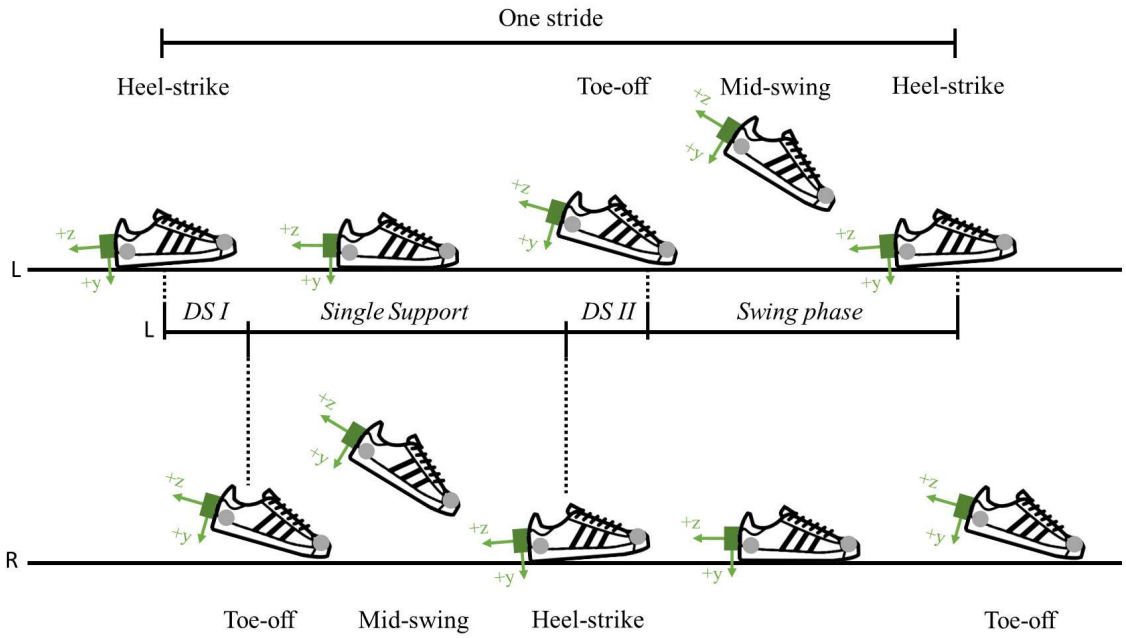


(b)

Figure 3.1: (a) Experiment setup of our proposed framework, where IMU unit is attached on the back of the shoe. Two markers attached on heel and toe, and two force plates (FP-1 and FP-2) were used for benchmark experiment. IMU frame is transformed to world coordinates that consisted of vertical direction (Ver) and antero-posterior direction (A-P) for spatial features calculation. (b) Graphical presentation of IMU sensor placement (green box), marker placement (gray dot), and gait events and phases representation on both L(Left) and R(Right) foot.

shoe, while toe markers were attached on the upper-front side of each shoe. The purpose of this experiment was to compare the performance of proposed framework in terms of gait event detection, as well as spatial/temporal parameters, with the ground truth, using a gold standard measurement from the motion capture and force plate system.

#### 3.2.3.2 Walkway experiment

Subjects were instructed to walk back and forth in a longer distance of 12 m for six repetitions at their own self-selected speed. The purpose of this experiment was to allow the subjects to walk more naturally, thereby providing an accurate assessment of each subject's natural gait.

### 3.2.4 Quantitative gait assessment

This section explains the overall procedure of the quantitative gait assessment (QGA) proposed in this study. As mentioned earlier, we used only two IMUs attached on the back of the shoes of each subject. Raw data from the IMU sensors were filtered using a 4th order Butterworth low pass filter with a cut-off frequency of 6 Hz. Following the filtering process, the data were processed according to the extracted gait features. The list of extracted features is presented in Table 4.1.

#### 3.2.4.1 Gait Event Detection

Gyroscope data were used to estimate three major gait events, i.e. initial contact (IC), toe-off (TO), and mid-swing (MSw). A heuristic-threshold based algorithm was constructed to detect these gait events. IC and TO were defined as the local maxima, whereas MSw was defined as the local minima detected from the gyro data. We set threshold of angular velocity, $\omega_n$, 30 deg $/s$ and -120 deg $/s$ as the starting point to search for local maxima and local minima for IC, TO and MSw events detection, respectively. These values were based on the observational study during benchmark experiment. Flowchart of event detection is depicted in Fig. 3.2.

We computed angular acceleration, $\alpha_n$, based on $\omega_n$ difference. When a local minimum is detected, marked by the change of sign in $\alpha_n$, and $\omega_n$ is under the specified threshold of -120 deg $/s$, we marked the data sample as MSw and hold the value of 1 in $msw$ variable. Meanwhile, when a local maximum is detected, also marked by the change of sign in $\alpha_n$, and $\alpha_n$ is greater than the specified threshold of 30 deg $/s$ and $msw$ value is 1, then we marked the data sample as IC and reset

Table 3.3: Overall extracted features

| Features ($f$) | Unit | Description |
|---|---|---|
| Stride time | $s$ | Time needed to complete one gait cycle (IC to IC) |
| Stance time | $s$ | Time elapsed when foot is in contact with the ground |
| Swing time | $s$ | Time elapsed when foot is not in contact with ground |
| Stride length | $m$ | Distance of one gait cycle |
| Heel vertical displacement | $m$ | Estimated maximum height of heel during swing phase |
| Gait speed | $m/s$ | Averaged walking speed of the subject |
| Walking distance | $m$ | Total distance covered by subject |
| Gait phase | % | Percentage of average gait phase consisted of iDS, SS, tDS, SW |
| Symmetry Index | dimensionless | Symmetry feature based on stance time |
| Asymmetry Indices | multi | Various indices based on the absolute mean difference between sides (L&R) |
| Variability Indices | multi | Various indices based on standard deviation of certain features |
| Activity class | dimensionless | 0 for other activities, 1 for walking, 2 for turning |
| Motion intensity | $g$ | Intensity of motion based on magnitude of acceleration |

the $msw$ value as well as hold the value of 1 in $ic$ variable. Otherwise, if there is another local maximum detected and $ic$ value is 1, then we marked it as TO and reset the $ic$ value and hold the value of 1 in $to$ variable.

#### 3.2.4.2 Activity class

In this part of the study, we introduced three activity classes named walking, turning, and others class, to easily distinguish certain movements performed by the subjects. Certain thresholds were defined to construct a finite state machine (FSM) transition rule between the activity classes, as depicted in Fig. 3.3 (a). The movement performed will fall under 'walking' class if there are sequences of IC event detected. As two IMUs were used, the inner-class states could detect separately between left and right events, thus could lead to more detailed double support analysis in walking class. Terminology of inner-class states is represented in Fig. 3.3 (b), whereas the inner-class transition rules are presented in flowchart in Fig. 3.2. On the other hand, if there is a significant change, defined as a threshold of 250 deg $/s$, in longitudinal angular velocity in both of feet, movement will be categorized to 'turning' class. In this study, we classify turning as a class to record the changing of direction of the subjects and also to avoid inaccurate gait event detection and further spatio/temporal features calculation during transition to non-gait activity. Any movement performed that did not satisfy any of the above described states was classified as the 'others' class.

#### 3.2.4.3 Temporal features

Temporal features were derived based on gait event detection. Stride time was calculated by the time difference between detected ICs. Stance time was calculated by the time difference between detected TO and detected IC before the respected TO event, while swing time was calculated by the time difference between the detected IC after TO event and the respective TO event itself. Double support was estimated from the detection of IC of left side to the detection of TO of right side and vice versa. Initial and terminal double support, $iDS$ and $tDS$, are interchangeable terms depending on the reference side. These descriptions are interpreted in Equation 3.2.1 to 3.2.5, where subscripts $i$, $L$ and $R$ are index of detected event, Left, and Right, respectively.

More over, we also present these temporal features in gait phase represented by percentage of each phase. Here we divided gait into four phases, consisted of iDS, SS, tDS, and SW, where SS and SW are single support and swing phase, respectively.

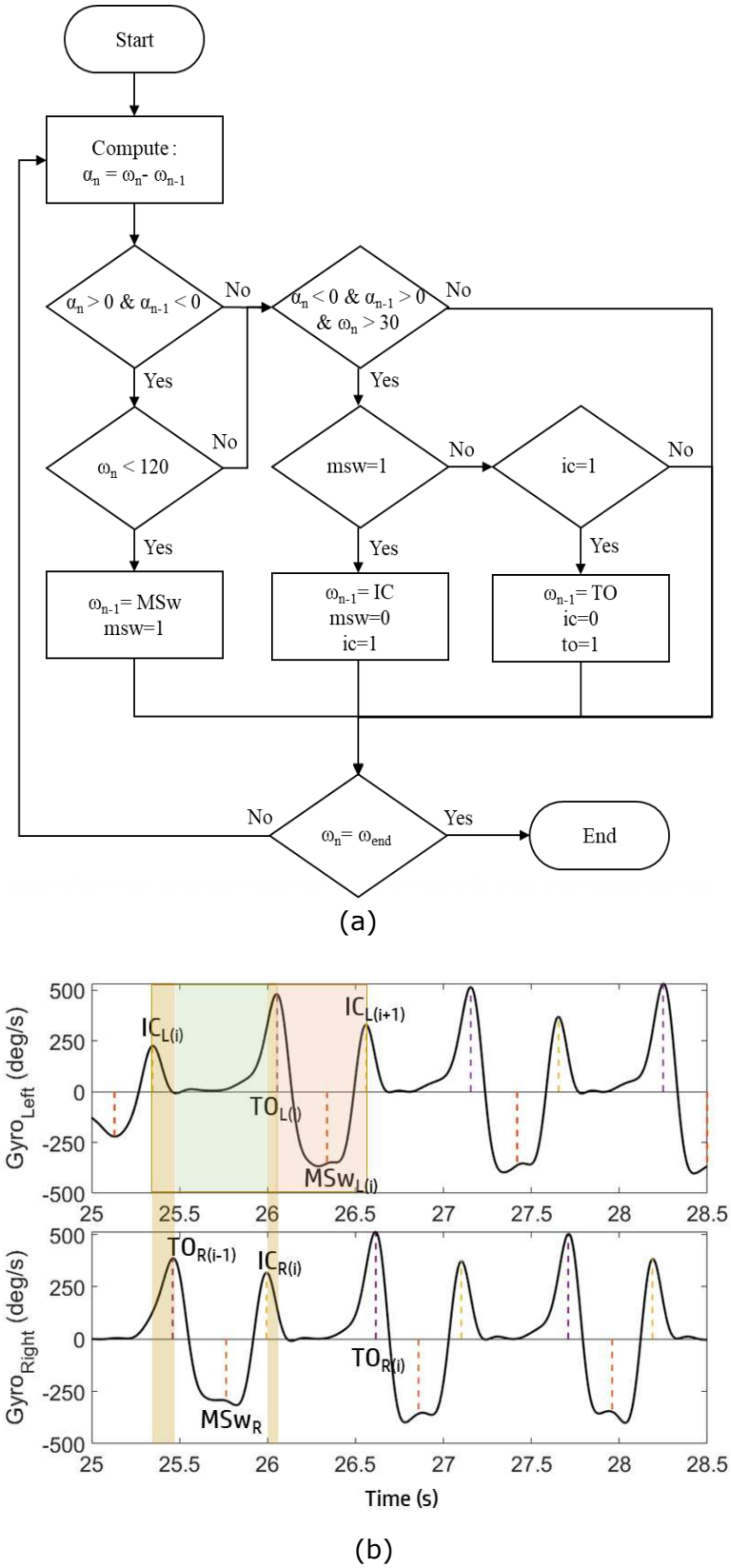


Figure 3.2: (a) Flowchart of gait event detection based on gyroscope data on the back of the shoes. (b) Example of gyro data used for gait event detection. Dashed line indicates IC, TO, and MSw events. Shades indicate gait phases (yellow: double support, green: single support, red: swing).

$$stride\ time = IC_{i+1} - IC_i \tag{3.2.1}$$

$$stance\ time = TO_i - IC_i \tag{3.2.2}$$

$$swing\ time = IC_{i+1} - TO_i \tag{3.2.3}$$

$$iDS_L = tDS_R = TO_R - IC_L \tag{3.2.4}$$

$$iDS_R = tDS_L = TO_L - IC_R \tag{3.2.5}$$

#### 3.2.4.4 Spatial features

Spatial parameters were extracted from the combination of accelerometer and gyroscope data. We calculate stride length in quaternion system. Raw data from IMU sensor that are recorded in Euler angles, were transformed into quaternion. Accelerometer was rotated into Earth's frame and gravity component was compensated by subtracting transformed accelerometer data that is perpendicular with ground with $g$, where $g$ is gravitational acceleration equal to 9.8 $m/s^2$. We followed a gradient descent algorithm [127] to estimate position based on IMU on quaternion system. This algorithm also include a magnetic distortion compensation algorithm and proven to reduce computational load. Further, we used a similar double integration method with [126], [128] to estimate velocity and lastly derived position. In this study, stride length is calculated per direction of walking to better estimate and avoid non-walking class data. On the other hand, we also introduced an estimation of heel vertical displacement (HVD) based on the transformed acceleration data to earth frame on vertical direction.

#### 3.2.4.5 Other gait features

We also derived other gait features based on the extracted spatial and/or temporal features. Symmetry Index (SI) is a derived feature from stance time of both sides. We averaged total stance time of left side to right side for every walking class per experiment performed. Minus sign in SI indicates an overall less stance time on left side while positive sign indicates an overall less stance time on right side. Motion Intensity (MI) [129], [130], is a derived feature from the magnitude of the accelerometer data, which relates to the intensity of certain movement performed by the subject. Furthermore, it could be used to assess the difference of intensity between left and right side of the foot.

Additionally, we also extract Asymmetry Indices (AIs) and Variability indices (VIs) as studied in [5]. AIs are various indices based on the comparison of absolute

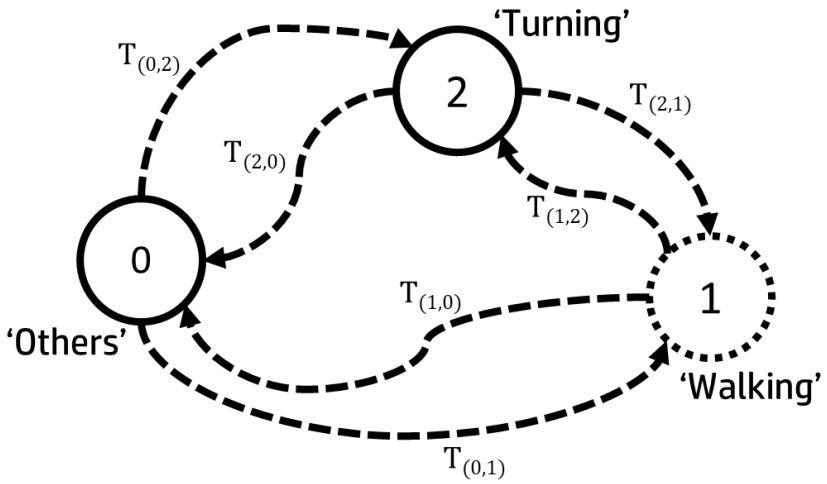


$$T_{(1,0)} = T_{(2,0)} \Rightarrow \nexists\{T_{(0,1)}, T_{(0,2)}\}$$

$$T_{(0,1)} = T_{(2,1)} \Rightarrow IC_{t-1} = IC_{t-2} = \ldots = IC_{t-n} = 1, \textit{ for } n \geq 3$$

$$T_{(0,2)} = T_{(1,2)} \Rightarrow (\omega_{y(L)} \,\&\, \omega_{y(R)}) > \text{threshold}$$

(a)

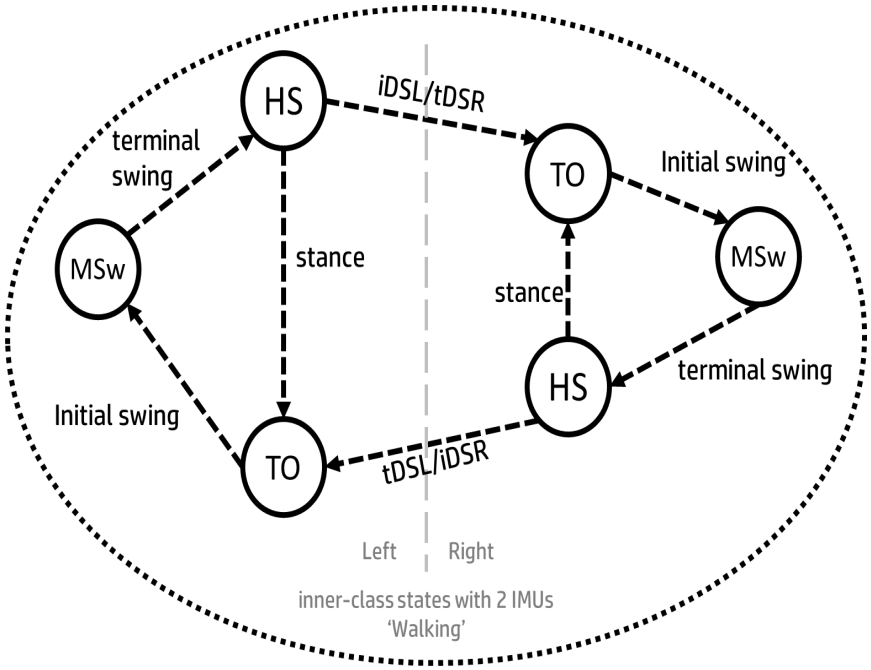


(b)

Figure 3.3: (a) Activity class transition rules (b) Notation of inner-class states that could be recognized using the proposed framework.

mean difference between left (L) and right (R) side. These AIs could potentially give important information about subject specific tendency of using left and right foot in gait. VIs are features derived based on standard deviation. These features can provide an insight into the variability found on certain spatial/temporal features. SI, AI, VI, and MI are formulated in Equation 3.2.6 to 3.2.9, where $n$ and $f$ are number of gait cycle detected and spatial/temporal features, respectively. For example if $f$ is stance time, then $AI_f$ will be $AI_{stance}$ where we calculate mean absolute error of stance time between left foot and right foot.

$$SI = \frac{\sum_1^n stancetime_L}{\sum_1^n stancetime_R} - 1 \tag{3.2.6}$$

$$AI_f = |mean(f_L) - mean(f_R)| \tag{3.2.7}$$

$$VI_f = S.D(f) \tag{3.2.8}$$

$$MI = |a| = \sqrt{{a_x}^2 + {a_y}^2 + {a_z}^2} \tag{3.2.9}$$

## 3.3 Results and Discussions

We asked each of the participants about their perception of their gait during the experiment. Their responses have been summarized in Table 4.2. S02 and S05 stated that, during the benchmark experiment, they walked slower than normal, while other subjects stated that they perceived their gait as normal. As we only used two force plates, we encouraged all subjects to step on it every time they walked by. Only one participant, S04, declared that they did not need to adjust their steps on the force plate. Meanwhile on walkway experiment, all participated subjects stated that they walked normally. These subjective perception could be used as references to interpret the results that are discussed below.

### 3.3.1 Benchmark experiment

A total of six subjects participated in this experiment. To synchronize motion capture, force plate system, and IMU sensors, all subjects performed jumping on the force plate (time was synchronized at maximum vertical acceleration from IMU and maximum vertical GRF from force plate). In addition to that, we introduced a bias correction of 0.07 s for time synchronization to IMU data based on the experiment trials. This correction factor is a lagging factor to compensate for the position of IMUs on feet that are not reflecting the acceleration of the whole body which correlates to the maximum GRF from the force plate. Further, we omitted the first

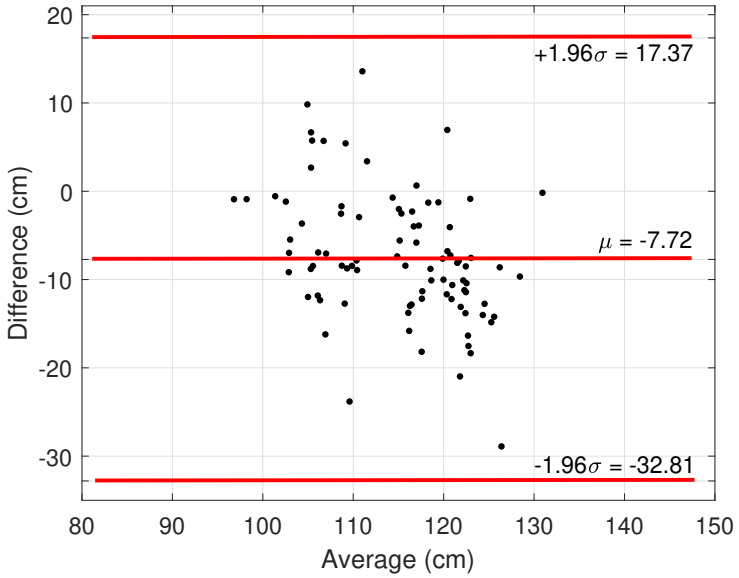


(a) Stride length

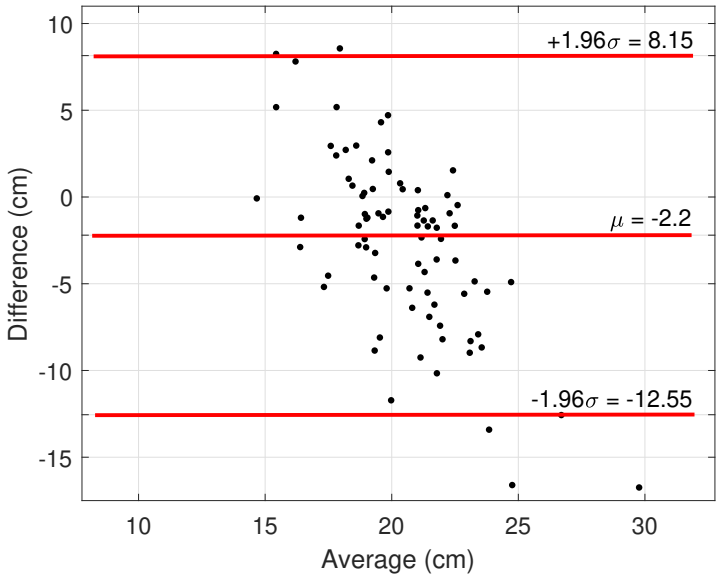


(b) Heel vertical displacement

Figure 3.4: Bland-Altman plot for spatial features. Red lines are mean and range of limit of agreement (LoA). The comparison results show that the proposed framework are within the LoA with mean of -7.72 cm and -2.2 cm for (a) stride length and (b) heel vertical displacement, respectively.

Table 3.4: Perception questionnaire

| Subject | Benchmark Experiment | | Walkway Experiment |
|---|---|---|---|
| | Perception | Step Adjusting | Perception |
| S01 | Normal | Maybe | Normal |
| S02 | Slower | Yes | Normal |
| S03 | Normal | Yes | Normal |
| S04 | Normal | No | Normal |
| S05 | Slower | Yes | N/A* |
| S06 | Normal | Maybe | N/A* |

*N/A = Not Available (subject was not participated)

Table 3.5: Summary of benchmark experiment: quantitative gait assessment

| Subject | Temporal features (s) | | | Spatial features (m) | | Gaitspeed (m/s) | Gait Phase (%) | | | | SI |
|---|---|---|---|---|---|---|---|---|---|---|---|
| | Stance time | Swing time | Stride time | Stride length | HVD | | iDS | SS | tDS | SW | |
| S01 | 0.66±0.09 | 0.45±0.09 | 1.12±0.11 | 1.25±0.05 | 0.21±0.03 | 0.98±0.22 | 6.46 | 45.71 | 6.11 | 41.72 | -0.032 |
| S02 | 0.66±0.12 | 0.50±0.08 | 1.19±0.13 | 1.26±0.05 | 0.24±0.06 | 1.00±0.10 | 6.48 | 43.33 | 7.38 | 42.81 | 0.053 |
| S03 | 0.65±0.21 | 0.45±0.15 | 1.18±0.24 | 1.12±0.04 | 0.21±0.05 | 0.89±0.15 | 8.59 | 42.27 | 8.76 | 40.39 | 0.068 |
| S04 | 0.71±0.19 | 0.48±0.12 | 1.22±0.20 | 1.19±0.06 | 0.20±0.06 | 0.93±0.06 | 8.11 | 44.10 | 8.37 | 39.42 | -0.018 |
| S05 | 0.87±0.04 | 0.60±0.03 | 1.47±0.04 | 1.09±0.06 | 0.20±0.02 | 0.63±0.17 | 12.75 | 40.48 | 8.39 | 38.38 | -0.039 |
| S06 | 0.67±0.22 | 0.48±0.15 | 1.25±0.23 | 1.11±0.05 | 0.21±0.03 | 0.85±0.13 | 9.14 | 39.77 | 8.41 | 42.77 | 0.104 |

continuous walking class until the first turning class and then started data analysis.

In terms of gait event detection reliability, the total of IC and TO events detected by force plates was 456 for all subjects. This number agrees with that obtained by our detection method based on IMU, exhibiting 100% detection rate. In total, we recorded 2286 gait events consisted of IC, TO, and MSw from all subjects during the benchmark experiment. We noticed there were a few missed or inaccurate event detection during the transition from walking to turning class and vice versa. This issue has been resolved automatically by introducing activity class, thus only IC, TO, and MSw during actual gait was recorded for analysis.

Table 3.5 summarizes a detailed gait assessment for each subject. Temporal features, spatial features, and gait speed are presented in mean ± S.D. Further more, we quantified gait phases in percentage of gait cycle, that could detail the iDS and tDS phases. Walking distance was not derived in this experiment as the walkway was short by approximately 4.5 m, and we did not explicitly instruct the subjects to follow a defined route or distance. Furthermore, for simplicity, we showed only SI among other proposed gait indices in this experiment as we focused on temporal/spatial agreement to the reference system and the comparison of our study

to various existing studies. In term of stance time, S05 had the longest stance time and also the shortest stride length compared to other subjects, which resulted in the slowest speed among all subjects. Quantitative results from S05 showed an agreement with subject perception, as depicted in Table 4.2. We confirmed that the step adjusting effort by subject influenced the gait and resulted in slower speed than normal, as observed in S05. Table 3.5 indicates that the largest deviation of SI (SI=0.104 or 10.4%) was found in S06. This finding was also correlated with the reported condition of S06 having lower limb injury.

Table 3.6 summarized the agreement of benchmark experiment results of each participated subject to the reference system. Temporal and spatial differences between IMU and motion capture-based measurements are calculated in terms of mean and standard deviation. The negative sign indicates an early detection of temporal features and an overestimation of spatial features, while the positive sign indicates a late detection of temporal parameters and an underestimation of spatial features.

Table 3.6 indicates that there was a 4.22±15.48 ms delay of IC detection and 8.31±21.02 ms early TO detection on average from all subjects. The lowest averaged temporal difference for IC and TO events was 1.32 ms and -0.31 ms observed from S02 and S05, respectively. On the other hand, we observed lowest temporal difference variability of 6.23 ms and 6.42 ms for IC and TO event from S02 and S01, respectively. Both lowest temporal differences and temporal differences variability are within one sampling time interval ($t_s = 0.01s$). We observed that the variability of gait event timing for each subject is dependent on sensor placement and data filtering as has been reported in [84].

For spatial features comparison with motion capture system, we observed that our proposed method tends to overestimate by an average of 7.72±12.8 cm for stride length and 2.22±5.28 cm for estimated HVD, as summarized in Table 3.6). We observed the best overall agreement of spatial features in S05 where stride length and HVD are -0.59±6.69 and 1.16±1.66, respectively. Fig. 3.4. showed bland-altman plot on spatial features. It could be seen that mean level of all spatial features from all participated subject showing a minus sign, thus our proposed method on extracting spatial features showed a trend to overestimate spatial features.

Even using two IMU sensors, we confirm that temporal feature could be well identified compared to motion capture system with minor temporal differences. The spatial feature has some gaps due to the measurement accuracy difference compared to the global measurement system, however IMU-based stride length estimation can still capture the relative change of the gait, while having absolute spatial errors.

However, in terms of HVD estimation, our proposed method suffered from inaccurate estimation that could reach 30% in terms of absolute error, even though we have implemented a linear correction algorithm based on all of the recorded gait data from all of the subjects. In our proposed method, for computational efficiency purposes, we estimated stride length and HVD in the same computation batch with IC as starting point. We found this became one of the factor contributing to the estimation error in HVD, as it should have been started from heel-off event instead of IC.

Furthermore, we compared our detection results with those of various existing studies in terms of temporal feature, as depicted in Table 3.7. Our results in IC detection performed better than all of previous studies, while TO detection performed better than [125], [126], [131], [132]. To conclude, we have demonstrated that our proposed method provides an acceptable performance compared with those of various existing studies.

Table 3.8 compares our spatial features result with those of existing studies. Using four gyroscope and inverted pendulum model (IPM), as studied in [123] resulted in better estimation compared to reference system. In [84], the mean accuracy using the similar double-integration method as presented in this study was more than 90%, compared to our study which is 93.23 % of mean accuracy. A study on [133] also used the double-integration method with better accuracy and precision of 2 cm and 5 cm, respectively. The difference was sensor location (dorsum of foot) and the integration method that started from foot-flat event to next foot-flat event. Even though this location and method performed better in estimating stride length, it may not be suitable for determining gait events or stride number as shown on this study [84]. A study on [134] used a deep-learning algorithm to estimate stride length, yet it took around 20 minutes per fold to train and a minimum of 4000 iterations to reach a stable error with precision, as shown in Table 3.8.

### 3.3.2 Walkway experiment

A total of four subjects agreed to participate in the walkway experiment. This experiment focused on presenting subject-specific gait features that had been extracted using our proposed framework. Table 3.9 shows an overall QGA based on our proposed framework.

We observed that all subjects took shorter time to complete a gait cycle, as seen from an overall less stride time in all subjects, compared to previous benchmark experiment. We also observed a longer stride length from all subjects compared

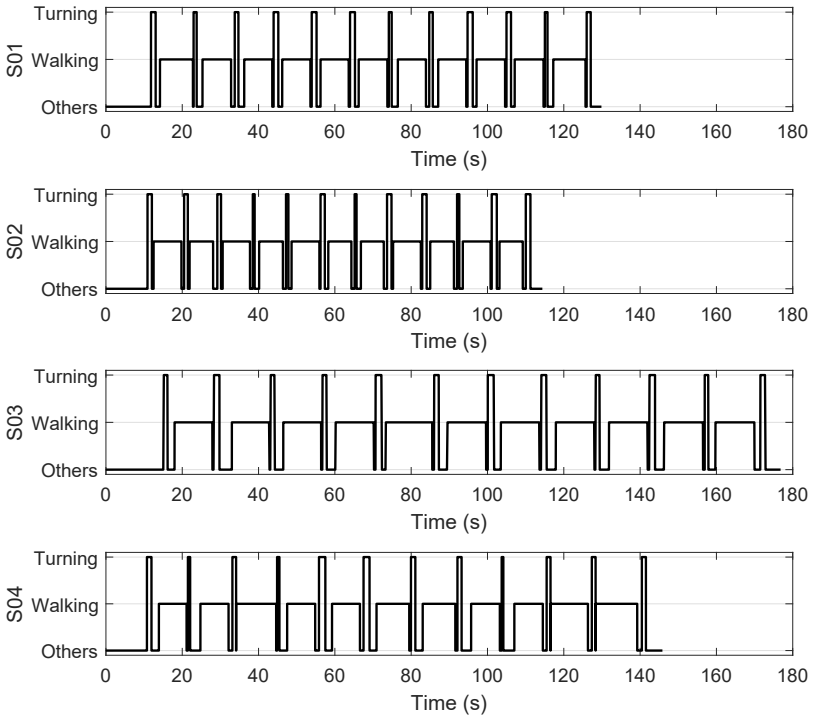


(a)

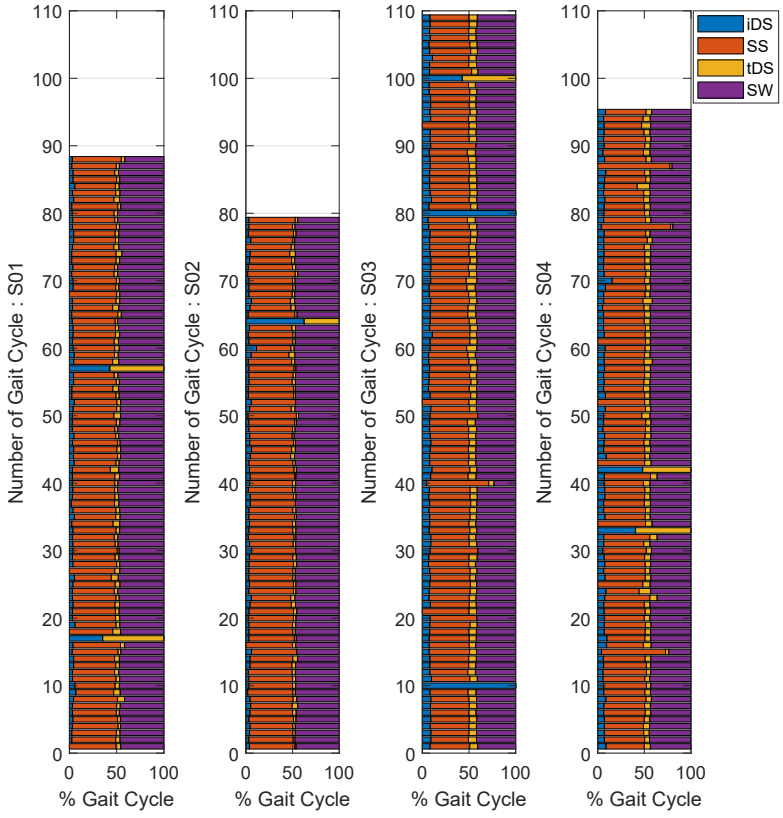


(b)

Figure 3.5: Results from walkway experiment from all participated subjects, presented with same scale of time and number of gait cycle (a) activity class (b) number of gait cycles and detailed percentage of gait phases.

Table 3.6: Benchmark experiment : Agreement to reference system

| Subject | Temporal Differences (ms) | | Spatial Differences (cm) | |
|---|---|---|---|---|
| | IC | TO | Stride length | HVD |
| S01 | 9.74±8.54 | -4.21±6.42 | -9.59±4.56 | 0.27±3.50 |
| S02 | 1.32±6.23 | -15.53±8.91 | -11.66±4.69 | -4.32±6.00 |
| S03 | 9.25±15.09 | -15.50±43.2 | -8.24±26.5 | -3.54±6.24 |
| S04 | 13.16±6.62 | -7.63±10.76 | -2.90±6.44 | -5.08±5.50 |
| S05 | 22.12±12.18 | -0.30±7.70 | -0.59±6.69 | 1.16±1.66 |
| S06 | 12.89±7.68 | -14.21±6.83 | -10.93±5.73 | -0.59±3.59 |
| Average | 4.22±15.48 | -8.31±21.02 | -7.72±12.8 | -2.22±5.28 |

data is presented in mean±S.D

Table 3.7: Benchmark experiment : Temporal differences comparison to existing studies presented in mean±S.D.

| Ref. | Sensor/ Location | Subjects | IC (ms) | TO (ms) |
|---|---|---|---|---|
| [125] | 1 IMU (Gyro.)/ shank | 10 | 12±11 | 51±21 |
| | 1 IMU(Gyro.+Acc.)/ L5 | 10 | 46±20 | 76±21 |
| [126] | 1 IMU(Gyro.)/ foot | 5 | 70±N/A | 35±N/A |
| [131] | 2 Acc./ below knee | 15 | 34±25 | 19±36 |
| [132] | 1 Gyro./ shank | 7 | -8±9 | 50±14 |
| [135] | 1 Gyro./ shank | 9 | -16.6±11.9 | 3.7±26.5 |
| Present Study | 1 IMU(Gyro)/foot | 6 | 4.22±15.48 | -8.31±21.02 |

N/A = Data not available ; Acc.=Accelerometer ; Gyro.=Gyroscope

to previous benchmark experiment. The walkway experiment was performed in a longer and wider space than the benchmark experiment, thus the walking distance was longer and the gait cycle time was shorter as subject tended to move in a more dynamic walking style. This slight change in walking style was well observed in our proposed method, which is a very important result as it demonstrates that the proposed method can accurately quantify the change of the gait under different environments. We can also note that both iDS and tDS time from all subjects were decreased in this experiment. This indicates that the subjects walks faster than during the benchmark experiment, which can be also observed in the gait speed feature.

We calculated the total walking distance covered by the subject based on stride length feature. We found that from 11 walking trials per subject in a 12 m walkway

Table 3.8: Benchmark experiment : Stride length comparison to existing studies presented in mean±S.D.[cm] (%Accuracy)

| Ref. | Sensor/Location/Method | Subjects | Stride Length |
|---|---|---|---|
| [123] | 4 Gyro./ shanks&thighs/ IPM | 11 | -2.7±N/A (N/A) |
| [84] | 1 IMU/ foot/ Double-integration | 15 | N/A (≥90.00) |
| [134] | 1 IMU/ foot/ Deep-learning | 15 | 4.11±3.57 (N/A) |
| [133] | 1 IMU/ foot/ Double-integration | 10 | 2±5 (N/A) |
| | 2 Gyro./ shanks/ SPM | 15 | -25.8±7.6 (N/A) |
| [136] | 2 Gyro./ shanks/ DPM | 15 | 3.8±6.6 (N/A) |
| | 3 Gyro./ shanks&thigh/ DPM | 15 | -0.2±8.4 (N/A) |
| Present Study | 1 IMU/foot/Double-integration | 6 | -7.72±12.8 (93.23) |

N/A = Data not available ; Gyro.=Gyroscope

resulted in 11.92±1.07 m total distance covered per trial, with 95% confidence interval (CI) of [11.61,12.24]. This confirmed that the accuracy of the proposed method for estimating stride length is the actual distance of 12 m with a 95% CI. In terms of SI, we observed a good symmetry from all subject, -0.03<SI<0.005, or not greater than 3% deviation from perfect symmetry (SI=0). In Table 3.9, we also verified AI and VI features based on all temporal features. Since two IMUs were used, we could detail the analysis for both left and right side of the foot based on these indices.

Fig. 3.5 shows activity class and detailed percentage of gait phases during walkway experiment. We presented the same scale of time and detected gait cycle to facilitate graphical comparison between subjects. Following the same protocols and overall walking distance, we observed that S02 was the fastest to complete this experiment, while S03 was the slowest. To further compare results between these subjects, we looked at number of stride (Fig. 3.5), stride length, stride time, double support phase, gait speed, and also MI (Table 3.9) to clearly see the differences. In Fig. 3.5 (b), we could observed that sometimes SS and SW is not detected and only show iDS and tDS. This occurrence happened not because of error in event detection, but merely shows a brief moment after turning, when both legs are on the ground, before the subject continue to walk. Furthermore, we could also correlate these result further with physical characteristics of the subject as presented in Table 3.2, thus generating a detailed gait assessment.

In terms of speed coverage, range of speed are 0.63-1.00 m/s and 1.15-1.49 m/s for benchmark experiment and walkway experiment, respectively. Average transition speed from walking gait to running gait is around 2.00 m/s [137]. In that case

Table 3.9: Summary of walkway experiment : Subject-specific QGA

| QGA | S01 | S02 | S03 | S04 |
|---|---|---|---|---|
| Stance time (s) | 0.56±0.09 | 0.54±0.07 | 0.65±0.26 | 0.61±0.19 |
| Swing time (s) | 0.48±0.08 | 0.47±0.06 | 0.45±0.11 | 0.45±0.08 |
| Stride time (s) | 1.05±0.09 | 1.02±0.07 | 1.13±0.25 | 1.08±0.19 |
| Stride length (m) | 1.50±0.08 | 1.54±0.16 | 1.30±0.07 | 1.46±0.12 |
| HVD (m) | 0.13±0.09 | 0.35±0.29 | 0.18±0.13 | 0.25±0.19 |
| Gait speed (m/s) | 1.42±0.08 | 1.49±0.17 | 1.15±0.08 | 1.36±0.15 |
| Walking dist. (m) | 134.03 | 115.44 | 142.5 | 132.67 |
| iDS (%) | 3.58 | 3.86 | 8.06 | 6.63 |
| SS (%) | 45.04 | 46.61 | 43.07 | 45.71 |
| tDS (%) | 4.35 | 2.91 | 7.45 | 6.23 |
| SW (%) | 47.03 | 46.62 | 41.43 | 41.42 |
| SI | -0.029 | -0.010 | 0.005 | -0.018 |
| $AI_{stance}$ (s) | 0.016 | 0.005 | 0.007 | 0.005 |
| $AI_{swing}$ (s) | 0.014 | 0.000 | 0.005 | 0.001 |
| $AI_{stride}$ (s) | 0.003 | 0.003 | 0.001 | 0.009 |
| $VI_{stance}$ (s) | 0.016(L)<br>0.021(R) | 0.011(L)<br>0.016(R) | 0.017(L)<br>0.016(R) | 0.020(L)<br>0.027(R) |
| $VI_{swing}$ (s) | 0.012(L)<br>0.011(R) | 0.011(L)<br>0.012 (R) | 0.009(L)<br>0.010(R) | 0.009(L)<br>0.010(R) |
| $VI_{swing}$ (s) | 0.029(L)<br>0.029(R) | 0.021(L)<br>0.027(R) | 0.021(L)<br>0.020(R) | 0.023(L)<br>0.034(R) |
| $MI_{swing}$ (g) | 2.02±0.14(L)<br>2.03±0.18(R) | 2.19±0.13(L)<br>2.12±0.16(R) | 1.83±0.13(L)<br>1.72±0.13(R) | 2.08±0.31(L)<br>1.98±0.26(R) |

we have covered and tested our proposed framework for roughly 0.63-1.49 m/s of walking speed and showed the accuracy and performance comparison to existing studies.

## 3.4 Conclusion

We have investigated our proposed framework of quantitative gait assessment keeping a feature-rich diversity using only two IMU sensors. By decreasing numbers of sensors, we need to sacrifice the performance of gait assessment. Through the comparison to motion capture system and existing studies, we have verified the potential and the limitation of our proposed framework toward compact sensing system but with feature-rich diversity on gait assessment. We have successfully derived major gait events, IC, TO, and MSw, and gait phases that can provide detailed double support analysis in initial and terminal phases. The agreement of IC and TO events compared to lab-based motion capture and force plate system were 4.22±15.48 ms delay on IC detection and -8.31±21.02 ms early on TO detection, respectively. Meanwhile, for spatial features, our proposed approach tend to overestimate by an average of 7.72±12.8 cm for stride length and 2.22±5.28 cm for estimated HVD. We also discussed a detailed comparison to various existing studies and found trade-offs in performance between number of sensors used, sensor placement, and algorithms to extract spatial/temporal features. While our proposed framework (number of sensor+sensor placement+algorithms) could not achieve better performance in terms of all spatial/temporal features, we demonstrated that for some features, it performed better than some existing studies and generally could maintain a good accuracy. Moreover, we have successfully detailed iDS and tDS phases that could be employed for gait research. We also showed that preliminary validation presented in this study could clearly distinguished normal subjects and subject with a recent history of lower limb injury based on the SI, therefore indicates a potential use for clinical research. Detecting asymmetricity is an essential QGA for stroke patients or patients who use prosthetic leg. Another factor to be noted is the time spent for preparation, which can be significantly reduced using only two sensors. This provides an advantage for clinical purposes as we can not spend much time for patients in practical scenarios. Based on the results of the walkway experiment, we are confident that this framework can be implemented to monitor gait in a free-living environment, thus assessing the subject with their natural gait without space limitation. However, HVD estimation error could reach 30%. An advanced correction algorithm and/or different estimation method are needed to resolve this error. Even though we have successfully tested our proposed framework for roughly 0.63-1.49 m/s of walking speed, there are some slower and faster walking speed that we have not covered. For this reason, a better benchmark experiment that could incorporate slow, normal, and fast walking instruction could be done in the future to cover all possible walking speed. Another future works for this study would be testing our proposed approach for online application as well as testing it for wider

audiences and combining the approach with other computational frameworks [138] to expand the range of application toward general motion assessment.

# Chapter 4

# Case studies using the proposed framework

This chapter further extends the application of the wearable-based quantitative gait analysis framework proposed in this thesis. Three case studies of mixed gait of treadmill walking and running, cognitive dual-task gait, and prolonged outdoor subject-specific gait are presented within this chapter.

## 4.1 Mixed gait of walking and running

This section investigates the application of the proposed framework from the previous chapter to include running gait analysis on a treadmill. A treadmill-based gait analysis enables a controlled speed experiment that is useful for tracking the gait performance of subjects across various speeds. Increased treadmill speed at some point will influence the subject to change their gait from walking gait to running gait. Some studies have argued that walk-run mixture at intermediate locomotion speed leads to optimization of metabolic energy [139]. Most of the state of the arts on wearable systems for gait analysis is developing a separate analysis between those two gait modalities [11]. We found that this study [36] discussed the assessment of temporal gait parameters using a gyroscope during treadmill walking and running. But again, each of the tested speeds was captured and analyzed separately in a different data recording session.

In this section, we address this problem by introducing a framework that can incorporate both walking and running gait analysis, seamlessly by means of constructing a finite state machine (FSM) followed by detailed inner-class states in a

single data recording session. Therefore, in this section, we proposed a controlled speed experiment on a treadmill to test our proposed framework. We have previously validated the performance of our algorithm to the gold standard measurement of motion capture and force plate systems on [100]. Although it has covered a wide range of self-selected speeds, it has not fully covered controlled slower and faster-walking speeds. Therefore we also aim to see the effect of those speeds on the gait of the subjects.

### 4.1.1 Methods

**Subjects**. Four subjects participated in the study with a mean age of 24±1.4 years, mean height of 171.8±6.1 cm and mean weight of 71.5±7.9 kg. All of the subjects reported that they have no severe lower limb related injuries in the past year prior to the experiment. All subjects had given informed consent prior to participation in this experiment.

**Data collections and preprocessing**. In this study, all subjects wore two IMU (Trigno Research+, Delsys, MA, USA) wireless systems on the back of the shoes as presented in Fig. 4.1a. We selected this location as it was found to have 93 % in terms of accuracy for detecting the stride number [84]. In this study, 3-axis gyroscope and 3-axis accelerometer data from each foot were considered. The sampling rate of the IMU sensors was set at 148 Hz. All the collected data were processed for analysis using MATLAB (Mathworks Inc., Natick, MA, USA). A 4th order Butterworth low pass filter was applied to all the collected data with a frequency cut-off of 6 Hz. After the filtering process, the data is ready to be used further for our designed algorithm to extract various temporal gait features.

**Experiment protocols**. Subjects were instructed to follow a pre-defined variable speed plan on a treadmill, starting from 2 km/h to 10 km/h, where the overall tested speed is $v = 2, 4, 5, 6, 8, 10$ km/h. During the experiment, subjects were also told to stop anytime if they felt uncomfortable. The purpose of this experiment was to see the effect of walking speed on temporal gait patterns for each subject. In addition to that, a comparison between subject-specific walking and running gait was also the interest of this experiment.

**Temporal gait analysis**. This section explains the overall procedure of the quantitative gait assessment (QGA) proposed in this study. As mentioned earlier, we used only two IMUs attached on the back of the shoes of each subject. Raw data from the IMU sensors were filtered using a 4th order Butterworth low pass filter with a cut-off frequency of 6 Hz. Following the filtering process, the data were

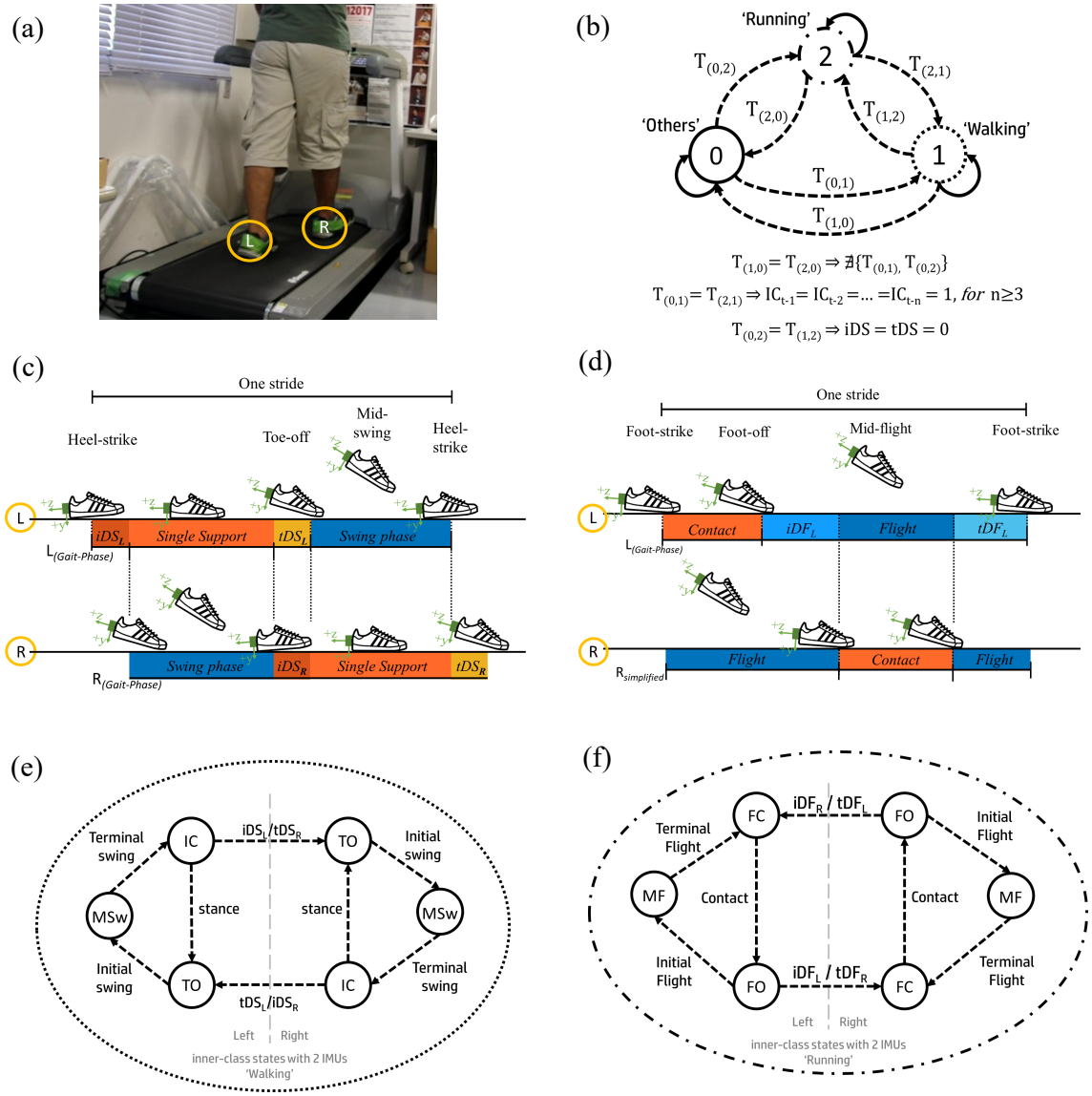


Figure 4.1: Proposed framework of seamless temporal gait analysis during walking and running on a treadmill. (a) Example of a subject following the experimental protocols of various speed treadmill walking and running with two IMUs attached on the back of the shoes. (b)The proposed FSM classes and transition rules are applied in this study. (c) Recognized gait events and phases for walking gait. (d) Recognized gait events and phases for running gait. (e) The corresponded inner class states of walking gait. (f) The corresponded inner class states of running gait.

Table 4.1: Overall extracted features

| Features ($f$) | Unit | Description |
|---|---|---|
| Gait events | - | Consists of IC, TO, MSw, for walking gait; and FC, FO, and MF, for running gait |
| Stride time | $s$ | Time needed to complete one gait cycle from IC to IC (walking/running) |
| Single Support time | $s$ | Time elapsed when one foot is in contact with the ground (walking) |
| Double Support time | $s$ | Time elapsed when both foot are in contact with the ground (walking) |
| Swing time | $s$ | Time elapsed when foot is not in contact with ground (walking) |
| Contact time | $s$ | Time elapsed when foot is in contact with ground (running) |
| Double Flight time | $s$ | Time elapsed when both foot are not in contact with the ground (running) |
| Flight time | $s$ | Time elapsed when one foot is not in contact with ground (running) |
| Gait phase | % | Percentage of average gait phase consisted of iDS, SS, tDS, SW for walking, and CP, iDF, FP, tDF for running |
| Symmetry Index | % | Symmetry feature based on stance time |
| Asymmetry Indices | s | Absolute mean difference of temporal features between sides (L&R) |
| Variability Indices | s | Various indices based on standard deviation of certain features |
| Activity class | - | 0 for other activities, 1 for walking, 2 for running |
| Motion intensity | $g$ | Intensity of motion based on magnitude of acceleration |

processed according to the extracted gait features. The list of extracted features is presented in Table 4.1.

**Gait Event Detection**. Gyroscope data were used to estimate three major gait events, i.e. initial contact (IC), toe-off (TO), and mid-swing (MSw). A heuristic-threshold based algorithm was constructed to detect these gait events. IC and TO were defined as the local maxima, whereas MSw was defined as the local minima detected from the gyro data. Our detailed heuristics algorithm is available on [100]. The same principles is applied to recognize running gait events, i.e. foot-contact

(FC), foot-off (FO), and mid-flight (MF).

**Activity class**. In this part of the study, we introduced three activity classes named walking, running, and others class, to easily distinguish certain movements performed by the subjects. Certain thresholds were defined to construct a finite state machine (FSM) transition rule between the activity classes, as depicted in Fig. 4.1a. The movement performed will fall under 'walking' class if there are sequences of IC event detected. As two IMUs were used, the inner-class states could detect separately between left and right events, thus could lead to more detailed double support analysis in walking class (Fig. 4.1b). On the other hand, if there is no initial and terminal double support detected, the movement will fall under 'running' class (Fig. 4.1c). Any movement performed that did not satisfy any of the above described states was classified as the 'others' class.

**Temporal features**. Temporal features were derived based on the extracted gait events. Since we used two IMU sensors, in this study we calculated a more detailed temporal features. Stride time was calculated by the time difference between detected ICs. Stance time was calculated by the time difference between detected TO and detected IC before the respected TO event, while swing time was calculated by the time difference between the detected IC after TO event and the respective TO event itself. Double support was estimated from the detection of IC of left side to the detection of TO of right side and vice versa. Initial and terminal double support, $iDS$ and $tDS$, are interchangeable terms depending on the reference side. Similar with walking gait, on the running gait, initial and terminal double flight, $iDF$ and $tDF$, are interchangeable terms depending on the reference side.

More over, we also present these temporal features in terms of the percentage of each gait phase. Here we divided walking gait into four phases, consisted of iDS, SS, tDS, and SW, where SS and SW are single support and swing phase, respectively. Meanwhile for running gait, we divided also into four phases, consisted of iDF, CP, tDF, FP, where CP and FP are contact phase and single flight phase, respectively.

**Other gait features**. We derived four kinds of gait indices based on the extracted temporal gait features. Symmetry Index (SI) is a derived feature from stance time of both sides. To calculate this feature, we averaged the total stance time of left side to right side for every walking or running class per experiment performed. Minus sign in SI indicates an overall less stance time on left side while positive sign indicates an overall less stance time on right side. Motion Intensity (MI) [129], [130] is a derived feature from the magnitude of the accelerometer data, which relates to the intensity of certain movement performed by the subject. Furthermore, it could

Table 4.2: Perception questionnaire

| Subjects | Comfort walking speed (km/h) | Transition speed (km/h) | Comfort running speed (km/h) |
|---|---|---|---|
| S01 | 5 | 6 to 8 | 10 |
| S02 | 5 | 6 to 8 | 10 |
| S03 | 4 | 6 to 8 | 10 |
| S04 | 4 | 6 to 8 | 8 |

be used to assess the difference of intensity between left and right side of the foot. Asymmetry Indices (AIs) are various indices based on absolute mean difference between left and right side. AIs could potentially give important information about subject specific tendency of using left and right foot in gait. Variability Indices (VIs) are derived based on standard deviation of temporal gait features. To give more specific speed-based analysis, we can further detailed SI, MI, AIs, and VIs based on speed to analyze how these indices changed over the increased speed of walking or running gait.

**Speed change detection**. In order to do a precise speed-based analysis, we introduce a speed change detection algorithm based on a simple moving average filter applied to MI data. A 20-points moving average filter, $MA_{20}$, was found sufficient to capture the changing dynamic of MI data, which highly correlated with the changing on gait speed, based on several preliminary experiment trials. We set a threshold at $75^{th}$ percentile of the difference in $MA_{20}$ value to determine if speed is constant or in transition. If $MA_{20}$ crossed the threshold value, we marked it as 'transition' state, while if it was under we marked it as 'constant' speed state.

### 4.1.2 Results and Discussions

We asked each of the participants about their perception of their gait during the experiment. Their responses have been summarized in Table 4.2. This will help us to compare the perception of subjects and actual data-based results. In terms of the agreement to gold standard measurement, our framework in this study has been benchmarked to motion capture and force plate system as well as compared to various existing studies. The detailed discussion on this issue is out of the scope of this study but is extensively discussed on previous chapter [100]. In the benchmark study, the temporal difference to force plate system were 4.22±15.48 ms (mean ± S.D.) and -8.31±21.02 ms (mean ± S.D.) for initial/foot contact and toe/foot-off events, respectively. Thus, in other words, we have verified that the accuracy of

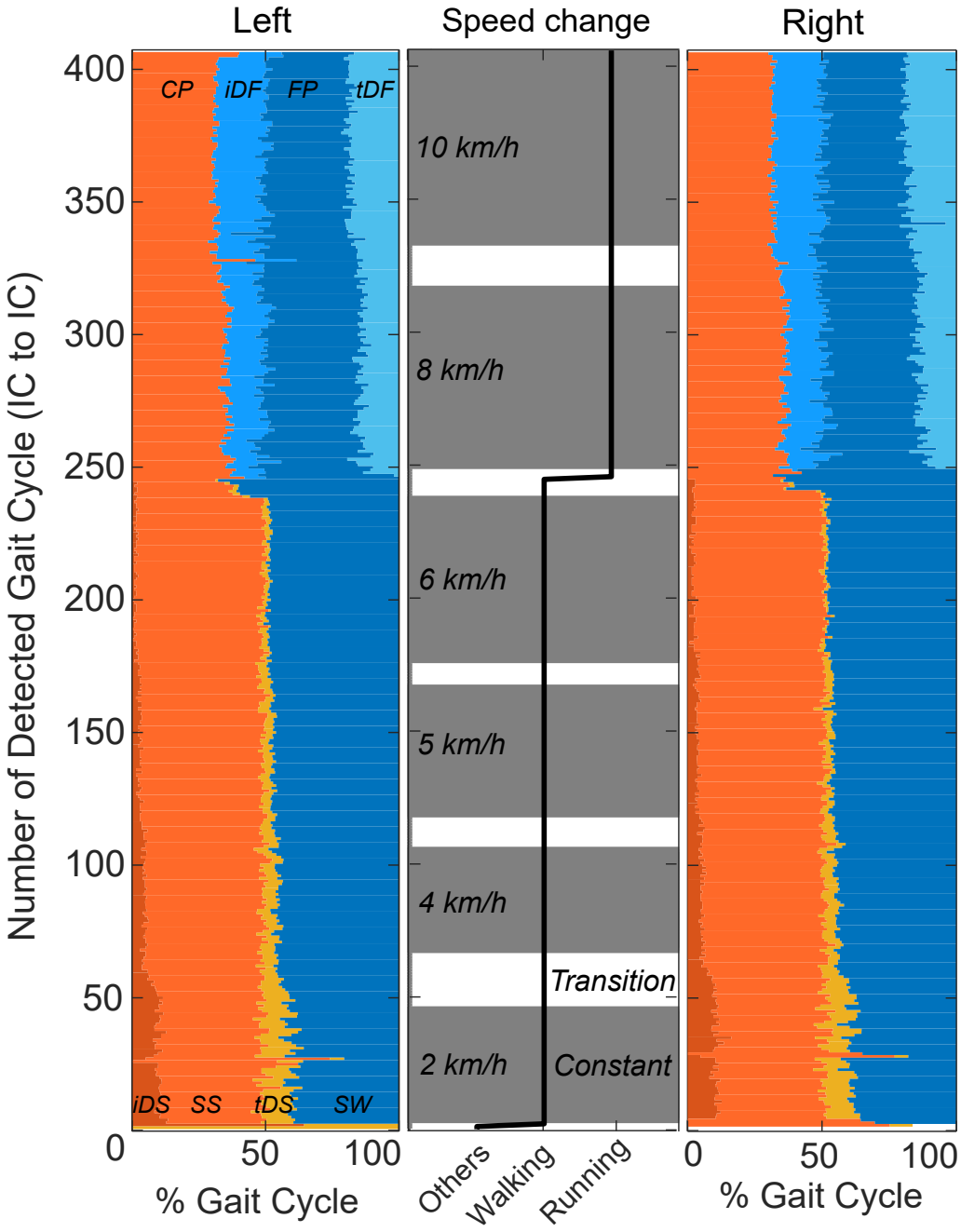


Figure 4.2: Result from S01: Percentage of gait phases from a single experiment trial, where left and right phases can be quantified separately. Mid-figure depict the recognized activity class and the changing of speed throughout the experiment trial.

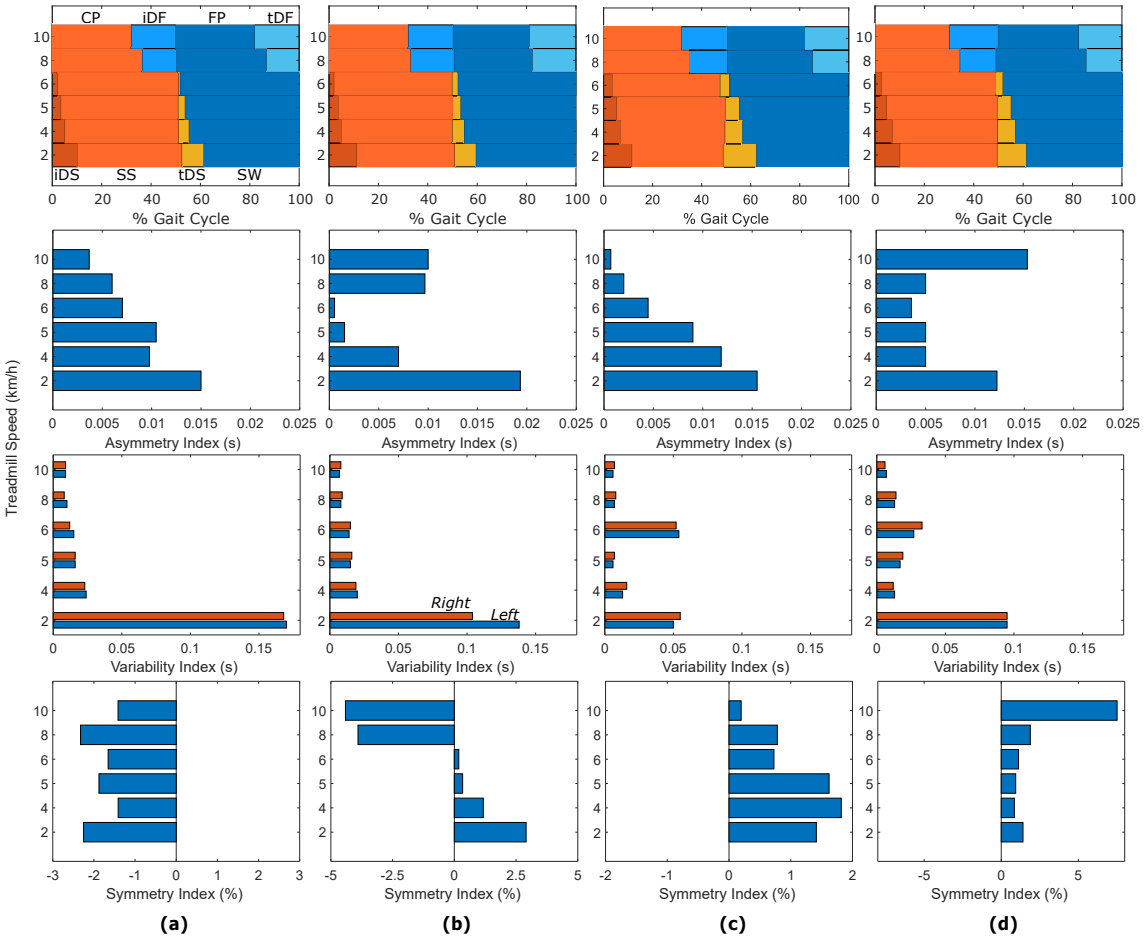


Figure 4.3: Summary of temporal gait features distinguished by treadmill speed. Columns represent subjects, i.e. (a) S01, (b) S02, (c) S03, and (d) S04. Top row to bottom represent percentage of gait shares, asymmetry index, variability index, and symmetry index, respectively.

Table 4.3: Quantitative gait assessment : A detailed report on temporal gait features distinguished by treadmill speed.

| Subject | Mean Temporal Features (s) | | | | | | | Gait Indices | | | Treadmill Speed |
|---|---|---|---|---|---|---|---|---|---|---|---|
| | iDS | SS/CP | tDS | iDF | SW/FP | tDF | Stride time | SI (%) | AI (s) | VI (s) | |
| S01 | 0.105 | 0.452 | 0.113 | | 0.432 | | 1.102 | -2.3 | 0.015 | 0.170(L) 0.168(R) | 2 km/h |
| | 0.047 | 0.432 | 0.052 | | 0.443 | | 0.973 | -1.4 | 0.009 | 0.024(L) 0.023(R) | 4 km/h |
| | 0.027 | 0.438 | 0.034 | | 0.449 | | 0.948 | -1.9 | 0.010 | 0.016(L) 0.016(R) | 5 km/h |
| | 0.011 | 0.422 | 0.019 | | 0.430 | | 0.882 | -1.7 | 0.007 | 0.015(L) 0.012(R) | 6 km/h |
| | | 0.250 | | 0.097 | 0.258 | 0.100 | 0.704 | -2.3 | 0.006 | 0.010(L) 0.080(R) | 8 km/h |
| | | 0.215 | | 0.126 | 0.220 | 0.127 | 0.688 | -1.4 | 0.004 | 0.009(L) 0.009(R) | 10 km/h |
| S02 | 0.134 | 0.636 | 0.178 | | 0.615 | | 1.564 | 2.9 | 0.019 | 0.138(L) 0.104(R) | 2 km/h |
| | 0.060 | 0.508 | 0.058 | | 0.502 | | 1.128 | 1.2 | 0.007 | 0.020(L) 0.019(R) | 4 km/h |
| | 0.038 | 0.478 | 0.039 | | 0.479 | | 1.034 | 0.3 | 0.001 | 0.015(L) 0.016(R) | 5 km/h |
| | 0.025 | 0.468 | 0.023 | | 0.469 | | 0.983 | 0.2 | <0.001 | 0.014(L) 0.015(R) | 6 km/h |
| | | 0.230 | | 0.131 | 0.238 | 0.132 | 0.731 | -3.9 | 0.009 | 0.008(L) 0.009(R) | 8 km/h |
| | | 0.212 | | 0.135 | 0.220 | 0.132 | 0.699 | -4.4 | 0.01 | 0.007(L) 0.008(R) | 10 km/h |
| S03 | 0.213 | 0.576 | 0.179 | | 0.555 | | 1.523 | 1.4 | 0.015 | 0.050(L) 0.055(R) | 2 km/h |
| | 0.085 | 0.479 | 0.780 | | 0.466 | | 1.108 | 1.8 | 0.011 | 0.013(L) 0.016(R) | 4 km/h |
| | 0.063 | 0.458 | 0.560 | | 0.449 | | 1.026 | 1.6 | 0.009 | 0.006(L) 0.007(R) | 5 km/h |
| | 0.041 | 0.413 | 0.320 | | 0.444 | | 0.930 | 0.7 | 0.004 | 0.054(L) 0.052(R) | 6 km/h |
| | | 0.270 | | 0.116 | 0.266 | 0.122 | 0.774 | 0.8 | 0.002 | 0.007(L) 0.008(R) | 8 km/h |
| | | 0.236 | | 0.136 | 0.234 | 0.142 | 0.747 | 0.2 | <0.001 | 0.006(L) 0.007(R) | 10 km/h |
| S04 | 0.186 | 0.601 | 0.159 | | 0.577 | | 1.522 | 1.4 | 0.012 | 0.095(L) 0.095(R) | 2 km/h |
| | 0.081 | 0.455 | 0.075 | | 0.450 | | 1.060 | 0.8 | 0.005 | 0.013(L) 0.012(R) | 4 km/h |
| | 0.056 | 0.423 | 0.048 | | 0.419 | | 0.946 | 0.9 | 0.005 | 0.017(L) 0.019(R) | 5 km/h |
| | 0.029 | 0.395 | 0.022 | | 0.403 | | 0.850 | 1.1 | 0.003 | 0.027(L) 0.033(R) | 6 km/h |
| | | 0.245 | | 0.104 | 0.251 | 0.106 | 0.706 | 1.9 | 0.005 | 0.013(L) 0.014(R) | 8 km/h |
| | | 0.224 | | 0.123 | 0.211 | 0.141 | 0.699 | 7.5 | 0.015 | 0.007(L) 0.006(R) | 10 km/h |

events detection falls roughly between 1-4 data samples (6.8 - 27.2 ms) at 148 Hz sampling rate.

Data preprocessing, processing, and analysis were all done using a commercial PC with Intel Core i7-8750H 2.2 GHz CPU. All of the above processes were done in a specialized MATLAB-based application that we developed to execute the proposed framework. A demo software of this study is available on:

*https://github.com/yonatancah/Temporal-Gait-Evaluation.*

Figure 4.2 serves as an example of data analysis performed under the proposed framework for a single experiment trial. Here, the percentage of gait phases from the left and right side of S01 are presented. A total of 406 gait cycles were detected from this experiment trial which lasted around 6 minutes and 20 seconds. The middle figure is showing the activity class as well as the point where 'constant' speed or in 'transition' occurred.

Table 4.3 presents a detailed report on temporal features distinguished by the treadmill speed. Here we extracted iDS, SS, tDS, and SW time for walking gait and CP, iDF, FP, and tDF time for running gait. Walking gait was observed for 2,4,5, and 6 km/h treadmill speed, while running gait was observed for 8 and 10 km/h treadmill speed consistently across all subjects. These results are in agreement with self-reported assessment by the subjects as presented in Table 4.2, where all subjects said that they changed from walk to run at 6 to 8 km/h transition. We observed that double support time, single support time, and contact phase time was decreased as treadmill speed increase across all subjects. On the other hand, even though we only have two speed representing running gait, i.e. 8 km/h and 10 km/h, we observed that double flight time was increased as treadmill speed increase. These results are also presented in top row of Figure 4.3 for every subjects.

On gait indices, we presented SI, AI, and VI with respect to treadmill speed on Table 4.3 and Figure 4.3. On the results of SI, we found that it was unique to each subjects. S01 showed an overall negative SI with an average of -1.83% SI in all tested treadmill speed. S02 showed a decrements trend in SI starting from 2.9% SI on 2 km/h speed to -4.4 % SI on 10 km/h speed, with an average of 2.15 % SI. To be more precise, on walking gait we observed an overall positive SI, while on running gait we observed an overall negative SI. These means that on walking gait S03 and S04 showed an overall positive SI with an average of 1.08 % and 2.27 % of SI, respectively.

On the results of VI, we observed that the highest temporal variability on both left and right sides occurred on the slowest treadmill speed, i.e. 2 km/h. Interestingly, only S03 experienced another comparable high variability on 6 km/h treadmill speed, where left side variability was 0.054 s compared to 0.050 s on 2 km/h, and right side variability were 0.055 s on 2 km/h and 0.052 s on 6 km/h. One of the importance of looking at VI is that we can distinguish the timing variability of each side which can be useful to assess if there is impairment of one of the sides of the subjects. It should be noted that gait index scores may not give an absolute definitive condition of subjects, but it can be used as a relative measure to make an intra-subject comparison such as tracking rehabilitation progress or to make an inter-subject comparison between groups of interest [140].

On the computational time, we observed an average of 10.84 $\pm$ 0.59 s to finish computation and extract all of the features depicted in Table 4.1, with average experiment time across all trials of 417.95 $\pm$ 26.55 s. Note that this result was achieved using the computational hardware mentioned early in this section and executed in MATLAB environment. Other processing hardware or programming

language may resulted in different computational cost. Looking at the computational cost of around 11 seconds to complete a roughly 7 minutes of data analysis, has made it highly possible for real-time or online system to be constructed using our proposed framework.

### 4.1.3 Conclusions

We have investigated our proposed framework of seamless extraction of temporal gait features for walking and running gait performed on a variable speed treadmill. By using two IMU sensors on both sides of foot and introducing activity class with detailed inner-class states, we can successfully extracted a detailed gait phases both on walking and running gait that incorporate double support and double flight phases, respectively. In this study we also introduced a moving-average based filtering technique to filter out transition data between speed changing, thus a precise speed-based analysis can be performed. In sport application, this approach will benefit to see the consistency and performance of an athlete given a specific speed of treadmill training, in addition to a video-based analysis [89]. To give a more in-depth analysis, we extracted several gait indices based on temporal features. This features is useful to be applied in clinical setting such as to track rehabilitation progress and to compare data between subjects of interest [5]. To conclude, the developed framework in this study may contribute to a more unobstructive gait analysis, where speed change and gait change can be anticipated and recognized, which reduce the amount of interruption to subjects during experiment. Future work for this study is to test it in an outdoor setting and considering a larger cohort and prolonged experiment time. Extending the framework to become an online process is also the future interest of this study.

## 4.2 Cognitive Dual-Task Gait

Walking is considered an automatic rhythmic motor behavior. This implies that gait can be performed without much attention. In daily life, the need to perform multiple tasks simultaneously is very common. The term dual-task gait refers to the condition where the secondary task is added into the walking or gait task. For example, we often have a conversation with someone while walking. Under these occasions, gait is considered as the primary task, while processing information and replying to a conversation are considered the secondary task. The added cognitive task load may influence the gait pattern of the subject, moreover on the elderly population [141]–[143]. The influence may negatively affect the performance of the

performed tasks as there is a competition between tasks for attentional resources [144].

Laboratory-based assessment is considered the gold standard for gait experiments. However, a recent study has suggested that the in-lab measure of gait does not accurately reflect the daily-living gait [145]. For this reason, wearable-based gait assessments have been proposed as an alternative solution to assess various gait experiments in both in and out-of-lab settings, with varying performance depending on the number of sensors used, location attachment to the body, and the implemented algorithm [146]. There have been several studies discussing wearable sensors for cognitive dual-task gait [147]–[149]. One accelerometer attached on low back over L5 vertebrae was investigated to assess gait balance control based on the analysis of acceleration data [147]. The use of six inertial sensors to assess dual-task gait from the extracted spatiotemporal and kinematics features was investigated on [148]. Meanwhile, another study [149] proposed the combination of pressure sensing insoles and four accelerometer to assess the difference between single-task and dual-task gait in fallers and non-fallers elderly population.

The increased number of sensors may give more ways to provide a detailed analysis as we can extract more gait information [148], [149], while using only one sensor such as on [147] may only provide analysis in descriptive statistic manners. This calls for an optimized number of sensors that can both be still practical and convenient to the wearer while also giving enough gait features to be analyzed for the dual-task gait experiment. Therefore, this case study investigates the use of two shoes-attached IMUs to distinguish single-task gait from cognitive dual-task gait from the quantification of temporal gait features as well as various gait index features.

### 4.2.1 Methods

**Subjects**. Two subjects, S01 (27 F) and S02 (27 M), with no history of severe lower-limb related injuries participated in this specific case study. Informed consent prior to participation in the experiment was given to the subject.

**Data collections and preprocessing**. Two IMUs (MetaMotionC, MbientLab, San Fransisco, CA, USA) were attached on the back of the shoes. Accelerometer and gyroscope data were logged during the time of the experiment, and later uploaded to the computer for data processing. Sampling rate of the sensors was set at 100 Hz. All of the collected data were processed using Python (version 3.7.3). On the pre-processing stage, 4th order Butterworth low-pass filter was applied to all the

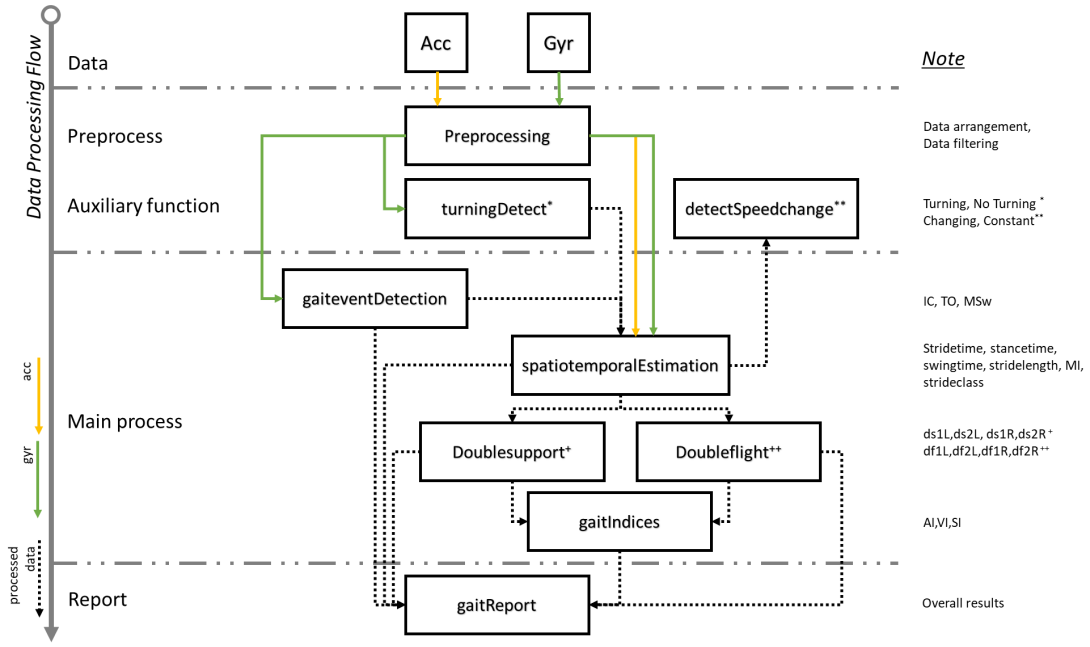


Figure 4.4: Data processing flow consisted of pre-process, auxiliary functions, main process, and report blocks.

collected data with a cut-off frequency of 6 Hz.

**Experiment protocols**. The experiment protocols were adapting the walkway protocol on Chapter 3. The first trial was subject performing single-task gait, where the subject walks at their preferred speed with no invervention. The second trial was subject performing dual-task gait, where the attention demanding task was the subject must solve crossword puzzles on their smartphone.

**Data processing**. The overall data processing flow is illustrated in Figure 4.4. Accelerometer and gyroscope data are fed to the pre-processing stage, where data arrangement and filtering were done. The output of this stage are then forwarded to various function such as for gait event detection algorithm and the estimation of spatio-temporal events on the main process. The detection of gait events, estimation of spatiotemporal features, and calculation of gait indices were following the same algorithm as Chapter 3.2.4. Detection of speed change as well as estimation of double flight phases were following the algorithm as discussed in Chapter 4.1.1. Finally, reporting function was introduced to summarize the results and provide analytics.

### 4.2.2 Results and Discussion

The comparison between single-task and dual-task gait is presented in this section. Graphical comparison between single-task and dual-task gait as seen from

the phase ratio and gait indices are presented in Figure 4.5-4.6 for S01 and S02, respectively.

For S01, stance phase, swing phase, and double-support phase ratio between single and dual-task gait were 58.43 % and 59.44 %, 41.57 % and 40.56 %, and 16.89 % and 19.42 %, respectively. The stance phase ratio was increased by 1.01 % when performing dual-task gait, and consequently swing phase ratio was decreased by the same percentage value of 1.01 %. Interestingly, we observed that the double-support phase was higher by 2.53 % on dual-task gait. In terms of gait indices, there was a higher variability across all gait variability indices when performing dual task-gait. A higher SI was also observed on dual-task (0.015) as compared to single-task (0.001), which translated to 98.5 % and 99.9 % of symmetry, respectively. This indicates that a worse gait symmetry was observed in dual-task gait as compared to the single-task gait, even though it was still on a high range of symmetry value

Meanwhile, for S02, stance phase, swing phase, and double-support phase ratio between single and dual-task gait were 51.19 % and 54.77 %, 48.81 % and 45.23 %, and 10.27 % and 15.56 %, respectively. The stance phase ratio was increased by 3.58 % when performing dual-task gait, and consequently swing phase ratio was decreased by the same percentage value of 3.58 %. Interestingly, we observed that the double-support phase was higher by 5.29 % on dual-task gait. In terms of gait indices, there was a decrease in variability, particularly on both swing and stance phase of right side when performing dual-task gait. A similar SI was also observed on dual-task (0.042) as compared to single-task (0.041), which translated to 95.8 % and 95.9 % of symmetry, respectively. This indicates that gait symmetry was not really affected when subject performing single-task or dual-task gait.

Both of S01 and S02 have higher double support phase when performing dual-task gait. A higher double-support phase may indicate a slower walking speed. This finding was further confirmed by looking at the total walking time depicted in Table. 4.4. Subject performing single-task gait complete the experiment faster compared to performing dual-task gait. This may indicate that there is an allocation of attention performing the secondary task that leads to a slight decrease in performance in terms of time to complete the gait experiment. In terms of cadence, we observed a decrease in cadence by an average of 2 steps/min for S01, and 11 steps/min for S02 when performing dual-task gait, with S02 having an overall higher cadence in both experiments.

In terms of motion intensity, there was a statistically significant difference between single-task and dual-task MI on the right side ($p < 0.1$). A significant dif-

Table 4.4: Gait report on single-task and dual-task gait experiment

| Gait features | S01 | | S02 | |
|---|---|---|---|---|
| | Single-task | Dual-task | Single-task | Dual-task |
| *Temporal gait features* | | | | |
| Total walking time (s) | 409.96 | 441.69 | 272.61 | 353.4 |
| Cadence (steps/min) | 78 | 76 | 99 | 88 |
| Average stance time (s) [L,R] | [0.90,0.90] | [0.94,0.92] | [0.61,0.63] | [0.75, 0.76] |
| Average swing time (s) [L,R] | [0.63,0.64] | [0.64,0.64] | [0.60,0.58] | [0.62, 0.63] |
| Double-support time (s) | 0.130 | 0.152 | 0.062 | 0.107 |
| *Gait events* | | | | |
| Detected IC [L,R] | [285,284] | [302,298] | [230,236] | [264, 269] |
| Detected TO [L,R] | [274,268] | [293,278] | [222, 225] | [258, 261] |
| Detected MSw [L,R] | [286,284] | [302,299] | [231, 237] | [265, 269] |
| *Gait indices* | | | | |
| Symmetry Index (%) | 99.9 | 98.5 | 95.9 | 95.8 |
| Asymmetry Indices (%) [Stance, Swing] | [0.09,1.1] | [1.39,0.04] | [2.63, 0.1] | [3.26, 0.79] |
| Variability Indices (Stance) [L,R] | [0.076,0.082] | [0.092,0.124] | [0.093, 0.087] | [0.094, 0.053] |
| Variability Indices (Swing) [L,R] | [0.081,0.027] | [0.113,0.134] | [0.013, 0.105] | [0.02, 0.027] |
| Motion Intensity (g) [L,R] | [1.207,1.283] | [1.164,1.214] | [1.261, 1.355] | [1.171, 1.233] |

ference ($p < 0.01$) between motion intensity on the left and the right side was also observed during this experiment. These correlations are depicted in Figure. 4.7.

### 4.2.3 Conclusions

This case study further expands the potential use of the proposed wearable-based quantitative gait analysis framework. While visual observation may not objectively show the differences between single-task and dual-task gait, the proposed framework could help in the extraction of temporal gait patterns that later can be derived into gait indices. By looking at these features, we could objectively find the differences between those two gait tasks. In this particular case study, a lesser motion intensity, an increase of double support time, and a reduced cadence were observed from all subjects participated in this study. For S01, we observed a higher gait temporal variability, and a worse gait symmetry were observed on the subject performing dual-task gait. Meanwhile for S02, we observed a decrease in swing and stance variability of right side when performing dual-task gait and a similar symmetry index on both experiments. These finding indicate that the gait pattern analyzed from each subject is unique and it should be noted that these findings may only be

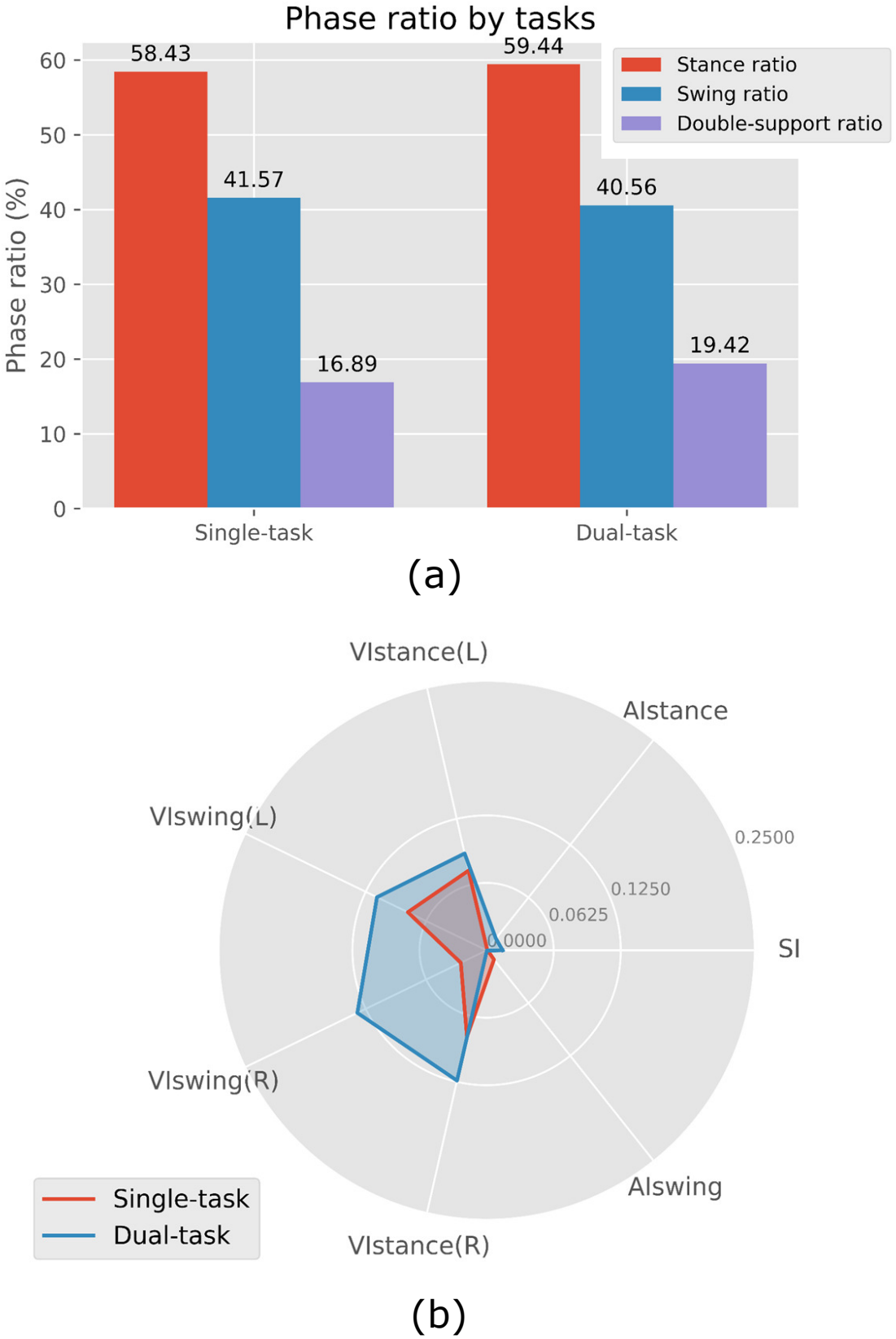


Figure 4.5: Results from S01: Comparison between single-task and dual-task gait (a) based on the phase ratio and (b) gait indices.

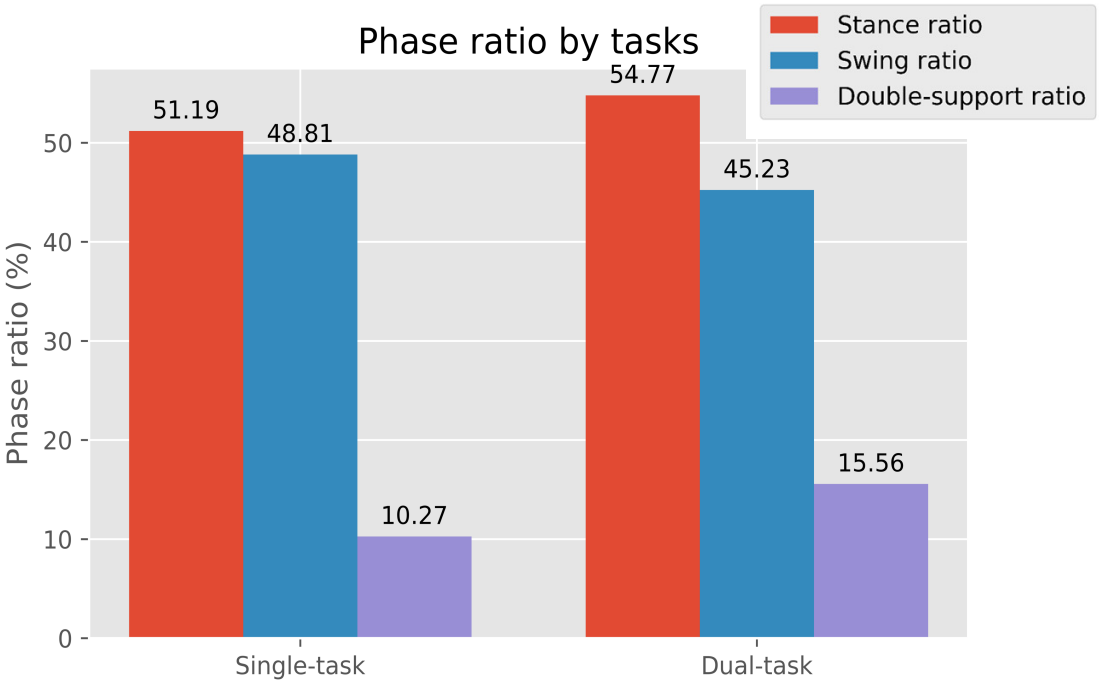


(a)

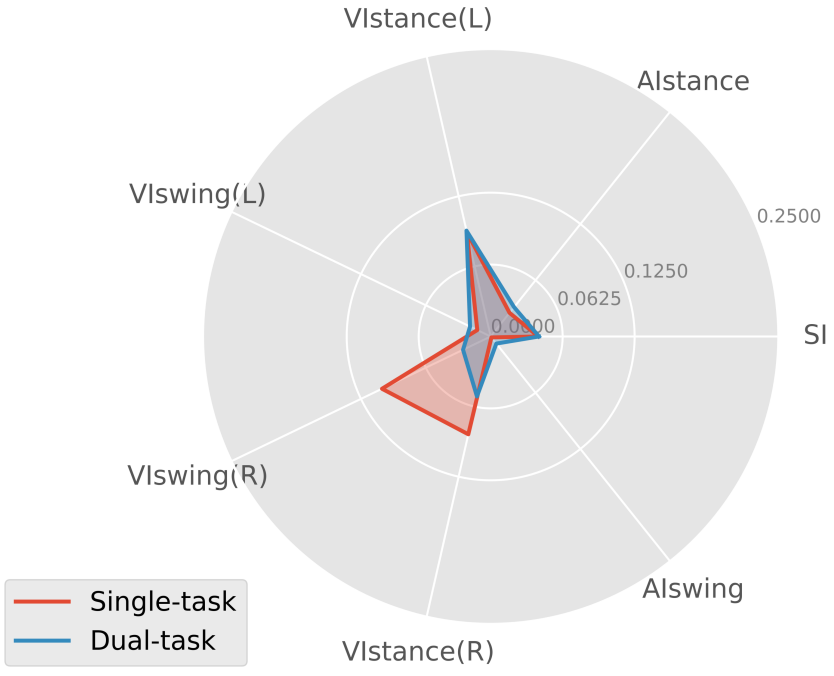


(b)

Figure 4.6: Results from S02: Comparison between single-task and dual-task gait (a) based on the phase ratio and (b) gait indices.

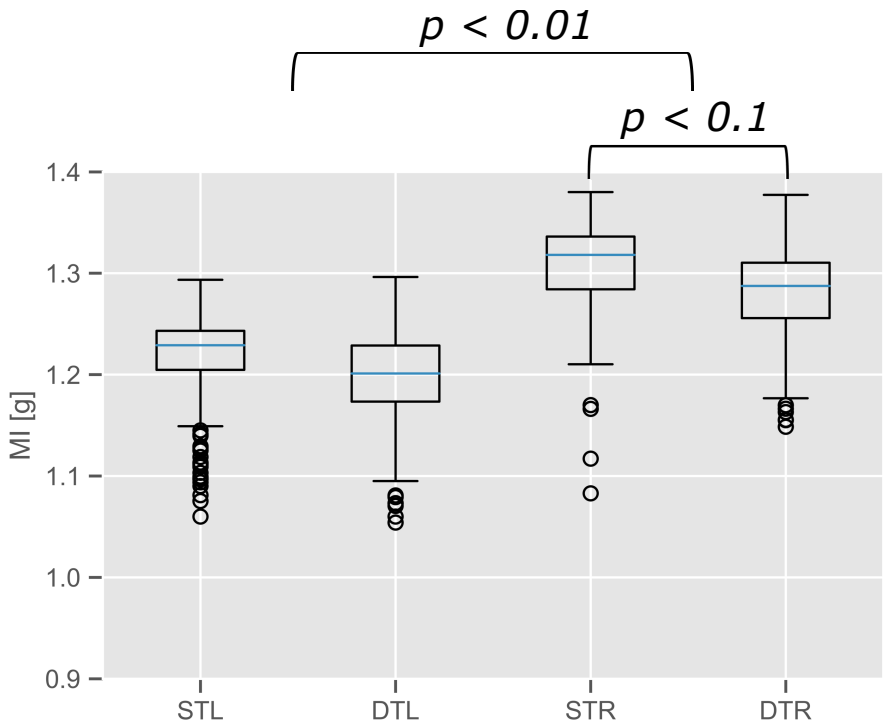


Figure 4.7: Motion intensity during single-task (ST) and dual-task (DT) gait. L and R denotes left and right side, respectively.

valid to the subject of this experiment. To draw a more general conclusion, this case study should be expanded to include more subjects.

## 4.3 Prolonged outdoor gait experiment

In this section, the use of the proposed framework over a prolonged outdoor experiment is investigated. A prolonged experiment is hypothesized to have a certain effect on the gait pattern of the subject. It is expected to see the changing of certain gait features during this experiment. Moreover, this study is intended to investigate if there is any sensor-related problem due to longer data recording sessions. All of these concerns are addressed within this section.

### 4.3.1 Methods

**Subjects**. Two subjects with no history of severe lower-limb related injuries or neurological conditions participated in this particular case study. Informed consent prior to participation in the experiment was given to the subject.

**Data collections and preprocessing**. Two IMUs (MetaMotionC, MbientLab, San Fransisco, CA, USA) were attached to the back of the shoes. Accelerometer and

gyroscope data were logged during the time of the experiment and later uploaded to the computer for data processing. The sampling rate of the sensors was set at 100 Hz. All of the collected data were processed using Python (version 3.7.3). On the pre-processing stage, 4th order Butterworth low-pass filter was applied to all the collected data with a cut-off frequency of 20 Hz to accommodate running gait.

**Experiment protocols**. This specific case study was designed to see the performance of the proposed framework under a prolonged experiment time. A total time of more than 10 minutes was considered sufficient to test for this case study, as the previous experiments were recorded less than 8 minutes per trial. There were two trials included for this study. The first trial was adopting the protocol from the walkway experiment on Section 3.2.3 which was modified to 18 repetitions instead of 6 repetitions on the original protocol. Thus, the first trial accounts for the controlled outdoor experiment with prolonged time. Contrary, in the second trial, the subjects were told to perform walk and run freely as they see fit as long as it lasted more than 10 minutes. Thus, the second trial accounts for the free outdoor gait experiment with prolonged time.

**Data processing**. The overall data processing flow is illustrated in Figure 4.4. Accelerometer and gyroscope data are fed to the pre-processing stage, where data arrangement and filtering were done. The output of this stage is then forwarded to various functions such as for gait event detection algorithm and the estimation of spatio-temporal events on the main process. The detection of gait events, estimation of spatiotemporal features, and calculation of gait indices were following the same algorithm as Chapter 3.2.4. Detection of speed change, as well as estimation of double flight phases, were following the algorithm as discussed in Chapter 4.1.1. Finally, reporting function was introduced to summarize the results and provide analytics.

### 4.3.2 Results and Discussions

Results on this case study are presented in this section. As mentioned on the experiment protocols on Section 4.3.1, there are a total of two experiments performed for this case study.

The first experiment lasted around 13 minutes. Walking and turning classes were detected throughout the experiment as depicted in Figure 4.8(A). The proposed turning detection algorithm resulted in 100 % detection accuracy in this trial. Since this trial is a three times extension of the protocols in Section 3.2.3, analysis in terms of gait indices was divided into three equivalent stages to see if there are significant

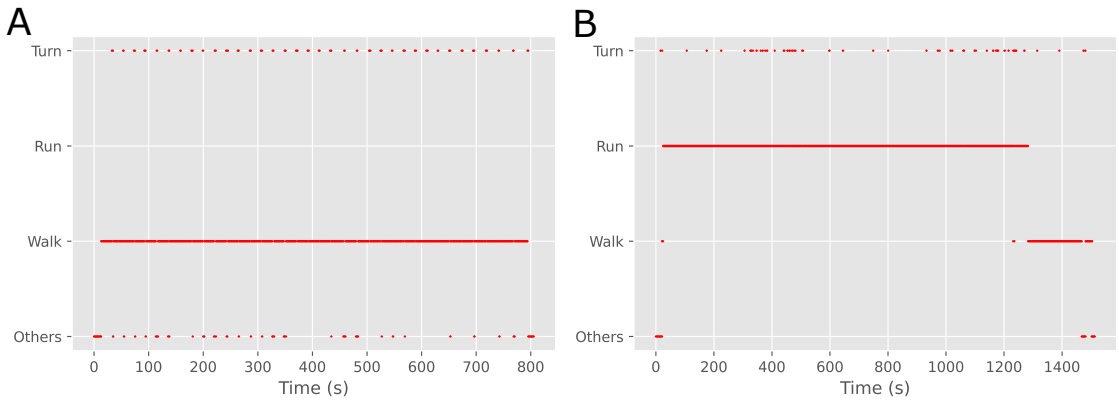


Figure 4.8: (A) Recorded activity class during the first trial, where walk and turn were detected during the experiment. (B) Recorded activity class during the second trial. Walk, Run, and Turn were detected during the experiment. Others class represented any other activity that were not classified yet, which include standing still.

changes on the subject performing the gait experiment.

Figure 4.9 (top) shows the changing of gait indices pattern during the first experiment. The first stage showed the most variability particularly on swing time on the left side. On to the second and third stages, all of the variability indices were decreased. The higher variability on the first stage may indicate that the subject was trying to adjust how they walk. Histogram plot on Figure 4.9 (top) has shown a clear difference between stance and swing time in this experiment, where stance time was higher than the swing time. The gait report regarding the first experiment is depicted in Table 4.5. This first experiment serves as an example to track the progress of the subject during the gait experiment. This could potentially be used in a clinical setting for tracking rehabilitation progress, particularly on gait-related progress as reflected by the extracted gait features.

The second experiment lasted around 23 minutes. Running followed by a shorter walking session with some occasional turning movements were detected throughout the experiment as depicted in Figure 4.8(B). From Figure 4.8(B), the turning class was detected more often during the actual running movement due to a higher intensity of foot movement, notably on the longitudinal axis of the sensors as we set a threshold to recognize turning movement. This has led to several misclassifications of turning class, which were supposed to be running class. Therefore, a more robust classification algorithm is needed to solve this issue.

The distribution of stance time and swing time during the second experiment is depicted in the histogram plot on Figure 4.9 (bottom). There were two concentrated regions of stance time distribution, the lower range around 0.2-0.4 s represented

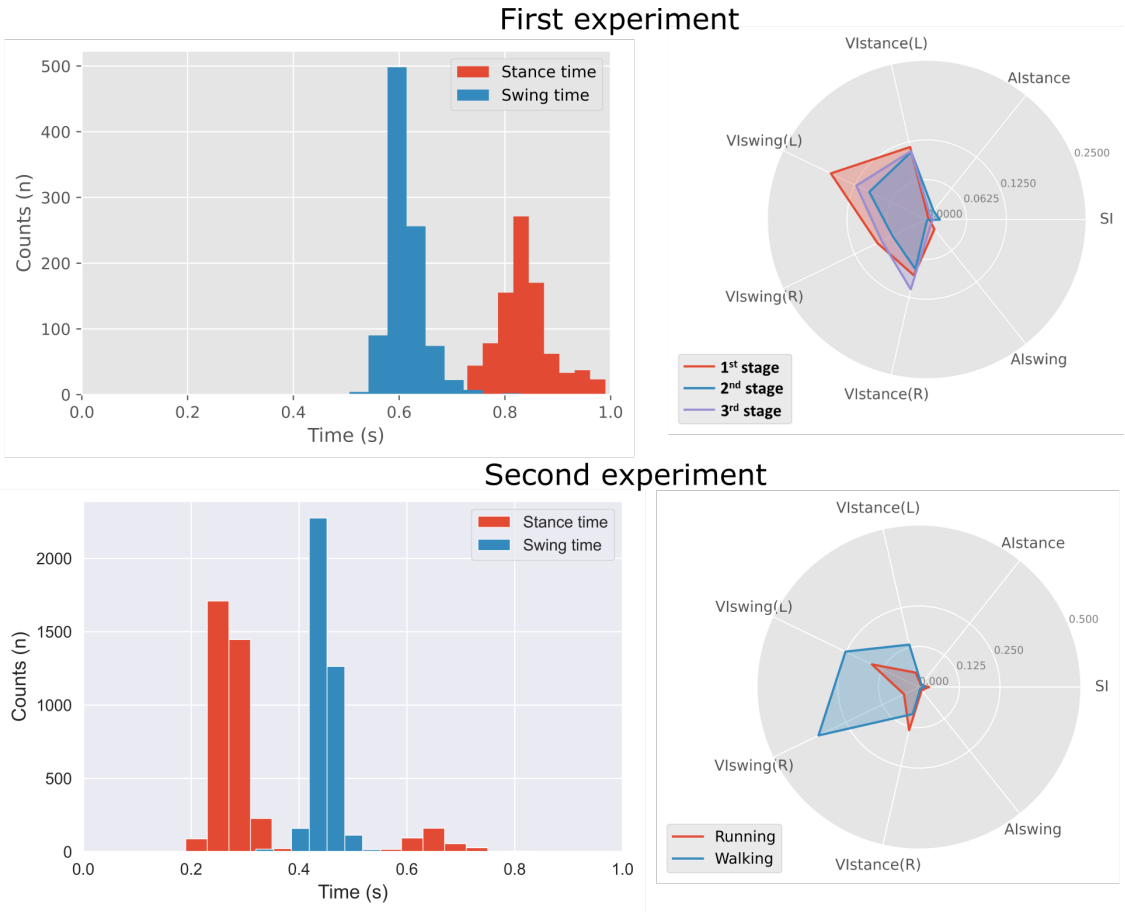


Figure 4.9: Histogram plot of temporal features (left) and temporal gait indices (right) analysis on this case study. The first experiment emphasise on a controlled outdoor gait experiment to observe gait changing during three stages of walking. The second experiment emphasise on a free outdoor gait experiment to observe the differences between two gait types of walking and running.

Table 4.5: Gait report on the first trial: the controlled outdoor gait experiment.

| Gait features | Overall |
|---|---|
| *Temporal gait features* | |
| Total walking time (s) | 755.25 |
| Cadence (steps/min) | 83 |
| Average stance time (s) [L,R] | [0.83,0.97] |
| Average swing time (s) [L,R] | [0.61,0.61] |
| Double-support time (s) | 0.134 |
| *Gait events* | |
| Detected IC [L,R] | [516,488] |
| Detected TO [L,R] | [492,479] |
| Detected MSw [L,R] | [517,488] |
| *Gait indices* | |
| Symmetry Index (%) | 97.57 |
| Asymmetry Indices (%) [Stance, Swing] | [2.00,0.55] |
| Variability Indices (Stance) [L,R] | [0.159,0.103] |
| Variability Indices (Swing) [L,R] | [0.038,0.031] |
| Motion Intensity (g) [L,R] | [1.26,1.31] |

running activity and the upper range around 0.6-0.8 s represented walking activity. Contrary, swing phase distribution was concentrated in one region around the 0.4-0.6 s range, with indistinguishable walking and running activities. This suggests that the stance time feature is more robust to recognize walking and running activities.

Figure 4.9 (right) and Table 4.6 depicted the comparison of temporal gait indices on subject performing the second experiment. A lower SI ($SI = 96.99\%$) was observed during running activity compared to walking ($SI = 98.18\%$). This may indicate that there was a slight gait inefficiency during the running session as compared to the walking session. Table 4.6 showed that the VI stance on the right side was three times more than the VI stance on the left side. Conversely, the VI swing on the left side was three times the VI stance on the right side. Meanwhile, the average stance time and swing time on both left and right sides were around the same value. This indicates that VI may contribute to a deeper understanding of the differences between sides, where the reported mean values were around similar values.

Further, the VI swing on both sides was significantly greater in the walking session compared to the running session. Since walking occurred after running, higher

Table 4.6: Gait report on the second trial: the free outdoor gait experiment.

| Gait features | Overall | Running | Walking |
|---|---|---|---|
| *Temporal gait features* | | | |
| Total walking time (s) | 1482.02 | 1269.04 | 212.98 |
| Cadence (steps/min) | 157 | 165 | 104 |
| Average stance time (s) [L,R] | [0.31,0.31] | [0.27,0.28] | [0.65,0.64] |
| Average swing time (s) [L,R] | [0.46,0.45] | [0.45,0.44] | [0.50,0.52] |
| Double-support time (s) | 0.084 | 0 | 0.084 |
| *Gait indices* | | | |
| Symmetry Index (%) | 98.11 | 96.99 | 98.18 |
| Asymmetry Indices (%) [Stance, Swing] | [0.60,1.13] | [0.85,1.29] | [1.16,0.59] |
| Variability Indices (Stance) [L,R] | [0.124,0.167] | [0.045,0.136] | [0.134,0.086] |
| Variability Indices (Swing) [L,R] | [0.172,0.116] | [0.161,0.051] | [0.251,0.344] |
| Motion Intensity (g) [L,R] | [2.37,2.30] | [2.38,2.46] | [1.542,1.584] |

variability may explain the cooling down activity where the subject is adjusting their gait into a slower pace from the high intensity of running gait. In terms of MI, it was expected that the MI on running session is always higher than MI on walking session as depicted in Table 4.6.

In addition to subject-specific analysis, an inter-subject analysis could also be performed using the proposed framework in this thesis. For example, Figure 4.10 depicted the inter-subject comparison as shown by gait index features and histogram of temporal gait features on subjects performing the same protocols adopted from Section 3.2.3. The result shows that there was a larger gap between the duration of stance time and swing time in S02 as compared to S01, shown by the histogram. This may indicate that S01 walk faster than S02 as the stance time was shorter. This hypothesis was further proved in Table 4.7, where the detailed quantitative comparisons are shown. The table shows that subject S01 completed the experiment with a total walking time of 177.46 s and cadence of 83 steps/min which were faster than S02 with 268.3 s and 75 steps/min of total walking time and cadence, respectively.

The symmetry index was relatively low in S01 with 93.64 % SI compared to 96.57 % SI on S02. There may be a correlation between walking speed and SI, where faster walking speed resulted in lower SI. Conversely, motion intensity was slightly lower on S01 compared to S02 even though S01 was walking faster. These unique findings are needed to be investigated further with a larger pool of participants.

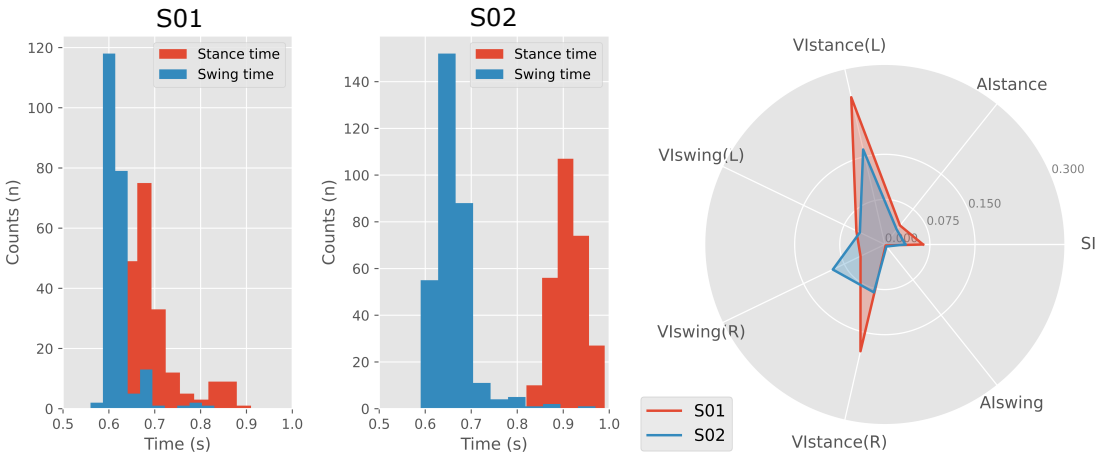


Figure 4.10: Inter-subject comparison between S01 and S02 as shown by the histogram of stance time and swing time, and the gait indices feature.

Table 4.7: Inter-subject comparison between S01 and S02

| Gait features | S01 | S02 |
|---|---|---|
| *Temporal gait features* | | |
| Total walking time (s) | 177.5 | 268.3 |
| Cadence (steps/min) | 83 | 75 |
| Average stance time (s) [L,R] | [0.78,0.78] | [0.94,1.02] |
| Average swing time (s) [L,R] | [0.67,0.60] | [0.65,0.66] |
| Double-support time (s) | 0.043 | 0.143 |
| *Gait events* | | |
| Detected IC [L,R] | [125,128] | [168,162] |
| Detected TO [L,R] | [117,116] | [163,160] |
| Detected MSw [L,R] | [128,128] | [169,162] |
| *Gait indices* | | |
| Symmetry Index (%) | 93.64 | 96.57 |
| Asymmetry Indices (%) [Stance, Swing] | [4.04,0.21] | [3.17,0.42] |
| Variability Indices (Stance) [L,R] | [0.251,0.182] | [0.162,0.082] |
| Variability Indices (Swing) [L,R] | [0.053,0.045] | [0.046,0.096] |
| Motion Intensity (g) [L,R] | [1.15,1.21] | [1.20,1.24] |

### 4.3.3 Conclusions

Two experiment trials performed in this section have demonstrated the use of the proposed framework in the previous chapter on a prolonged outdoor gait experiment. Two trials were presented in this chapter which serves as an example to assess gait for potential clinical application and sport application. The first trial empha-

sized assessing gait over a prolonged time with specific instruction. By extracting the gait index features, an objective comparison between walking stages could be drawn. The second trial emphasized assessing gait in a free-living situation, where the subject can do any activity as they see fit. Further, an inter-subject comparison was demonstrated as an extension of what the proposed framework can achieve, which may potentially be used in clinical applications.

## 4.4 General Conclusions

This chapter demonstrated the potential application of what the proposed framework of wearable-based gait analysis in this thesis could do. The mixed gait of walking and running with variable speeds, cognitive dual-task gait, and prolonged outdoor use of the system was presented and discussed within this chapter. The preliminary experiments have shown promising results and are deemed potential to be used for the respected applications. Nevertheless, follow-up experiments with a larger cohort should be done to ensure the robustness of the proposed framework in a bigger population test.

# Chapter 5

# Machine learning for gait analysis

## 5.1 Introduction

This chapter addresses the use of machine learning algorithms for gait analysis purposes. By doing various gait experiments from previous studies in Chapter 3 and Chapter 4, we have collected several gait databases performed by various subjects. These gait database are used in this chapter to construct specific machine learning model. Several studies have implemented machine learning algorithms to their proposed framework of wearable-based quantitative gait analysis. The overall contributions of the machine learning algorithm were mostly for classification problems such as gait event or gait phase classifications [58], [78], [94], [106], and gait activity/terrain classification [109], as concluded from the systematic review presented in Chapter 2. With the positive trend and widespread implementation of big data research, the trained machine learning models will become more robust and may become an alternative algorithm for gait research.

In this chapter, several machine learning algorithms were proposed to be applied in some gait-related applications. In the first section, machine learning algorithms such as support vector machines (SVM) and boosting algorithms were designed to classify gait phases. Further, temporal convolutional networks (TCN) were studied to predict the gait outcomes of a subject. Lastly, reinforcement learning was proposed as a control algorithm for swing phase control in a prosthetic knee device.

## 5.2 Gait phases classification

In this section, three candidates of machine learning algorithms were considered. The first one was SVM, which is commonly used as classification algorithm in various applications [58], [78], [102]. The second and third algorithms were based on ensemble meta algorithms or also called boosting algorithms, which are adaptive boosting (AdaBoost) [150] and extreme gradient boosting (XGBoost) [151], respectively. The problem addressed in this section is whether the proposed algorithms could distinguish and classify gait phases of stance and swing phases, respectively from a series of data obtained from two IMU sensors.

### 5.2.1 Methods

**Data collection and preprocessing**. Data were collected from seven subjects who participated in the previous study in Chapter 4. All subjects wore two IMUs (MetaMotionC, MbientLab, San Fransisco, CA, USA or Trigno Research+, Delsys, MA, USA) on the back of their shoes. Several walking trials were performed in either indoor or outdoor setting with level ground walking adopting the experimental protocols in Section 3.2.3. Some of the experiments may contains running gait and also included for this study. Data pre-processing and the extraction of gait events were following the same method as depicted in Figure 4.4 from Chapter 4.

A total of ten datasets from seven subjects were considered. The datasets were annotated according to subject number (S) and trial number (T), respectively, as depicted in Table 5.1. Gait phases were classified into two distinct phases called the stance phase and swing phase. Ground truth for these phases was extracted using the validated method from Chapter 3. Since all data within a trial were fully used, it may contain a non-gait phase such as fully standing or when performing turning motion. For this reason, another class called 'other' was introduced to accommodate these data. Thus, a total of three classes (stance, swing, and other) were formulated as the target for the proposed model.

**Model training**. Three machine learning models, i.e. SVM, AdaBoost, and XGBoost were proposed and compared for gait phase classification. The same types and number of features were used to train those algorithms in order to fairly compare the performance from each model. Features extracted in this simulation were the magnitude of both acceleration and angular velocity from both left and right sensors. Hyper-parameters from each model were tweaked following grid search techniques to find the optimum values from a given dataset.

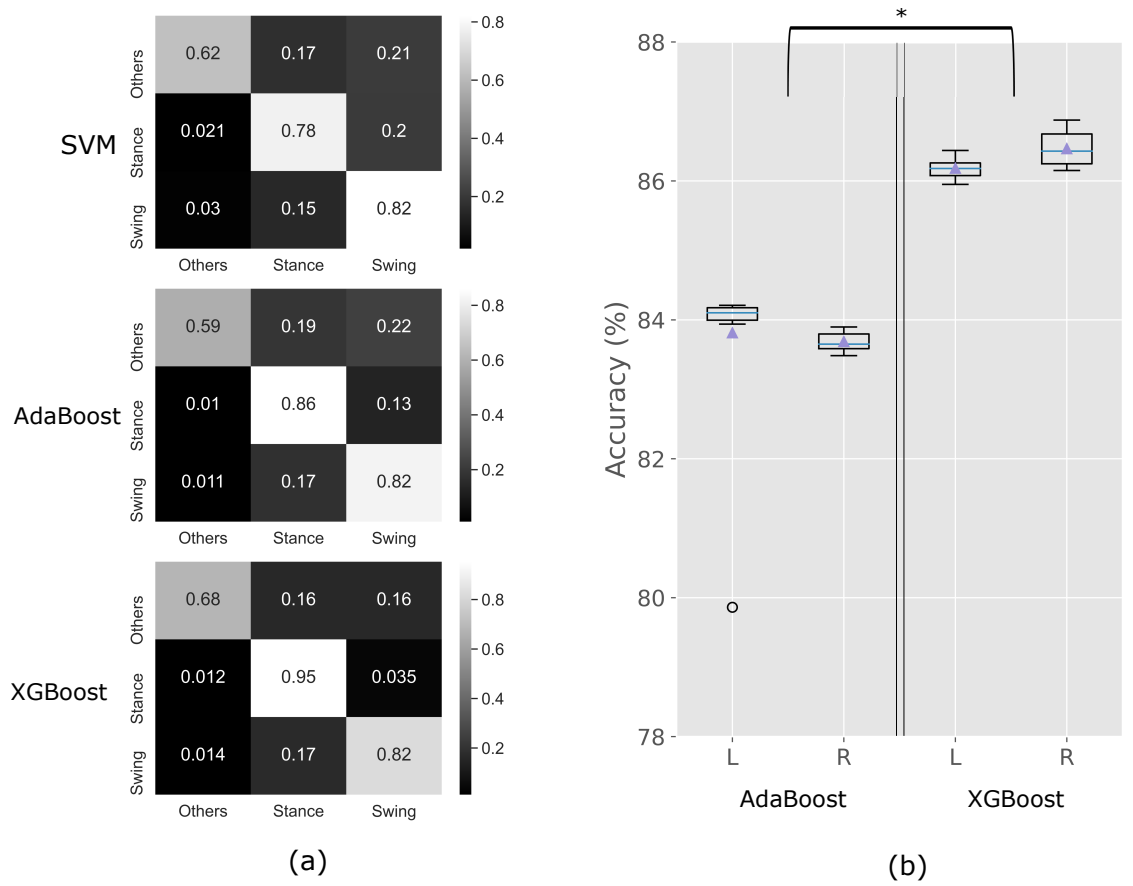


Figure 5.1: (a) Confusion matrices of all models trained with all dataset, where values shown indicates the classification accuracy of each class, vertical and horizontal axes are true class and predicted class, respectively. XGBoost leads on stance phase classification with 95 % rate, while all models performed at the same level of 82 % accuracy on swing phase classification. (b) 5-fold cross validation metrics from both AdaBoost and XGBoost classifiers with respect to left and right sensors. $*p < 0.001$ shows a statistical differences between the two models as computed based on two-tailed T-test.

### 5.2.2 Results and Discussions

In this study, a few simulation strategies were performed to see the effect of a different combination of training datasets in constructing the classification model. In the first simulation, only 70 % of S01.T01 dataset was used to train each of the models. The full results are depicted in Table. 5.1. XGBoost outperform other algorithms in four out of six datasets, where the best performance was on the S01.T01 dataset with 91.65 % accuracy. On the other hand, SVM outperform in two out of six datasets, where the best performance was on S02.T03 dataset with 79.24 % accuracy. As expected, the highest performance of each model was achieved when tested in S01.T01 dataset, where the 70 % of the data were used to train the model. On the contrary, the worst performance occurred when the trained model was employed to S01.T02 dataset, where it contains running gait. This result is also

expected as there are distinctions between gait phases during running and walking. This first simulation was intended to see if a model trained from a specific subject can also be used for another dataset and subjects. Here, we could see that the classification accuracy decreases when the trained model is tested on other datasets. Therefore, the next simulation will consider employing all datasets for training.

The second simulation was consisted of training the model with 70 % of all the datasets from simulation I, which include several experiment trials from both S01 and S02. The full results are depicted in Table 5.2 and confusion matrices are shown in Figure 5.1 (a). An overall best performance was obtained by the XGBoost model with a mean classification accuracy of 86.45 % and the range of accuracy when tested to individual dataset were 79.11 % - 92.23 %. Interestingly, we observed an increase in performance of all the models on classifying gait in dataset S01.T02, which contains running gait. This indicates that all the proposed models can also accommodate running gait phases by introducing part of running gait data to be trained.

Finally, on the third simulation we considered to increase more the size of dataset which include all of the subjects from Chapter 3 and Chapter 4 (S01-S07). The full results are depicted in Table 5.3. An overall best performance was also obtained by the XGBoost model with a mean classification accuracy of 84.54 % with range of 75.64 % - 87.86 % accuracy when tested to individual dataset. On the other hand, AdaBoost classifier achieved a mean classification accuracy of 82.26 % with range of 75.27 % - 86.50 % accuracy when tested to individual dataset, and SVM classifier achieved a mean classification accuracy of 78.31 % with range of 67.06 % - 84.79 % when tested to individual dataset.

It can be observed that the performance dropped from simulation II to simulation III, where there were 1.61 % and 1.91 % decrements in performance for AdaBoost and XGBoost classifier, respectively. The decrease in performance of the boosting models from simulation II to simulation III was partially due to the increase in the dataset which contains gait patterns from new subjects. This was correlated with the finding on [152] where the performance of classifiers depends on the extent to which a dataset represents the original distribution rather than its size. In simulation III, we introduced the dataset from five new subjects, where they may have different gait speed profile and different gait pattern in general that leads to a change in the original distribution from the previous simulation II.

One important point to be noted is the computational complexity when training the data. As the training size increased, SVM needs a longer time to train with a

Table 5.1: Simulation I: Training the machine learning model based only one dataset (S01.T01). Value in **bold** represent the best performance on each dataset.

| Dataset | Training/Test (%) | Test Accuracy (%) | | |
|---|---|---|---|---|
| | | SVM | AdaBoost | XGBoost |
| S01.T01 | 70/30 | 89.48 | 82.38 | **91.65** |
| S01.T02$^{+}$ | 0/100 | **54.67** | 36.15 | 43.13 |
| S02.T01 | 0/100 | 85.52 | 74.25 | **85.83** |
| S02.T02 | 0/100 | 77.24 | 72.03 | **80.37** |
| S02.T03 | 0/100 | **79.24** | 69.57 | 77.36 |
| S02.T04 | 0/100 | 74.60 | 71.27 | **78.34** |

$^{+}$this dataset contains running gait

Table 5.2: Simulation II: Training the classification model based on all of the dataset from previous simulation (S01-S02). Value in **bold** represent the best performance on each dataset.

| Dataset | Training / Test (%) | Test Accuracy (%) | | |
|---|---|---|---|---|
| | | SVM | AdaBoost | XGBoost |
| S01.T01 | 0/100 | 70.18 | 77.66 | **79.11** |
| S01.T02$^{+}$ | 0/100 | 75.28 | 81.27 | **82.50** |
| S02.T01 | 0/100 | 71.46 | 78.51 | **79.74** |
| S02.T02 | 0/100 | 80.99 | 87.11 | **90.48** |
| S02.T03 | 0/100 | 85.34 | 89.50 | **92.23** |
| S02.T04 | 0/100 | 81.96 | 87.77 | **91.08** |
| S01-S02 | 70/30 | 78.04 | 83.87 | **86.45** |

$^{+}$this dataset contains running gait

theoretical complexity of $O(n^3)$, where $n$ is equal to the number of training samples. On the other hand, since AdaBoost and XGBoost were both a tree-based ensemble, the time complexity is $O(n)$. Thus, the time needed to both train and test was significantly increased at the expense of $n$ power of 3 for SVM. For this reason alone, we did not continue to consider SVM for the classification model, moreover if the dataset is getting larger.

Next, to properly validate the model performance of AdaBoost and XGBoost, $k$-fold cross validation method was employed, with $k$ equal to 5 and repeated for three times. The result of this validation is depicted in Figure 5.1 (b). We seperate the model trained for gait phase classification based on left and right sensors. The mean cross validation of the XGBoost (left= $86.5\% \pm 0.2\%$, right= $86.2\% \pm 0.2\%$)

Table 5.3: Simulation III: Training the classification model based on all of the dataset available (S01-S07). Value in **bold** represent the best performance on each dataset.

| Dataset | Training / Test (%) | Test Accuracy (%) | | |
|---|---|---|---|---|
| | | SVM | AdaBoost | XGBoost |
| S01.T01 | 0/100 | 67.06 | 75.27 | **75.64** |
| S01.T02$^{+}$ | 0/100 | 75.28 | 78.65 | **82.50** |
| S02.T01 | 0/100 | 79.23 | 85.01 | **86.29** |
| S02.T02 | 0/100 | 76.44 | 80.21 | **81.97** |
| S02.T03 | 0/100 | 81.96 | 86.50 | **87.26** |
| S03.T01 | 0/100 | 71.92 | 77.41 | **81.13** |
| S04.T01$^{+}$ | 0/100 | 83.84 | 83.05 | **86.80** |
| S05.T01$^{+}$ | 0/100 | 84.79 | 84.97 | **87.86** |
| S06.T01$^{+}$ | 0/100 | 82.24 | 84.55 | **87.44** |
| S07.T01$^{+}$ | 0/100 | 83.63 | 84.48 | **86.21** |
| S01-S07 | 70/30 | 78.31 | 82.26 | **84.54** |

$^{+}$this dataset contains running gait

outperformed the AdaBoost (left= $83.7\% \pm 0.1\%$, right= $83.5\% \pm 0.1\%$). It is worth to note that both of the classifier models have high precision with only within 0.1 - 0.2 % from the mean.

To conclude, XGBoost with a mean accuracy of 84.54 % was suited the best to classify stance and swing phases during both walking and running based on the available dataset. It is important to note that the dataset used in this study was not cleaned and thus we purposefully introduce the third class called 'other' to accommodate any other data that were not stance and swing. By following this approach, we would like to demonstrate the performances of the selected classifiers for a real-world condition that mostly contains 'dirty' data. Therefore, based on the lesser time complexity and overall higher accuracy despite the condition of the 'dirty' dataset, it is highly likely that XGBoost can be used for real-time classification. To improve the performance of the proposed classifier, future works must consider to have several experiment trials from a subject.

## 5.3 Gait activity prediction

In this section, machine learning algorithms are trained to predict certain gait activities from continuous gait data. Temporal convolutional networks (TCN), which

was first proposed by S. Bai et. al. in 2018 [153], was considered for the main algorithm in this study. Since its first introduction, there have been many studies tried to implement this technique in various time-series or sequence model problems [154]–[156]. There has been an attempt to combine CNN and TCN [157] applied to process EEG dataset for mental workload assessment. The main advantages of TCN are lower memory requirements, parallel processing of long sequences, and a more stable training scheme [153].

### 5.3.1 Methods

In this case, gait can be considered a time series data as it has causality properties where data in the past will be highly correlated with data in the future. The mathematical expression for this principle is depicted in Equation 5.3.1, where $yt$ depends only on $x_0, ..., x_T$ without any information from future inputs such as $x_{t+1}, ..., x_{t+n}$. For instance, in normal gait, the stance phase will be followed by the swing phase and so on. TCN consists of a fully convolutional network with causal convolution. Since it is challenging to apply a simple causal convolution to a sequence modeling task, a dilated convolution was introduced that enables a larger receptive field [153]. The mathematical expression of dilated convolution is depicted in Equation 5.3.2, where $F(s)$ is the dilated convolutional operation on sequence $s$, $i$ is the index of the sequence, $d$ is the dilation factor, $k$ is the filter size, and $(s - d \cdot i)$ accounts for the direction of the past. Overall, the general architecture of a TCN is depicted in Figure 5.2.

$$y_0, ..., y_T = f(x_0, ..., x_T) \tag{5.3.1}$$

$$F(s) = (x *_d f)(s) = \sum_{i=0}^{k-1} f(i) \cdot x_{s-d \cdot i} \tag{5.3.2}$$

The research question of this study is whether TCN can predict the activity class of a subject. Activity class here is defined as the same as the previous definition on Section 3.2.4, where we have mainly walking and turning activities, apart from the occasional 'other' activity. Data used to train and test for this study are from the collection of datasets gathered on several experiments in this thesis, which is also part of the dataset used in Section 5.2. Several simulations were performed to ensure the best performance possible from the trained algorithm.

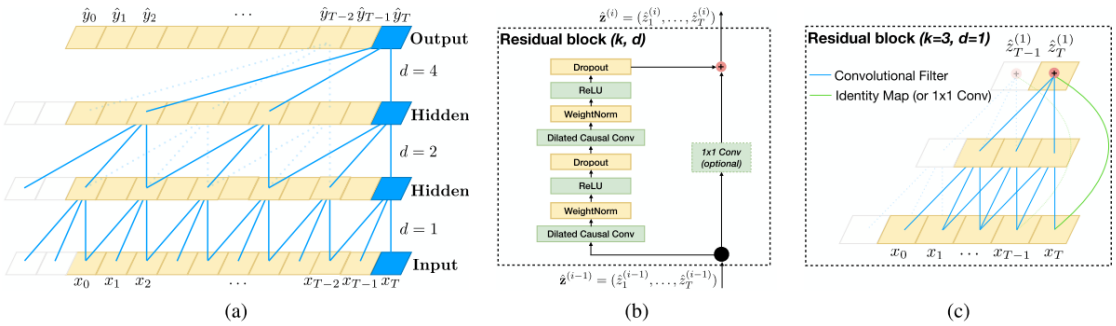


Figure 5.2: TCN architecture [153]. (a) Dilated causal convolution with dilation factors $d = 1, 2, 4$, and filter size $k = 3$. (b) Residual block where a fully convolutional network (1x1) is added to the output of dilated convolution. (c) Example of residual connection in TCN, where blue lines are filters and green lines are identity mappings.

TCN model parameters that can be tuned for model training are the number of filters (layer depth), filter size, and dilation factor number. Apart from the model parameter, there are a few general parameters that can be set to define the model such as the predicted time steps and the ratio of input to output length, which are the focus of this study.

### 5.3.2 Results and Discussions

In this study, a 50-time steps prediction was set as the goal or output for the model to predict gait activity. In addition to that, an input-output ratio of 3 to 1 was considered to define the model, which means that 150 historical time steps data is used to predict the next 50 time steps of gait activity. After a few simulations of trial and error of TCN model parameters, we set the maximum depth of layer to 3, dropout at 0.7, and kernel size at 3. In addition to TCN, other ML-based models such as RNN and LSTM were also simulated to compare how the model perform to this particular problem of gait activity prediction.

$$MAPE = \frac{1}{n} \sum_{i=1}^{n} \left| \frac{A_t - F_t}{A_t} \right| \tag{5.3.3}$$

Table 5.4 and Figure 5.3 depicted the overall comparison between the trained ML models. Mean absolute percentage error (MAPE) metric was used to evaluate the model performance as expressed in Equation 5.3.3, where $A_t$ stands for actual value at time t, $F_t$ stands for forecasted value at time t, and $n$ represent the number of time steps calculated. The result shows that TCN outperforms both RNN and LSTM at 50, 100, and 150-time steps prediction, while LSTM outperforms RNN

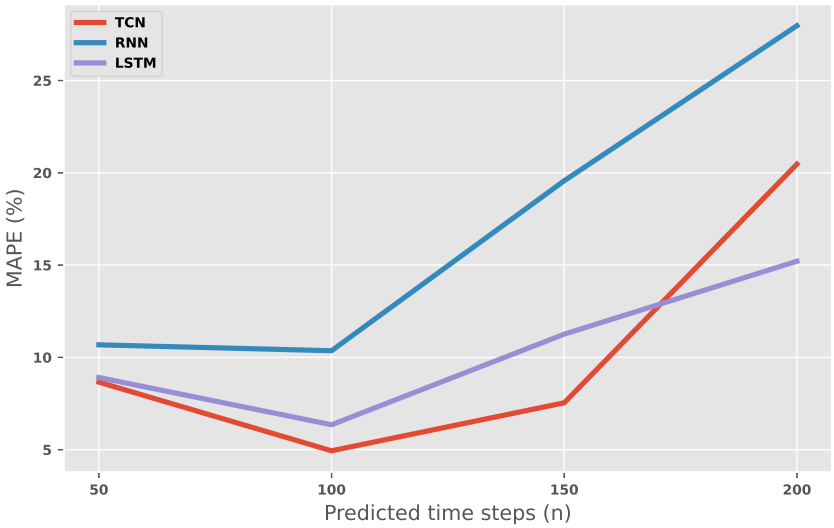


Figure 5.3: TCN, RNN, and LSTM performances against the changing of time steps prediction. TCN performs better in 50, 100, and 150 predicted time steps, while LSTM was superior on a longer 200 time steps prediction. The performance of all models were worsen as the prediction horizon increased.

and TCN at the 200-time steps prediction. Overall, the best performing model was TCN with 4.94 % MAPE at 100-time steps prediction. Another thing to be noted is that all of the models got worsened as the time steps prediction increased, where the best performance was on 100-time steps prediction.

A simple prediction problem is presented in this section, where the model tries to predict whether in the next $t$ time steps the subject will turn. This study serves as the preliminary test for the state of the art of TCN model for the gait-related application. To the best of our knowledge, this is the first attempt at the TCN model used in gait-related applications since it is first proposed in 2018. Therefore, the future work for this study is to define a more sophisticated problem in the gait-related application, such as the prediction of falls or the prediction of certain conditions such as FoG in PD patients.

## 5.4 Swing phase control

In this section, a more advanced example of machine learning implementation to gait-related applications is presented, where it is used as part of the control algorithm. A reinforcement learning (RL) based control was implemented to control a semi-active prosthetic knee during the swing phase [158]. Model-free reinforcement Q-learning control (RQLC) with a reward shaping function was proposed as the voltage controller of a magnetorheological damper-based prosthetic knee.

Table 5.4: Performance of TCN, RNN, and LSTM in MAPE (%) with various ratio input-output and predicted time steps ($t_F$). Value in **bold** represent the best performance of each model.

| | TCN | | | RNN | | | LSTM | | |
|---|---|---|---|---|---|---|---|---|---|
| $t_F$ | Ratio of input/output length | | | | | | | | |
| | 3 | 6 | 10 | 3 | 6 | 10 | 3 | 6 | 10 |
| 50 | 8.66 | 33.93 | 100.76 | 10.68 | 15.48 | 14.28 | 8.91 | 8.95 | 15.85 |
| 100 | **4.94** | 17.65 | 65.54 | **10.36** | 14.90 | 18.02 | **6.35** | 6.37 | 10.56 |
| 150 | 7.54 | 12.86 | 56.08 | 19.57 | 26.66 | 23.00 | 11.26 | 10.00 | 16.35 |
| 200 | 20.47 | 10.53 | 61.51 | 27.97 | 37.63 | 28.00 | 15.21 | 13.01 | 22.41 |

### 5.4.1 Methods

The overall of the proposed method is depicted in Figure 5.4. Dataset were obtained from real-world experiment of a subject performing treadmill walk with variable speeds. These dataset were then fed to the simulated environment consisted of system models and the proposed RQLC algorithm. System models are consisted of the double pendulum model to simulate the swing phase, and the MR damper dynamics to simulate the damping mechanism of the prosthetic knee.

RQLC algorithm, which adapting the Q-learning method, is consisted of the Q-function and the reward function blocks. The mathematical description of Q-function is depicted in Equation 5.4.1. The designed reward function is following the formula from [158], which was designed as a function of the performance index that accounts for the trajectory of the subject-specific knee angle ($\theta_K$). The RL-based control algorithm was trained to adapt to several walking speed datasets under one control policy and subsequently compared its performance with that of other control algorithms such as user-adaptive control [159] and neural network predictive (NNPC) control [160].

$$Q_{(\theta_{K(t)},\dot{\theta_{K(t)}},a_t)} \leftarrow Q_{(\theta_{K(t)},\dot{\theta_{K(t)}},a_t)} + \alpha \left[ \sum_{t=1}^{n} \beta_t R_t + \gamma \max Q_{(\theta_{K(t+1)},\dot{\theta_{K(t+1)}},a_t)} - Q_{(\theta_{K(t)},\dot{\theta_{K(t)}},a_t)} \right] \tag{5.4.1}$$

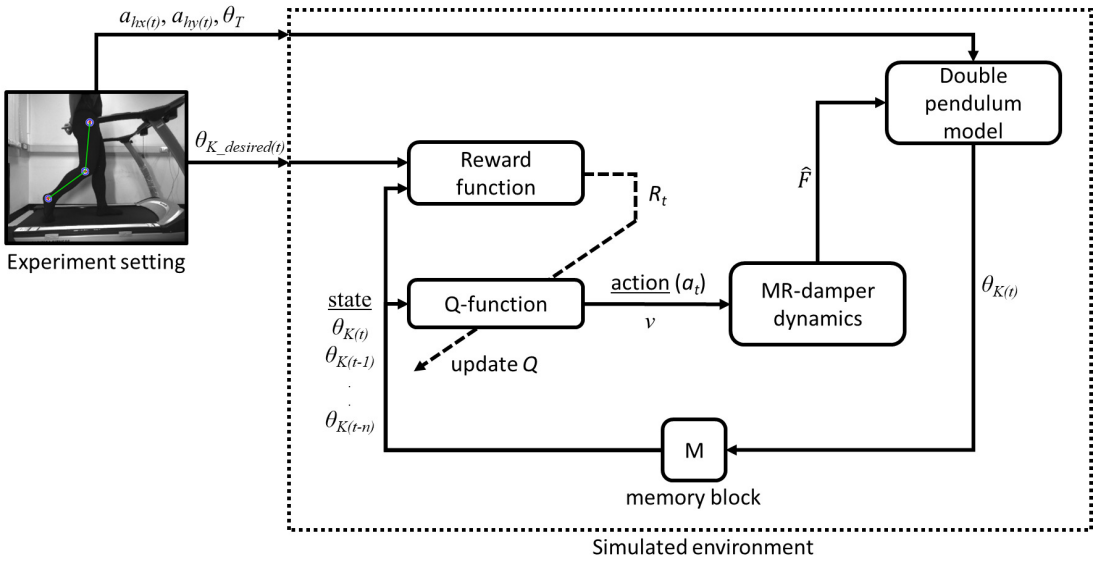


Figure 5.4: The proposed RL-based control algorithm. Data collected from the real-world experiment is fed to the simulated environment which consisted of the system models and the RQLC algorithm. Systems model is consisted of double pendulum model to simulate swing phase, and MR-damper dynamics model to simulate the damping mechanism of prosthetic knee.

### 5.4.2 Results and Discussions

In this study, we investigated our proposed control algorithm for the swing phase controller in the MR-damper-based prosthetic knee. The proposed controller was designed with the structure of a tabular reinforcement Q-learning algorithm, a subset in machine learning algorithms. The Q-learning control comprised a $Q$-function that stores its value in a Q-matrix and a reward function following the reward shaping function proposed in this study. The advantages of using this control structure are that it can be trained online, and also it is a model-free control algorithm that does not require prior knowledge of the system to be controlled. A variable reward as a function of $PI$ showed a faster convergence trend over that of a single reward function and was concluded as the better reward mechanism [158].

The proposed controller is then compared to the user-adaptive controller [159] and the NNPC algorithm [160]. The comparison of 2.4, 3.6, and 5.4 km/h walking speed are depicted in Fig.5.5. and Table 5.5. The table depicts that for the walking speed of 2.4 km/h, Q-learning method performed the best with 0.78 of $NRMSE$, compared to NNPC (0.81) and User-adaptive (2.70). Further, for the walking speed of 3.6 km/h, the best performance was achieved by NNPC with 0.61 of $NRMSE$, compared with Q-learning (0.88) and User-adaptive (3.65). Lastly, for the walking speed of 5.4 km/h, Q-learning performed the best with the lowest $NRMSE$ of 0.52, compared with NNPC (2.42) and User-adaptive (3.46). Overall, Q-learning method

perform within 1% of $NRMSE$, which followed the designed common reward function for different walking speed.

This control structure also shows adaptability to various walking speeds. Moreover, we have successfully trained a unified control policy for every simulated walking speed. $PI$ verified with the experimental result indicates that this control structure performs better than the user-adaptive control. Moreover, in some of the walking speeds, this control structure performs better than the NNPC algorithm. The total performance over different walking speeds showed promising results by using the proposed approach.

In terms of cost function, knee trajectory is only one of the parameters to be optimized among other correlated systems, such as ankle and foot prostheses, to achieve better gait symmetry and reduce metabolic costs. Although there has not been a detailed study about the acceptable criterion in terms of the $NRMSE$ performance index of the knee trajectory in a prosthetic knee, this study aims to mimic the biological knee trajectory, which is shown by $PI$.

On the applicability point of view, our proposed Q-learning control had no prior knowledge of the structure and characteristics of MR-damper. Signals observed by Q-learning control were the states of knee angle and its derivatives, as well as the reward signal $R_t$ that was given based on the performance of the controller to shape the control policy. Based on this facts, our proposed Q-learning control can potentially be used for other structure of MR-damper or even other impedance-based machine for semi-active prosthetic.

Although we cannot provide detailed comparison of our proposed method with another RL-based method in [161], a brief comparison is discussed as follows. The ADP-based RL algorithm resulted in 2.5 degrees of $RMSE$ on the robotic knee kinematics. The average performance of our proposed method was 0.73 of $NRMSE$ or was 1.59 degrees if converted to average $RMSE$. Conversely, in this study, we employed the RL algorithm to control the output of the control voltage for the MR damper, resulting in only one simple output variable. Meanwhile, this study [161] used the RL algorithm to tune a total of 12 impedance parameters of the robotic knee; thus, the output variables are 12. We also treated the swing phase as one state, while in [161], the swing phase was divided into swing flexion and swing extension where the ADP tuner would tune the impedance parameters accordingly with respect to each state.

In this study, we focused on developing a unique control that can adapt and accommodate a range of subject-specific walking speed. Unique means that it can

Table 5.5: Comparison between user adaptive, NNPC, and RQLC control

| Walking speed (km/h) | NRMSE(%) | | |
|---|---|---|---|
| | User-adaptive | NNPC | RQLC |
| 2.4 | 2.70 | 0.81 | 0.78* |
| 3.6 | 3.65 | 0.61* | 0.88 |
| 5.4 | 3.46 | 2.42 | 0.52* |
| Average | 3.27 | 1.28 | 0.73* |

*= best performance

only be valid for the subject. The reason was, like any other prosthetic, it is tuned personally to the wearer. In this study, the control policy that we train is valid only for the subject whose data we used. However, the idea of our proposed control framework and algorithm can be applied to other subjects.

While it has shown a promising result, we also identified some of the limitations of our study. Using the computational hardware mentioned at the previous section and source code implemented in MATLAB, the overall calculation and online update $Q$-function process consumed approximately 40.4 ms, while each evaluation of NNPC with pre-trained swing phase model consumed approximately 13.2 ms [160]. Changing the source code implementation in C language and using dedicated processing hardware could shorten the calculation time to be within the proposed control interval of 20 ms.

There are several areas that can be explored for future works. First, another training strategy can be explored further to shorten the calculation time. Second, this study proposed a tabular-discretized $Q$-function stored in a Q-matrix. A continuous $Q$-function could also be explored to better cover all the states and actions. Third is to test our proposed control strategy to other subjects and possibly to test a transfer learning approach from control policy that was learnt in this study for dataset from other subjects.

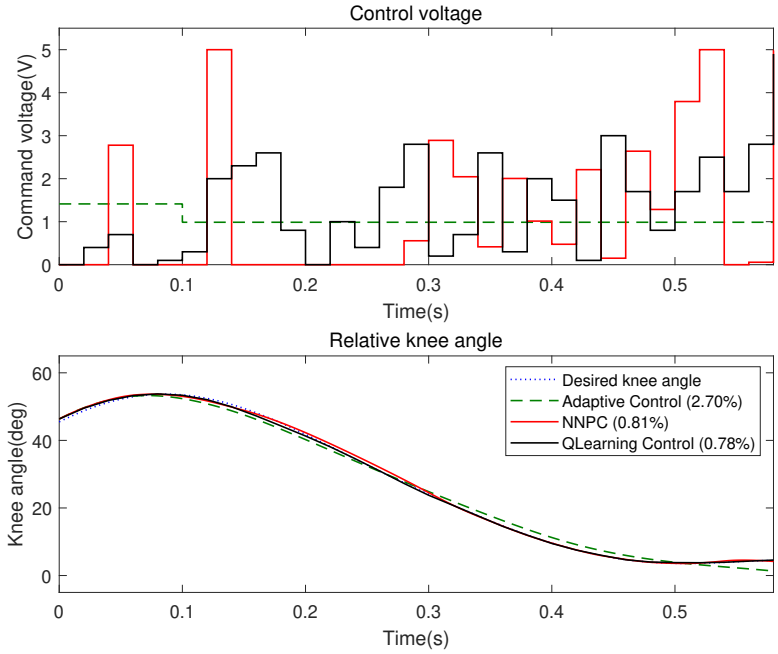


(a)

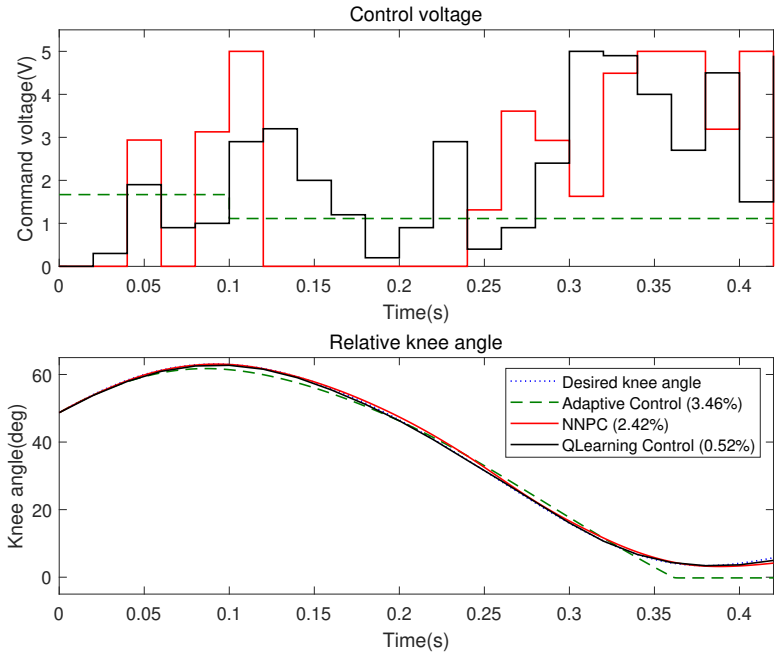


(b)

Figure 5.5: Comparison between user-adaptive control (green dashed line), NNPC (red line), and q-learning control (black line) for the slowest and fastest walking speed (a) 2.4 km/h, (b) 5.4 km/h.

# Chapter 6

# Concluding remarks

## 6.1 Summary

This thesis focused on the topic of wearable sensors for quantitative gait analysis. It was motivated by the question of whether the current state-of-the-art wearable sensors could address the challenge to provide a quantitative gait analysis. Theoretical, experimental, and simulation approaches were simultaneously conducted to investigate this grand question. Several principal outcomes have been obtained from this thesis, such as the theoretical contribution in making the systematic review which emphasized the recent advances on quantitative gait analysis through wearable sensors, the proposition of using two IMUs attached on the back of shoes to extract rich quantitative gait features in several applications, and the integration of machine learning algorithm to enrich the IMU-based gait analysis. Each of the outcomes was addressed extensively in each chapter and summarized as the following.

In chapter 2, a systematic review was conducted to gain a deeper perspective on the recent advancement of wearable sensors for gait analysis topic. PRISMA guidelines were adapted to find relevant studies using the formulated keywords. Over the course of the last ten years, a total of 76 studies were extensively discussed in this thesis regarding their impact on this research area. Wearable IMUs attached to the lower limb region were found to be the most common approach for gait analysis. Spatio-temporal features were the most common quantitative gait features extracted from wearable sensors. The application of wearable-based gait analysis was found ranging from clinical applications such as assessing gait of people with PD, stroke, and other pathological conditions related to gait, to sports applications such as running gait analysis. Several studies have also shown the interest in using machine

learning algorithms for classification problems, correction algorithms, crosschecking functions, and scoring functions. The importance of validation to a reference system or gold standard measurements such as motion capture and force plate systems was highlighted to ensure the performance accuracy and practicality of the proposed wearable approach.

In chapter 3, responding to the systematic review done in chapter 2, the proposition of using two IMU sensors to extract rich quantitative gait features was discussed. Reducing the number of sensors may compromise the accuracy of gait quantification, nevertheless, it would improve the practicality and ease of use for the wearer. In this thesis, two IMU sensors attached to the back of the shoes were proposed. The proposed system was validated to the gold standard measurement of gait analysis consisting of motion capture system and force plate systems. Results of the validation experiment show a good agreement to the reference system with 4.22 ms and 8.31 ms of temporal differences in detecting initial contact and toe-off events, respectively. On the other hand, stride length and heel vertical displacement were overestimated by an average of 7.72 cm and 2.22 cm, respectively, which were still in the range of the limit of agreement. A total of 17 features ranging from gait events/ gait phases, spatio-temporal features, and other gait features were successfully extracted using the proposed framework. Moreover, the preliminary validation presented in this chapter could clearly distinguish normal subjects from the subject with pathological gait issues.

In chapter 4, several case studies were presented to extend the application of the proposed framework. The first case study investigates the use of the proposed framework to extract temporal gait features seamlessly on subjects performing both walking and running gait in one session. The second case study expands the potential use of the proposed framework to assess the quantitative differences between single-task and dual-task gait performed by the subject. The third case study tested the proposed framework on a prolonged time, where both controlled outdoor and free outdoor experiments were performed. Although the results from all the case studies have shown a potential implementation in both clinical and sports applications, validation experiments that involve a larger pool of subjects are needed to ensure the consistency of the proposed framework.

In chapter 5, machine learning algorithms were proposed to classify gait phases, predict certain gait activity, and as swing phase control algorithm for the prosthetic knee. Three machine learning models consisting of SVM, AdaBoost, and XGBoost were trained for the classification problem, while RNN, LSTM, and TCN were trained for the prediction problem. Varying performances were observed from

each of the trained models, where XGBoost performed the best with an overall mean cross-validation accuracy of 84.54 % for gait phase classification and TCN performed the best with an average MAPE of 4.95 % on predicting gait activity within 100 predicted time steps. On the swing phase control problem, our proposed model-free reinforcement Q-learning control showed better performance on average compared to user-adaptive and NNPC from existing studies.

## 6.2 Contributions

The main contributions of this thesis are the following.

- The systematic review of state of the arts on quantitative gait analysis using wearable sensors.
- The proposition and validation of wearable-based gait analysis using two IMUs on back of the shoes to extract a feature-rich gait features.
- The demonstration of the proposed framework in three case studies, i.e. mixed walking and running gait, cognitive dual-task gait, and on a prolonged outdoor gait experiment.
- The proposition and validation of machine learning algorithms for gait phase classification, prediction of gait activity, and swing phase control of prosthetic knee.

## 6.3 Future Work

There are several things that can be considered for further investigations and improvements regarding the studies in this thesis. The following discussed the potential future works.

First, this study has verified the use of two shoes-attached IMUs for a feature-rich quantitative gait analysis on a control group of healthy subjects. Since there are various pathological conditions that can affect the gait pattern, the performance of the proposed framework in this thesis may be affected. Therefore, this calls for further benchmark experiments of the framework proposed in this thesis for specific clinical application. Another improvement that could be done regarding this matter is to try another algorithms that could potentially improve the performance of the system.

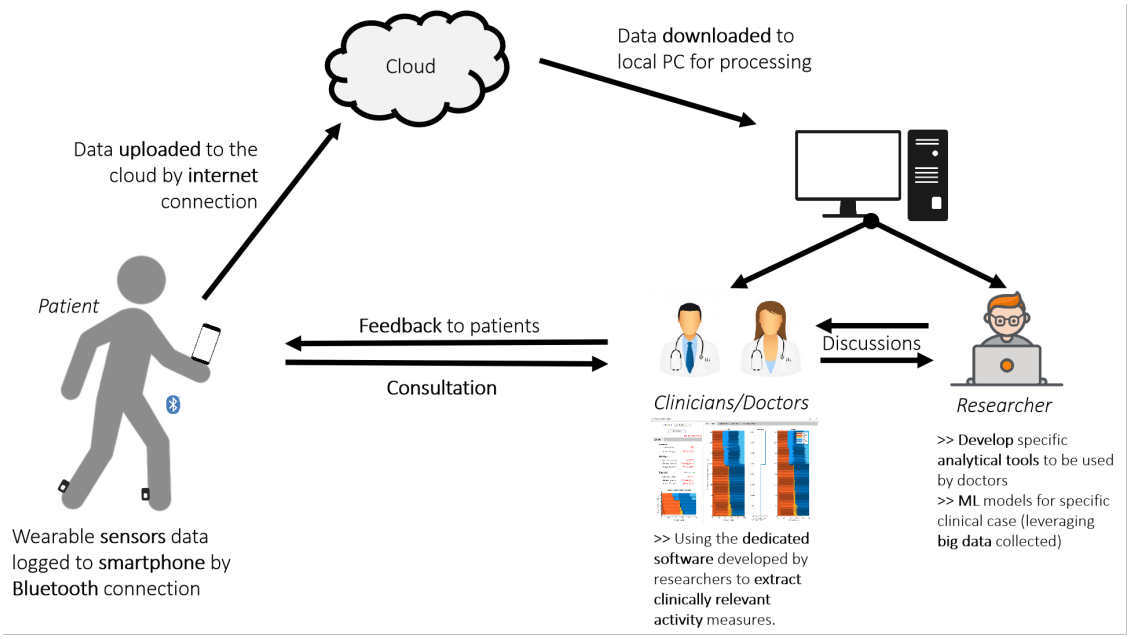


Figure 6.1: Future perspectice: a framework of real-world scenario of remote monitoring through shoes-attached sensors.

Second, this thesis has explored the possibility of using the proposed framework for various gait analysis application. Nevertheless, due to the limitation in the number of the subjects, the findings in this thesis may be limited only to the participated subjects. Therefore, the future work should consider a larger cohort to draw a more general conclusion.

Third, the proposition of machine learning algorithm in this thesis need to be explored further. In this thesis SVM and TCN were proposed for gait phase classification and prediction of gait activity, respectively. Although a comparison to a few other learning algorithms were presented, there still a need to further investigate the performance of the algorithms to other methods. Another thing to consider is to include more data to ensure the robustness of the model. On the swing phase control problem, another RL-based algorithm could also be explored to better cover all the states and actions.

### 6.3.1 Future Perspective

Since 2020 we have been asked to minimize physical contact to restrict the spread of the COVID-19 virus. This issue has highlighted an urgent need for tools to facilitate remote monitoring for certain patients. The positive trend on digital health and wearable sensors research may provide a solution to monitor physical activity while also giving relevant clinical outcomes based on the real-world continuous mea-

sure from body-worn sensors. By the time this thesis is written, there is an ongoing consortium held by several institutions in the European Union with a purpose of pushing widespread adaptation of digital measures of mobility to be used in both clinical trials and health care in general [162]. Although the proposed sensor location is different with what are proposed in this thesis, several gait features extracted such as the measure of symmetry index and variability indices were also adapted on their project [162]. Therefore, the proposition in this thesis may become an alternative solution to facilitate remote monitoring as illustrated in Figure 6.1, where patients wearing wearable IMUs on their foot to collect data of activity of daily life. The data was sent through Bluetooth connection to their phone and then uploaded to the dedicated cloud, where both doctors and researchers can download to analyze the data.

# Publications

Below are the list of publications made througout the author's PhD study at Tohoku University.

**Peer-reviewed journal articles**

Y. Hutabarat, D. Owaki, and M. Hayashibe, *"Quantitative Gait Assessment with Feature-Rich Diversity Using Two IMU Sensors,"* in **IEEE Trans. Med. Robot. Bionics**, 2020. doi: 10.1109/TMRB.2020.3021132

Y. Hutabarat, D. Owaki, and M. Hayashibe, *"Recent Advances in Quantitative Gait Analysis using Wearable Sensors: A Review,"* in **IEEE Sensors Journal**, 2021. doi: 10.1109/JSEN.2021.3119658

Y. Hutabarat, K.Ekkachai, M. Hayashibe, and W. Kongprawechnon, *"Reinforcement Q-Learning Control with Reward Shaping Function for Swing Phase Control in a Semi-Active Prosthetic Knee,"* in **Frontiers in Neurorobotics**, 2020. doi: 10.3389/fnbot.2020.565702

**Peer-reviewed conference proceedings**

Y. Hutabarat, D. Owaki, and M. Hayashibe, *"Seamless Temporal Gait Evaluation During Walking and Running Using Two IMU Sensors,"* in **EMBC 2021.**

**Submitted manuscript**

Y. Hutabarat, D. Owaki, and M. Hayashibe, *"Temporal Variation Quantification During Cognitive Dual-Task Gait Using Two IMU Sensors,"* submitted to **EMBC 2022.**

# Bibliography


[1] Y.-S. Lee, C.-S. Ho, Y. Shih, S.-Y. Chang, F. J. Róbert, and T.-Y. Shiang, "Assessment of walking, running, and jumping movement features by using the inertial measurement unit," *Gait Posture*, vol. 41, no. 4, pp. 877–881, 2015, ISSN: 0966-6362. DOI: https://doi.org/10.1016/j.gaitpost.2015.03.007.

[2] Q. Mei, J. Fernandez, W. Fu, N. Feng, and Y. Gu, "A comparative biomechanical analysis of habitually unshod and shod runners based on a foot morphological difference," *Human Movement Science*, vol. 42, pp. 38–53, 2015, ISSN: 0167-9457. DOI: https://doi.org/10.1016/j.humov.2015.04.007.

[3] B. H. Dobkin, X. Xu, M. Batalin, S. Thomas, and W. Kaiser, "Reliability and validity of bilateral ankle accelerometer algorithms for activity recognition and walking speed after stroke," *Stroke*, vol. 42, no. 8, pp. 2246–2250, 2011, ISSN: 00392499. DOI: 10.1161/STROKEAHA.110.611095.

[4] C. Punin, B. Barzallo, R. Clotet, *et al.*, "A Non-Invasive Medical Device for Parkinson's Patients with Episodes of Freezing of Gait," *Sensors (Basel, Switzerland)*, vol. 19, no. 3, 2019, ISSN: 14248220. DOI: 10.3390/s19030737.

[5] S. Del Din, A. Godfrey, and L. Rochester, "Validation of an Accelerometer to Quantify a Comprehensive Battery of Gait Characteristics in Healthy Older Adults and Parkinson's Disease: Toward Clinical and at Home Use," *IEEE Journal of Biomedical and Health Informatics*, vol. 20, no. 3, pp. 838–847, 2016, ISSN: 21682194. DOI: 10.1109/JBHI.2015.2419317.

[6] G. Rescio, A. Leone, and P. Siciliano, "Supervised machine learning scheme for electromyography-based pre-fall detection system," *Expert Systems with Applications*, vol. 100, pp. 95–105, Jun. 2018, ISSN: 09574174. DOI: 10.1016/j.eswa.2018.01.047.

[7] T. Virmani, H. Gupta, J. Shah, and L. Larson-Prior, "Objective measures of gait and balance in healthy non-falling adults as a function of age," *Gait*

*Posture*, vol. 65, pp. 100–105, Sep. 2018, ISSN: 09666362. DOI: 10.1016/j.gaitpost.2018.07.167.

[8] M. B. Nebel, E. L. Sims, F. J. Keefe, *et al.*, "The Relationship of Self-Reported Pain and Functional Impairment to Gait Mechanics in Overweight and Obese Persons With Knee Osteoarthritis," *Archives of Physical Medicine and Rehabilitation*, vol. 90, no. 11, pp. 1874–1879, Nov. 2009, ISSN: 00039993. DOI: 10.1016/j.apmr.2009.07.010. eprint: NIHMS150003.

[9] M. Benedetti, V. Agostini, M. Knaflitz, V. Gasparroni, M. Boschi, and R. Piperno, "Self-reported gait unsteadiness in mildly impaired neurological patients: an objective assessment through statistical gait analysis," *Journal of NeuroEngineering and Rehabilitation*, vol. 9, no. 1, p. 64, 2012, ISSN: 1743-0003. DOI: 10.1186/1743-0003-9-64.

[10] S. Fritz and M. Lusardi, "White paper: "walking speed: The sixth vital sign"," *Journal of Geriatric Physical Therapy*, vol. 32, no. 2, pp. 2–5, 2009, ISSN: 15398412. DOI: 10.1519/00139143-200932020-00002.

[11] L. C. Benson, C. A. Clermont, E. Bošnjak, and R. Ferber, "The use of wearable devices for walking and running gait analysis outside of the lab: A systematic review.," *Gait posture*, vol. 63, pp. 124–138, Jun. 2018, ISSN: 1879-2219 (Electronic). DOI: 10.1016/j.gaitpost.2018.04.047.

[12] G. Quer, J. M. Radin, M. Gadaleta, *et al.*, "Wearable sensor data and self-reported symptoms for COVID-19 detection," *Nature Medicine*, vol. 27, no. 1, pp. 73–77, Jan. 2021, ISSN: 1078-8956. DOI: 10.1038/s41591-020-1123-x.

[13] J. Dunn, L. Kidzinski, R. Runge, *et al.*, "Wearable sensors enable personalized predictions of clinical laboratory measurements," *Nature Medicine*, 2021, ISSN: 1078-8956. DOI: 10.1038/s41591-021-01339-0.

[14] D. Trojaniello, A. Ravaschio, J. M. Hausdorff, and A. Cereatti, "Comparative assessment of different methods for the estimation of gait temporal parameters using a single inertial sensor: application to elderly, post-stroke, Parkinson's disease and Huntington's disease subjects," *Gait Posture*, vol. 42, no. 3, pp. 310–316, Sep. 2015, ISSN: 09666362. DOI: 10.1016/j.gaitpost.2015.06.008.

[15] S. Bolink, E. Lenguerrand, L. Brunton, *et al.*, "Assessment of physical function following total hip arthroplasty: Inertial sensor based gait analysis is supplementary to patient-reported outcome measures," *Clinical Biomechanics*, vol. 32, pp. 171–179, Feb. 2016, ISSN: 02680033. DOI: 10.1016/j.clinbiomech.2015.11.014.

[16] P. P. Panciani, K. Migliorati, A. Muratori, M. Gelmini, A. Padovani, and M. Fontanella, "Computerized gait analysis with inertial sensor in the management of idiopathic normal pressure hydrocephalus.," *European journal of physical and rehabilitation medicine*, vol. 54, no. 5, pp. 724–729, Oct. 2018, ISSN: 1973-9095 (Electronic). DOI: 10.23736/S1973-9087.18.04949-3.

[17] F. De Cillis, F. De Simio, and R. Setola, "Long-term gait pattern assessment using a tri-axial accelerometer," *Journal of Medical Engineering Technology*, vol. 41, no. 5, pp. 346–361, Jul. 2017, ISSN: 0309-1902. DOI: 10.1080/03091902.2017.1293741.

[18] A. Rodríguez-Molinero, A. Samà, C. Pérez-López, *et al.*, "Analysis of Correlation between an Accelerometer-Based Algorithm for Detecting Parkinsonian Gait and UPDRS Subscales," *Frontiers in Neurology*, vol. 8, no. SEP, Sep. 2017, ISSN: 1664-2295. DOI: 10.3389/fneur.2017.00431.

[19] I. Carpinella, D. Cattaneo, G. Bonora, *et al.*, "Wearable Sensor-Based Biofeedback Training for Balance and Gait in Parkinson Disease: A Pilot Randomized Controlled Trial.," eng, *Archives of physical medicine and rehabilitation*, vol. 98, no. 4, 622–630.e3, Apr. 2017, ISSN: 1532-821X (Electronic). DOI: 10.1016/j.apmr.2016.11.003.

[20] B. M. Bartels, A. Moreno, M. J. Quezada, H. Sivertson, J. Abbas, and N. Krishnamurthi, "Real-Time Feedback Derived from Wearable Sensors to Improve Gait in Parkinson's Disease," *Technology Innovation*, vol. 20, no. 1, pp. 37–46, Nov. 2018, ISSN: 1949-8241. DOI: 10.21300/20.1-2.2018.37.

[21] L. Angelini, I. Carpinella, D. Cattaneo, *et al.*, "Is a Wearable Sensor-Based Characterisation of Gait Robust Enough to Overcome Differences Between Measurement Protocols? A Multi-Centric Pragmatic Study in Patients with Multiple Sclerosis," *Sensors*, vol. 20, no. 1, p. 79, Dec. 2019, ISSN: 1424-8220. DOI: 10.3390/s20010079.

[22] S. Shirai, I. Yabe, I. Takahashi-Iwata, *et al.*, "The Responsiveness of Triaxial Accelerometer Measurement of Gait Ataxia Is Higher than That of the Scale for the Assessment and Rating of Ataxia in the Early Stages of Spinocerebellar Degeneration," *The Cerebellum*, vol. 18, no. 4, pp. 721–730, Aug. 2019, ISSN: 1473-4222. DOI: 10.1007/s12311-019-01025-5. [Online]. Available: http://link.springer.com/10.1007/s12311-019-01025-5.

[23] B. Hobbs and P. Artemiadis, "A Review of Robot-Assisted Lower-Limb Stroke Therapy: Unexplored Paths and Future Directions in Gait Rehabilitation," *Frontiers in Neurorobotics*, vol. 14, no. April, 2020, ISSN: 16625218. DOI: 10.3389/fnbot.2020.00019.

[24] A. Liberati, D. G. Altman, J. Tetzlaff, *et al.*, "The PRISMA statement for reporting systematic reviews and meta-analyses of studies that evaluate health care interventions: explanation and elaboration," *Journal of clinical epidemiology*, vol. 62, no. 10, e1–34, 2009, ISSN: 18785921. DOI: 10.1016/j.jclinepi.2009.06.006. eprint: arXiv:1011.1669v3.

[25] D. Kobsar, Z. Masood, H. Khan, *et al.*, "Wearable Inertial Sensors for Gait Analysis in Adults with Osteoarthritis—A Scoping Review," *Sensors*, vol. 20, no. 24, p. 7143, Dec. 2020, ISSN: 1424-8220. DOI: 10.3390/s20247143.

[26] I. T. G. de Oliveira Gondim, C. d. C. B. de Souza, M. A. B. Rodrigues, I. M. Azevedo, M. d. G. W. de Sales Coriolano, and O. G. Lins, "Portable accelerometers for the evaluation of spatio-temporal gait parameters in people with Parkinson's disease: an integrative review," *Archives of Gerontology and Geriatrics*, vol. 90, p. 104 097, Sep. 2020, ISSN: 01674943. DOI: 10.1016/j.archger.2020.104097.

[27] P. R. F. Junior, R. C. F. de Moura, C. S. Oliveira, and F. Politti, "Use of wearable inertial sensors for the assessment of spatiotemporal gait variables in children: A systematic review," *Motriz: Revista de Educação Física*, vol. 26, no. 3, pp. 1–11, 2020, ISSN: 1980-6574. DOI: 10.1590/s1980-6574202000030139.

[28] S. Díaz, J. B. Stephenson, and M. A. Labrador, "Use of Wearable Sensor Technology in Gait, Balance, and Range of Motion Analysis," *Applied Sciences*, vol. 10, no. 1, p. 234, Dec. 2019, ISSN: 2076-3417. DOI: 10.3390/app10010234.

[29] P. Dasgupta, J. VanSwearingen, A. Godfrey, M. Redfern, M. Montero-Odasso, and E. Sejdic, "Acceleration Gait Measures as Proxies for Motor Skill of Walking: A Narrative Review," *IEEE Transactions on Neural Systems and Rehabilitation Engineering*, vol. 29, pp. 249–261, 2021, ISSN: 1534-4320. DOI: 10.1109/TNSRE.2020.3044260.

[30] A. Saboor, T. Kask, A. Kuusik, *et al.*, "Latest Research Trends in Gait Analysis Using Wearable Sensors and Machine Learning: A Systematic Review," *IEEE Access*, vol. 8, pp. 167 830–167 864, 2020, ISSN: 2169-3536. DOI: 10.1109/ACCESS.2020.3022818.

[31] W. Tao, T. Liu, R. Zheng, and H. Feng, "Gait analysis using wearable sensors," *Sensors*, vol. 12, no. 2, pp. 2255–2283, 2012, ISSN: 14248220. DOI: 10.3390/s120202255.

[32] I. H. Lopez-Nava and A. Munoz-Melendez, "Wearable Inertial Sensors for Human Motion Analysis: A Review," *IEEE Sensors Journal*, vol. 16, no. 22, pp. 7821–7834, Nov. 2016, ISSN: 1530-437X. DOI: 10.1109/JSEN.2016.2609392.

[33] R. Caldas, M. Mundt, W. Potthast, F. Buarque de Lima Neto, and B. Markert, "A systematic review of gait analysis methods based on inertial sensors and adaptive algorithms," *Gait and Posture*, vol. 57, no. February, pp. 204–210, 2017, ISSN: 18792219. DOI: 10.1016/j.gaitpost.2017.06.019.

[34] T. Watanabe, H. Saito, E. Koike, and K. Nitta, "A preliminary test of measurement of joint angles and stride length with wireless inertial sensors for wearable gait evaluation system," *Computational Intelligence and Neuroscience*, vol. 2011, pp. 1–12, 2011, ISSN: 1687-5265. DOI: 10.1155/2011/975193.

[35] S. Zhu, H. Anderson, and Y. Wang, "A Real-Time On-Chip Algorithm for IMU-Based Gait Measurement," *Lecture Notes in Computer Science (including subseries Lecture Notes in Artificial Intelligence and Lecture Notes in Bioinformatics)*, vol. 7674 LNCS, pp. 93–104, 2012. DOI: 10.1007/978-3-642-34778-8_9.

[36] D. McGrath, B. R. Greene, K. J. O'Donovan, and B. Caulfield, "Gyroscope-based assessment of temporal gait parameters during treadmill walking and running," *Sports Engineering*, vol. 15, no. 4, pp. 207–213, 2012. DOI: 10.1007/s12283-012-0093-8.

[37] F. Bugané, M. Benedetti, G. Casadio, *et al.*, "Estimation of spatial-temporal gait parameters in level walking based on a single accelerometer: Validation on normal subjects by standard gait analysis," *Computer Methods and Programs in Biomedicine*, vol. 108, no. 1, pp. 129–137, Oct. 2012, ISSN: 01692607. DOI: 10.1016/j.cmpb.2012.02.003.

[38] H. Rouhani, J. Favre, X. Crevoisier, and K. Aminian, "Measurement of multi-segment foot joint angles during gait using a wearable system.," *Journal of biomechanical engineering*, vol. 134, no. 6, p. 61 006, Jun. 2012, ISSN: 1528-8951 (Electronic). DOI: 10.1115/1.4006674.

[39] A. Dalton, H. Khalil, M. Busse, A. Rosser, R. van Deursen, and G. ÓLaighin, "Analysis of gait and balance through a single triaxial accelerometer in presymptomatic and symptomatic Huntington's disease," *Gait Posture*, vol. 37, no. 1, pp. 49–54, Jan. 2013, ISSN: 09666362. DOI: 10.1016/j.gaitpost.2012.05.028.

[40] O. Tirosh, R. Begg, E. Passmore, and N. Knopp-Steinberg, "Wearable textile sensor sock for gait analysis," in *2013 Seventh International Conference on Sensing Technology (ICST)*, 2013, pp. 618–622. DOI: 10.1109/ICSensT.2013.6727727.

[41] J. C. Van Den Noort, A. Ferrari, A. G. Cutti, J. G. Becher, and J. Harlaar, "Gait analysis in children with cerebral palsy via inertial and magnetic sensors," *Medical and Biological Engineering and Computing*, vol. 51, no. 4, pp. 377–386, 2013. DOI: 10.1007/s11517-012-1006-5.

[42] B. Mariani, M. C. Jiménez, F. J. G. Vingerhoets, and K. Aminian, "On-Shoe Wearable Sensors for Gait and Turning Assessment of Patients With Parkinson's Disease," *IEEE Transactions on Biomedical Engineering*, vol. 60, no. 1, pp. 155–158, Jan. 2013, ISSN: 0018-9294. DOI: 10.1109/TBME.2012.2227317.

[43] S. Tadano, R. Takeda, and H. Miyagawa, "Three Dimensional Gait Analysis Using Wearable Acceleration and Gyro Sensors Based on Quaternion Calculations," *Sensors*, vol. 13, no. 7, pp. 9321–9343, Jul. 2013, ISSN: 1424-8220. DOI: 10.3390/s130709321.

[44] F. Martínez-Martí, M. S. Martínez-García, S. G. García-Díaz, J. García-Jiménez, A. J. Palma, and M. A. Carvajal, "Embedded sensor insole for wireless measurement of gait parameters," *Australasian Physical Engineering Sciences in Medicine*, vol. 37, no. 1, pp. 25–35, Mar. 2014, ISSN: 0158-9938. DOI: 10.1007/s13246-013-0236-7.

[45] D. Jarchi, C. Wong, R. M. Kwasnicki, B. Heller, G. A. Tew, and Guang-Zhong Yang, "Gait Parameter Estimation From a Miniaturized Ear-Worn Sensor Using Singular Spectrum Analysis and Longest Common Subsequence," *IEEE Transactions on Biomedical Engineering*, vol. 61, no. 4, pp. 1261–1273, Apr. 2014, ISSN: 0018-9294. DOI: 10.1109/TBME.2014.2299772.

[46] A. Brégou Bourgeois, B. Mariani, K. Aminian, P. Y. Zambelli, and C. J. Newman, "Spatio-temporal gait analysis in children with cerebral palsy using, foot-worn inertial sensors," *Gait and Posture*, vol. 39, no. 1, pp. 436–442, Jan. 2014, ISSN: 0966-6362. DOI: 10.1016/j.gaitpost.2013.08.029.

[47] A. Godfrey, S. Del Din, G. Barry, J. C. Mathers, and L. Rochester, "Within trial validation and reliability of a single tri-axial accelerometer for gait assessment," in *2014 36th Annual International Conference of the IEEE Engineering in Medicine and Biology Society*, IEEE, Aug. 2014, pp. 5892–5895, ISBN: 978-1-4244-7929-0. DOI: 10.1109/EMBC.2014.6944969.

[48] T. Liu, Y. Inoue, K. Shibata, K. Shiojima, and M. M. Han, "Triaxial joint moment estimation using a wearable three-dimensional gait analysis system," *Measurement*, vol. 47, pp. 125–129, 2014, ISSN: 0263-2241. DOI: https://doi.org/10.1016/j.measurement.2013.08.020.

[49] Y. Mengüç, Y.-L. Park, H. Pei, *et al.*, "Wearable soft sensing suit for human gait measurement," *The International Journal of Robotics Research*, vol. 33, no. 14, pp. 1748–1764, Dec. 2014, ISSN: 0278-3649. DOI: 10.1177/0278364914543793.

[50] K. Ben Mansour, N. Rezzoug, and P. Gorce, "Analysis of several methods and inertial sensors locations to assess gait parameters in able-bodied subjects," *Gait and Posture*, vol. 42, no. 4, pp. 409–414, 2015. DOI: 10.1016/j.gaitpost.2015.05.020.

[51] C. M. Kanzler, J. Barth, A. Rampp, *et al.*, "Inertial sensor based and shoe size independent gait analysis including heel and toe clearance estimation," in *2015 37th Annual International Conference of the IEEE Engineering in Medicine and Biology Society (EMBC)*, 2015, pp. 5424–5427. DOI: 10.1109/EMBC.2015.7319618.

[52] S. Crea, C. Cipriani, M. Donati, M. C. Carrozza, and N. Vitiello, "Providing time-discrete gait information by wearable feedback apparatus for lower-limb amputees: usability and functional validation.," *IEEE Transactions on Neural Systems and Rehabilitation Engineering*, vol. 23, no. 2, pp. 250–7, Mar. 2015, ISSN: 1558-0210. DOI: 10.1109/TNSRE.2014.2365548.

[53] S. Shirai, I. Yabe, M. Matsushima, Y. M. Ito, M. Yoneyama, and H. Sasaki, "Quantitative evaluation of gait ataxia by accelerometers.," *Journal of the neurological sciences*, vol. 358, no. 1-2, pp. 253–258, Nov. 2015, ISSN: 1878-5883 (Electronic). DOI: 10.1016/j.jns.2015.09.004.

[54] C. Buckley, B. Galna, L. Rochester, and C. Mazzà, "Attenuation of Upper Body Accelerations during Gait: Piloting an Innovative Assessment Tool for Parkinson's Disease," *BioMed Research International*, vol. 2015, pp. 1–6, 2015, ISSN: 2314-6133. DOI: 10.1155/2015/865873.

[55] H. Chang, Y. Hsu, S. Yang, J. Lin, and Z. Wu, "A Wearable Inertial Measurement System With Complementary Filter for Gait Analysis of Patients With Stroke or Parkinson's Disease," *IEEE Access*, vol. 4, pp. 8442–8453, 2016. DOI: 10.1109/ACCESS.2016.2633304.

[56] S. Byun, J. W. Han, T. H. Kim, and K. W. Kim, "Test-Retest Reliability and Concurrent Validity of a Single Tri-Axial Accelerometer-Based Gait Analysis in Older Adults with Normal Cognition," *PLOS ONE*, vol. 11, no. 7, A. Fasano, Ed., e0158956, Jul. 2016, ISSN: 1932-6203. DOI: 10.1371/journal.pone.0158956.

[57] D. Jarchi, B. Lo, C. Wong, E. Ieong, D. Nathwani, and G.-Z. Yang, "Gait Analysis From a Single Ear-Worn Sensor: Reliability and Clinical Evaluation for Orthopaedic Patients," *IEEE Transactions on Neural Systems and Rehabilitation Engineering*, vol. 24, no. 8, pp. 882–892, Aug. 2016, ISSN: 1534-4320. DOI: 10.1109/TNSRE.2015.2477720.

[58] W. Chen, Y. Xu, J. Wang, and J. Zhang, "Kinematic Analysis of Human Gait Based on Wearable Sensor System for Gait Rehabilitation," *Journal of Medical and Biological Engineering*, vol. 36, no. 6, pp. 843–856, 2016. DOI: 10.1007/s40846-016-0179-z.

[59] C. Soaz and K. Diepold, "Step Detection and Parameterization for Gait Assessment Using a Single Waist-Worn Accelerometer," *IEEE Transactions on Biomedical Engineering*, vol. 63, no. 5, pp. 933–942, May 2016, ISSN: 0018-9294. DOI: 10.1109/TBME.2015.2480296.

[60] L. Donath, O. Faude, E. Lichtenstein, G. Pagenstert, C. Nüesch, and A. Mündermann, "Mobile inertial sensor based gait analysis: Validity and reliability of spatiotemporal gait characteristics in healthy seniors.," *Gait posture*, vol. 49, pp. 371–374, Sep. 2016, ISSN: 1879-2219 (Electronic). DOI: 10.1016/j.gaitpost.2016.07.269.

[61] A. Pacilli, I. Mileti, M. Germanotta, *et al.*, "A Wearable Setup for Auditory Cued Gait Analysis in Patients with Parkinson's Disease," in *2016 IEEE International Symposium on Medical Measurements and Application (MEMEA)*, ser. IEEE International Symposium on Medical Measurements and Applications Proceedings-MeMeA, IEEE; IEEE Instrumentat Measurement Soc, IEEE, 2016, pp. 551–556, ISBN: 978-1-4673-9172-6.

[62] N. Carbonaro, F. Lorussi, and A. Tognetti, "Assessment of a Smart Sensing Shoe for Gait Phase Detection in Level Walking," *Electronics*, vol. 5, no. 4, p. 78, Nov. 2016, ISSN: 2079-9292. DOI: 10.3390/electronics5040078.

[63] C. Tunca, N. Pehlivan, N. Ak, B. Arnrich, G. Salur, and C. Ersoy, "Inertial Sensor-Based Robust Gait Analysis in Non-Hospital Settings for Neurological Disorders," *Sensors*, vol. 17, no. 4, p. 825, Apr. 2017, ISSN: 1424-8220. DOI: 10.3390/s17040825.

[64] V. Agostini, L. Gastaldi, V. Rosso, M. Knaflitz, and S. Tadano, "A Wearable Magneto-Inertial System for Gait Analysis (H-Gait): Validation on Normal Weight and Overweight/Obese Young Healthy Adults," *Sensors*, vol. 17, no. 10, p. 2406, Oct. 2017, ISSN: 1424-8220. DOI: 10.3390/s17102406.

[65] A. Suppa, A. Kita, G. Leodori, *et al.*, "l-DOPA and Freezing of Gait in Parkinson's Disease: Objective Assessment through a Wearable Wireless System.," *Frontiers in neurology*, vol. 8, p. 406, 2017, ISSN: 1664-2295 (Print). DOI: 10.3389/fneur.2017.00406.

[66] S. Qiu, Z. Wang, H. Zhao, and O. Hu, "Heterogeneous data fusion for three-dimensional gait analysis using wearable MARG sensors," *International Journal of Computational Science and Engineering*, vol. 14, no. 3, p. 222, 2017, ISSN: 1742-7185. DOI: 10.1504/IJCSE.2017.084154.

[67] M. Boutaayamou, V. Denöel, O. Brüls, *et al.*, "Algorithm for temporal gait analysis using wireless foot-mounted accelerometers," *Communications in Computer and Information Science*, vol. 690, pp. 236–254, 2017. DOI: 10.1007/978-3-319-54717-6_14.

[68] Y. Moon, R. S. McGinnis, K. Seagers, *et al.*, "Monitoring gait in multiple sclerosis with novel wearable motion sensors.," *PloS one*, vol. 12, no. 2, e0171346, 2017, ISSN: 1932-6203 (Electronic). DOI: 10.1371/journal.pone.0171346.

[69] K. Orlowski, F. Eckardt, F. Herold, N. Aye, J. Edelmann-Nusser, and K. Witte, "Examination of the reliability of an inertial sensor-based gait analysis system.," *Biomedizinische Technik. Biomedical engineering*, vol. 62, no. 6, pp. 615–622, Nov. 2017, ISSN: 1862-278X (Electronic). DOI: 10.1515/bmt-2016-0067.

[70] S. A. Moore, A. Hickey, S. Lord, S. Del Din, A. Godfrey, and L. Rochester, "Comprehensive measurement of stroke gait characteristics with a single accelerometer in the laboratory and community: a feasibility, validity and reliability study," *Journal of NeuroEngineering and Rehabilitation*, vol. 14, no. 1, p. 130, Dec. 2017, ISSN: 1743-0003. DOI: 10.1186/s12984-017-0341-z.

[71] X. Chen, S. Liao, S. Cao, D. Wu, and X. Zhang, "An Acceleration-Based Gait Assessment Method for Children with Cerebral Palsy," *Sensors*, vol. 17, no. 5, p. 1002, May 2017, ISSN: 1424-8220. DOI: 10.3390/s17051002.

[72] S. Rogan, R. de Bie, and E. Douwe de Bruin, "Sensor-based foot-mounted wearable system and pressure sensitive gait analysis," *Zeitschrift für Gerontologie und Geriatrie*, vol. 50, no. 6, pp. 488–497, Aug. 2017, ISSN: 0948-6704. DOI: 10.1007/s00391-016-1124-z.

[73] J. L. Lanovaz, A. R. Oates, T. T. Treen, J. Unger, and K. E. Musselman, "Validation of a commercial inertial sensor system for spatiotemporal gait measurements in children," *Gait Posture*, vol. 51, pp. 14–19, Jan. 2017, ISSN: 09666362. DOI: 10.1016/j.gaitpost.2016.09.021.

[74] S. Khandelwal and N. Wickström, "Evaluation of the performance of accelerometer based gait event detection algorithms in different real-world scenarios using the MAREA gait database," *Gait Posture*, vol. 51, pp. 84–90, Jan. 2017, ISSN: 09666362. DOI: 10.1016/j.gaitpost.2016.09.023.

[75] G. Pacini Panebianco, M. C. Bisi, R. Stagni, and S. Fantozzi, "Analysis of the performance of 17 algorithms from a systematic review: Influence of sensor position, analysed variable and computational approach in gait timing estimation from IMU measurements," *Gait Posture*, vol. 66, pp. 76–82, Oct. 2018, ISSN: 09666362. DOI: 10.1016/j.gaitpost.2018.08.025.

[76] R. Mc Ardle, R. Morrisa, A. Hickey, *et al.*, "Gait in Mild Alzheimer's Disease: Feasibility of Multi-Center Measurement in the Clinic and Home with Body-Worn Sensors: A Pilot Study," *Journal of Alzheimer's Disease*, vol. 63, no. 4, pp. 1557–1557, May 2018, ISSN: 13872877. DOI: 10.3233/JAD-189003.

[77] H. De Vroey, F. Staes, I. Weygers, *et al.*, "The implementation of inertial sensors for the assessment of temporal parameters of gait in the knee arthroplasty population," *Clinical Biomechanics*, vol. 54, pp. 22–27, 2018. DOI: 10.1016/j.clinbiomech.2018.03.002.

[78] C. Caramia, D. Torricelli, M. Schmid, *et al.*, "IMU-Based Classification of Parkinson's Disease From Gait: A Sensitivity Analysis on Sensor Location and Feature Selection," *IEEE Journal of Biomedical and Health Informatics*, vol. 22, no. 6, pp. 1765–1774, Nov. 2018, ISSN: 2168-2194. DOI: 10.1109/JBHI.2018.2865218.

[79] S. Qiu, L. Liu, H. Zhao, Z. Wang, and Y. Jiang, "MEMS Inertial Sensors Based Gait Analysis for Rehabilitation Assessment via Multi-Sensor Fusion.," *Micromachines*, vol. 9, no. 9, Sep. 2018, ISSN: 2072-666X (Print). DOI: 10.3390/mi9090442.

[80] W. Teufl, M. Lorenz, M. Miezal, *et al.*, "Towards inertial sensor based mobile gait analysis: Event-detection and spatio-temporal parameters," *Sensors (Switzerland)*, vol. 19, no. 1, Jan. 2018, ISSN: 1424-8220. DOI: 10.3390/s19010038.

[81] M. Fusca, F. Negrini, P. Perego, L. Magoni, F. Molteni, and G. Andreoni, "Validation of a wearable IMU system for gait analysis: Protocol and application to a new system," *Applied Sciences (Switzerland)*, vol. 8, no. 7, 2018. DOI: 10.3390/app8071167.

[82] N. Roth, C. F. Martindale, H. Gaßner, Z. Kohl, J. Klucken, and B. M. Eskofer, "Synchronized sensor insoles for clinical gait analysis in home-monitoring applications," *Current Directions in Biomedical Engineering*, vol. 4, no. 1, pp. 433–437, 2018. DOI: 10.1515/cdbme-2018-0103.

[83] E. Papi, Y. N. Bo, and A. H. McGregor, "A flexible wearable sensor for knee flexion assessment during gait," *Gait Posture*, vol. 62, pp. 480–483, May 2018, ISSN: 09666362. DOI: 10.1016/j.gaitpost.2018.04.015.

[84] A. R. Anwary, H. Yu, and M. Vassallo, "Optimal Foot Location for Placing Wearable IMU Sensors and Automatic Feature Extraction for Gait Analysis," *IEEE Sensors Journal*, vol. 18, no. 6, pp. 2555–2567, Mar. 2018, ISSN: 1530437X. DOI: 10.1109/JSEN.2017.2786587.

[85] A. M. Keppler, T. Nuritidinow, A. Mueller, *et al.*, "Validity of accelerometry in step detection and gait speed measurement in orthogeriatric patients.," *PloS one*, vol. 14, no. 8, e0221732, 2019, ISSN: 1932-6203 (Electronic). DOI: 10.1371/journal.pone.0221732.

[86] S. Qiu, L. Liu, Z. Wang, *et al.*, "Body Sensor Network-Based Gait Quality Assessment for Clinical Decision-Support via Multi-Sensor Fusion," *IEEE Access*, vol. 7, pp. 59 884–59 894, 2019. DOI: 10.1109/ACCESS.2019.2913897.

[87] S. Qiu, Z. Wang, H. Zhao, *et al.*, "Body Sensor Network-Based Robust Gait Analysis: Toward Clinical and at Home Use," *IEEE Sensors Journal*, vol. 19, no. 19, pp. 8393–8401, 2019. DOI: 10.1109/JSEN.2018.2860938.

[88] P. Pierleoni, A. Belli, L. Palma, *et al.*, "Validation of a Gait Analysis Algorithm for Wearable Sensors," in *2019 International Conference on Sensing and Instrumentation in IoT Era (ISSI)*, IEEE, Aug. 2019, pp. 1–6, ISBN: 978-1-7281-1022-6. DOI: 10.1109/ISSI47111.2019.9043647.

[89] F. García-Pinillos, P. Á. Latorre-Román, V. M. Soto-Hermoso, *et al.*, "Agreement between the spatiotemporal gait parameters from two different wearable devices and high-speed video analysis," *PLOS ONE*, vol. 14, no. 9, D. Boullosa, Ed., e0222872, Sep. 2019, ISSN: 1932-6203. DOI: 10.1371/journal.pone.0222872.

[90] L. Meng, U. Martinez-Hernandez, C. Childs, A. A. Dehghani-Sanij, and A. Buis, "A Practical Gait Feedback Method Based on Wearable Inertial Sensors for a Drop Foot Assistance Device," *IEEE Sensors Journal*, vol. 19, no. 24, pp. 12 235–12 243, Dec. 2019, ISSN: 1530-437X. DOI: 10.1109/JSEN.2019.2938764.

[91] N. Lefeber, M. Degelaen, C. Truyers, I. Safin, and D. Beckwee, "Validity and Reproducibility of Inertial Physilog Sensors for Spatiotemporal Gait Analysis in Patients With Stroke," *IEEE Transactions on Neural Systems and Rehabilitation Engineering*, vol. 27, no. 9, pp. 1865–1874, Sep. 2019, ISSN: 1534-4320. DOI: 10.1109/TNSRE.2019.2930751.

[92] Wang, Kim, Shin, and Min, "Preliminary Clinical Application of Textile Insole Sensor for Hemiparetic Gait Pattern Analysis," *Sensors*, vol. 19, no. 18, p. 3950, Sep. 2019, ISSN: 1424-8220. DOI: 10.3390/s19183950.

[93] R. De Ridder, J. Lebleu, T. Willems, C. De Blaiser, C. Detrembleur, and P. Roosen, "Concurrent Validity of a Commercial Wireless Trunk Triaxial Accelerometer System for Gait Analysis.," *Journal of sport rehabilitation*, vol. 28, no. 6, Aug. 2019, ISSN: 1543-3072 (Electronic). DOI: 10.1123/jsr.2018-0295.

[94] J. Yang, T.-H. Huang, S. Yu, *et al.*, "Machine Learning Based Adaptive Gait Phase Estimation Using Inertial Measurement Sensors," in *2019 Design of Medical Devices Conference*, vol. 19, American Society of Mechanical Engineers, Apr. 2019, pp. 12 235–12 243, ISBN: 978-0-7918-4103-7. DOI: 10.1115/DMD2019-3266.

[95] D. Phan, N. Nguyen, P. N. Pathirana, M. Horne, L. Power, and D. Szmulewicz, "A Random Forest Approach for Quantifying Gait Ataxia With Truncal and Peripheral Measurements Using Multiple Wearable Sensors," *IEEE Sensors Journal*, vol. 20, no. 2, pp. 723–734, 2020. DOI: 10.1109/JSEN.2019.2943879.

[96] M. Lueken, L. Mueller, M. G. Decker, C. Bollheimer, S. Leonhardt, and C. Ngo, "Evaluation and Application of a Customizable Wireless Platform: A Body Sensor Network for Unobtrusive Gait Analysis in Everyday Life.," *Sensors (Basel, Switzerland)*, vol. 20, no. 24, Dec. 2020, ISSN: 1424-8220 (Electronic). DOI: 10.3390/s20247325.

[97] N. Muthukrishnan, J. J. Abbas, and N. Krishnamurthi, "A Wearable Sensor System to Measure Step-Based Gait Parameters for Parkinson's Disease Rehabilitation," *Sensors*, vol. 20, no. 22, p. 6417, Nov. 2020, ISSN: 1424-8220. DOI: 10.3390/s20226417.

[98] N. Mani, P. Haridoss, and B. George, "A Wearable Ultrasonic based Ankle Angle and Toe Clearance Sensing System for Gait Analysis," *IEEE Sensors Journal*, p. 1, 2020. DOI: 10.1109/JSEN.2020.3047900.

[99] S. Qiu, H. Wang, J. Li, *et al.*, "Towards Wearable-Inertial-Sensor-Based Gait Posture Evaluation for Subjects with Unbalanced Gaits," *Sensors*, vol. 20, no. 4, p. 1193, Feb. 2020, ISSN: 1424-8220. DOI: 10.3390/s20041193.

[100] Y. Hutabarat, D. Owaki, and M. Hayashibe, "Quantitative Gait Assessment With Feature-Rich Diversity Using Two IMU Sensors," *IEEE Transactions on Medical Robotics and Bionics*, vol. 2, no. 4, pp. 639–648, 2020. DOI: 10.1109/TMRB.2020.3021132.

[101] F. Amitrano, A. Coccia, C. Ricciardi, *et al.*, "Design and Validation of an E-Textile-Based Wearable Sock for Remote Gait and Postural Assessment.," *Sensors (Basel, Switzerland)*, vol. 20, no. 22, Nov. 2020, ISSN: 1424-8220 (Electronic). DOI: 10.3390/s20226691.

[102] J. Figueiredo, S. P. Carvalho, J. P. Vilas-Boas, L. M. Gonçalves, J. C. Moreno, and C. P. Santos, "Wearable Inertial Sensor System towards Daily Human Kinematic Gait Analysis: Benchmarking Analysis to MVN BIOMECH," *Sensors*, vol. 20, no. 8, p. 2185, Apr. 2020, ISSN: 1424-8220. DOI: 10.3390/s20082185.

[103] D. Renggli, C. Graf, N. Tachatos, *et al.*, "Wearable Inertial Measurement Units for Assessing Gait in Real-World Environments.," *Frontiers in physiology*, vol. 11, p. 90, 2020, ISSN: 1664-042X (Print). DOI: 10.3389/fphys.2020.00090.

[104] L. Zhou, C. Tunca, E. Fischer, *et al.*, "Validation of an IMU Gait Analysis Algorithm for Gait Monitoring in Daily Life Situations," in *2020 42nd Annual International Conference of the IEEE Engineering in Medicine Biology Society (EMBC)*, 2020, pp. 4229–4232. DOI: 10.1109/EMBC44109.2020.9176827.

[105] I. A. Vajs, V. N. Bobić, M. D. urić-Jovičić, and M. M. Janković, "Open-source application for real-time gait analysis using inertial sensors," in *2020 28th Telecommunications Forum (TELFOR)*, 2020, pp. 1–4. DOI: 10.1109/TELFOR51502.2020.9306636.

[106] H. Zhao, Z. Wang, S. Qiu, J. Li, F. Gao, and J. Wang, "Evaluation of Inertial Sensor Configurations for Wearable Gait Analysis," *Studies in Computational Intelligence*, vol. 844, pp. 197–212, 2020. DOI: 10.1007/978-3-030-24405-7_13.

[107] S. Vítečková, H. Horáková, K. Poláková, R. Krupička, E. Růžička, and H. Brožová, "Agreement between the GAITRite® System and the Wearable Sensor BTS G-Walk® for measurement of gait parameters in healthy adults and Parkinson's disease patients.," *PeerJ*, vol. 8, e8835, 2020, ISSN: 2167-8359 (Print). DOI: 10.7717/peerj.8835.

[108] C. Pradeau, N. Sturbois-Nachef, and E. Allart, "Concurrent validity of the ZeroWire® footswitch system for the measurement of temporal gait parameters.," *Gait posture*, vol. 82, pp. 133–137, Oct. 2020, ISSN: 1879-2219 (Electronic). DOI: 10.1016/j.gaitpost.2020.09.003.

[109] L.-F. Shi, C.-X. Qiu, D.-J. Xin, and G.-X. Liu, "Gait recognition via random forests based on wearable inertial measurement unit," *Journal of Ambient Intelligence and Humanized Computing*, vol. 11, no. 11, pp. 5329–5340, Nov. 2020, ISSN: 1868-5137. DOI: 10.1007/s12652-020-01870-x.

[110] W. Zijlstra and A. L. Hof, "Assessment of spatio-temporal gait parameters from trunk accelerations during human walking," *Gait and Posture*, vol. 18, no. 2, pp. 1–10, 2003, ISSN: 09666362. DOI: 10.1016/S0966-6362(02)00190-X.

[111] K. Aminian, B. Najafi, C. Büla, P.-F. Leyvraz, and P. Robert, "Spatio-temporal parameters of gait measured by an ambulatory system using miniature gyroscopes," *Journal of Biomechanics*, vol. 35, no. 5, pp. 689–699, May 2002, ISSN: 00219290. DOI: 10.1016/S0021-9290(02)00008-8. eprint: arXiv:1011.1669v3.

[112] S. Studenski, S. Perera, K. Patel, *et al.*, "Gait speed and survival in older adults.," *JAMA*, vol. 305, no. 1, pp. 50–8, Jan. 2011, ISSN: 1538-3598. DOI: 10.1001/jama.2010.1923.

[113] K. Aminian, F. Dadashi, B. Mariani, C. Lenoble-Hoskovec, B. Santos-Eggimann, and C. J. Büla, "Gait analysis using shoe-worn inertial sensors: How is foot clearance related to walking speed?" In *UbiComp 2014 - Proceedings of the 2014 ACM International Joint Conference on Pervasive and Ubiquitous Computing*, 2014, pp. 481–485. DOI: 10.1145/2632048.2632071.

[114] R. de Souza Baptista, A. P. L. Bo, and M. Hayashibe, "Automatic Human Movement Assessment With Switching Linear Dynamic System: Motion Segmentation and Motor Performance," *IEEE Transactions on Neural Systems and Rehabilitation Engineering*, vol. 25, no. 6, pp. 628–640, Jun. 2017, ISSN: 1534-4320. DOI: 10.1109/TNSRE.2016.2591783.

[115] M. Sharifi Renani, C. A. Myers, R. Zandie, M. H. Mahoor, B. S. Davidson, and C. W. Clary, "Deep Learning in Gait Parameter Prediction for OA and TKA Patients Wearing IMU Sensors," *Sensors*, vol. 20, no. 19, p. 5553, Sep. 2020, ISSN: 1424-8220. DOI: 10.3390/s20195553.

[116] A. Tura, L. Rocchi, M. Raggi, A. G. Cutti, and L. Chiari, "Recommended number of strides for automatic assessment of gait symmetry and regularity in above-knee amputees by means of accelerometry and autocorrelation analysis," *Journal of NeuroEngineering and Rehabilitation*, vol. 9, no. 1, p. 11, Feb. 2012, ISSN: 1743-0003. DOI: 10.1186/1743-0003-9-11.

[117] V. Belluscio, E. Bergamini, M. Tramontano, R. Formisano, M. G. Buzzi, and G. Vannozzi, "Does Curved Walking Sharpen the Assessment of Gait Disorders? An Instrumented Approach Based on Wearable Inertial Sensors," *Sensors*, vol. 20, no. 18, p. 5244, Sep. 2020, ISSN: 1424-8220. DOI: 10.3390/s20185244.

[118] L. Sloot, M. van der Krogt, and J. Harlaar, "Self-paced versus fixed speed treadmill walking," *Gait Posture*, vol. 39, no. 1, pp. 478–484, Jan. 2014, ISSN: 09666362. DOI: 10.1016/j.gaitpost.2013.08.022.

[119] M. D. Chang, S. Shaikh, and T. Chau, "Effect of treadmill walking on the stride interval dynamics of human gait," *Gait Posture*, vol. 30, no. 4, pp. 431–435, Nov. 2009, ISSN: 09666362. DOI: 10.1016/j.gaitpost.2009.06.017.

[120] D. Owaki, Y. Sekiguchi, K. Honda, A. Ishiguro, and S. I. Izumi, "Short-term effect of prosthesis transforming sensory modalities on walking in stroke patients with hemiparesis," *Neural Plasticity*, vol. 2016, 2016, ISSN: 16875443. DOI: 10.1155/2016/6809879.

[121] S. Biesmans and P. Markopoulos, "Design and evaluation of sonis, a wearable biofeedback system for gait retraining," *Multimodal Technologies and Interaction*, vol. 4, no. 3, pp. 1–13, 2020. DOI: 10.3390/mti4030060.

[122] K. R. Sheerin, D. Reid, D. Taylor, and T. F. Besier, "The effectiveness of real-time haptic feedback gait retraining for reducing resultant tibial acceleration with runners," *Physical Therapy in Sport*, vol. 43, pp. 173–180, May 2020, ISSN: 1466853X. DOI: 10.1016/j.ptsp.2020.03.001.

[123] E. Allseits, V. Agrawal, J. Lučarević, R. Gailey, I. Gaunaurd, and C. Bennett, "A practical step length algorithm using lower limb angular velocities," *Journal of Biomechanics*, vol. 66, pp. 137–144, Jan. 2018, ISSN: 00219290. DOI: 10.1016/j.jbiomech.2017.11.010.

[124] L. Wang, Y. Sun, Q. Li, and T. Liu, "Estimation of Step Length and Gait Asymmetry Using Wearable Inertial Sensors," *IEEE Sensors Journal*, vol. 18, no. 9, pp. 3844–3851, May 2018, ISSN: 1530-437X. DOI: 10.1109/JSEN.2018.2815700.

[125] F. A. Storm, C. J. Buckley, and C. Mazzà, "Gait event detection in laboratory and real life settings: Accuracy of ankle and waist sensor based methods," *Gait and Posture*, vol. 50, pp. 42–46, 2016, ISSN: 18792219. DOI: 10.1016/j.gaitpost.2016.08.012.

[126] A. Sabatini, C. Martelloni, S. Scapellato, and F. Cavallo, "Assessment of Walking Features From Foot Inertial Sensing," *IEEE Transactions on Biomedical Engineering*, vol. 52, no. 3, pp. 486–494, Mar. 2005, ISSN: 0018-9294. DOI: 10.1109/TBME.2004.840727.

[127] S. O. Madgwick, A. J. Harrison, and R. Vaidyanathan, "Estimation of IMU and MARG orientation using a gradient descent algorithm," *IEEE International Conference on Rehabilitation Robotics*, pp. 0–6, 2011, ISSN: 19457898. DOI: 10.1109/ICORR.2011.5975346.

[128] Y. Thong, M. Woolfson, J. Crowe, B. Hayes-Gill, and D. Jones, "Numerical double integration of acceleration measurements in noise," *Measurement*, vol. 36, no. 1, pp. 73–92, Jul. 2004, ISSN: 02632241. DOI: 10.1016/j.measurement.2004.04.005.

[129] M. Zhang and A. Sawchuk, "A Feature Selection-Based Framework for Human Activity Recognition Using Wearable Multimodal Sensors," in *Proceedings of the 6th International ICST Conference on Body Area Networks*, vol. 1, ACM, 2011, pp. 92–98, ISBN: 978-1-936968-29-9. DOI: 10.4108/icst.bodynets.2011.247018.

[130] A. Derungs, C. Schuster-Amft, and O. Amft, "Physical Activity Comparison Between Body Sides in Hemiparetic Patients Using Wearable Motion Sensors in Free-Living and Therapy: A Case Series," *Frontiers in Bioengineering and Biotechnology*, vol. 6, no. OCT, Oct. 2018, ISSN: 2296-4185. DOI: 10.3389/fbioe.2018.00136.

[131] R. Selles, M. Formanoy, J. Bussmann, P. Janssens, and H. Stam, "Automated estimation of initial and terminal contact timing using accelerometers; development and validation in transtibial amputees and controls," *IEEE Transactions on Neural Systems and Rehabilitation Engineering*, vol. 13, no. 1, pp. 81–88, Mar. 2005, ISSN: 1534-4320. DOI: 10.1109/TNSRE.2004.843176.

[132] B. R. Greene, D. McGrath, R. O'Neill, K. J. O'Donovan, A. Burns, and B. Caulfield, "An adaptive gyroscope-based algorithm for temporal gait analysis," *Medical Biological Engineering Computing*, vol. 48, no. 12, pp. 1251–1260, Dec. 2010, ISSN: 0140-0118. DOI: 10.1007/s11517-010-0692-0.

[133] N. Kitagawa and N. Ogihara, "Estimation of foot trajectory during human walking by a wearable inertial measurement unit mounted to the foot," *Gait Posture*, vol. 45, pp. 110–114, Mar. 2016, ISSN: 09666362. DOI: 10.1016/j.gaitpost.2016.01.014.

[134] J. Hannink, T. Kautz, C. F. Pasluosta, *et al.*, "Mobile Stride Length Estimation With Deep Convolutional Neural Networks," *IEEE Journal of Biomedical and Health Informatics*, vol. 22, no. 2, pp. 354–362, Mar. 2018, ISSN: 2168-2194. DOI: 10.1109/JBHI.2017.2679486. eprint: 1609.03321.

[135] K. Aminian, C. Trevisan, B. Najafi, *et al.*, "Evaluation of an ambulatory system for gait analysis in hip osteoarthritis and after total hip replacement," *Gait Posture*, vol. 20, no. 1, pp. 102–107, Aug. 2004, ISSN: 09666362. DOI: 10.1016/S0966-6362(03)00093-6.

[136] A. Salarian, P. R. Burkhard, F. J. G. Vingerhoets, B. M. Jolles, and K. Aminian, "A Novel Approach to Reducing Number of Sensing Units for Wearable Gait Analysis Systems," *IEEE Transactions on Biomedical Engineering*, vol. 60, no. 1, pp. 72–77, 2013.

[137] A. Rotstein, O. Inbar, T. Berginsky, and Y. Meckel, "Preferred transition speed between walking and running: Effects of training status," *Medicine and Science in Sports and Exercise*, vol. 37, no. 11, pp. 1864–1870, 2005, ISSN: 01959131. DOI: 10.1249/01.mss.0000177217.12977.2f.

[138] R. de Souza Baptista, A. P. L. Bo, and M. Hayashibe, "Automatic Human Movement Assessment With Switching Linear Dynamic System: Motion Segmentation and Motor Performance," *IEEE Transactions on Neural Systems and Rehabilitation Engineering*, vol. 25, no. 6, pp. 628–640, Jun. 2017, ISSN: 1534-4320. DOI: 10.1109/TNSRE.2016.2591783.

[139] L. L. Long and M. Srinivasan, "Walking, running, and resting under time, distance, and average speed constraints: Optimality of walk-run-rest mixtures," *Journal of the Royal Society Interface*, vol. 10, no. 81, 2013, ISSN: 17425662. DOI: 10.1098/rsif.2012.0980.

[140] N. U. Ahamed, D. Kobsar, L. C. Benson, C. A. Clermont, S. T. Osis, and R. Ferber, "Subject-specific and group-based running pattern classification using a single wearable sensor," *Journal of Biomechanics*, vol. 84, pp. 227–233, Feb. 2019, ISSN: 00219290. DOI: 10.1016/j.jbiomech.2019.01.001.

[141] W. A. Sparrow, E. J. Bradshaw, E. Lamoureux, and O. Tirosh, "Ageing effects on the attention demands of walking," *Human Movement Science*, vol. 21, no. 5-6, pp. 961–972, 2002, ISSN: 01679457. DOI: 10.1016/S0167-9457(02)00154-9.

[142] V. Dubost, R. W. Kressig, R. Gonthier, *et al.*, "Relationships between dual-task related changes in stride velocity and stride time variability in healthy older adults," *Human Movement Science*, vol. 25, no. 3, pp. 372–382, Jun. 2006, ISSN: 01679457. DOI: 10.1016/j.humov.2006.03.004. [Online]. Available: https://linkinghub.elsevier.com/retrieve/pii/S0167945706000285.

[143] J. Howcroft, E. D. Lemaire, J. Kofman, and W. E. McIlroy, "Dual-Task Elderly Gait of Prospective Fallers and Non-Fallers: A Wearable-Sensor Based Analysis.," *Sensors (Basel, Switzerland)*, vol. 18, no. 4, Apr. 2018, ISSN: 1424-8220 (Electronic). DOI: 10.3390/s18041275.

[144] J. Nonnekes, V. Dibilio, C. Barthel, T. Solis-Escalante, B. R. Bloem, and V. Weerdesteyn, "Understanding the dual-task costs of walking: a StartReact study," *Experimental Brain Research*, vol. 238, no. 5, pp. 1359–1364, 2020, ISSN: 14321106. DOI: 10.1007/s00221-020-05817-8. [Online]. Available: https://doi.org/10.1007/s00221-020-05817-8.

[145] I. Hillel, E. Gazit, A. Nieuwboer, *et al.*, "Is every-day walking in older adults more analogous to dual-task walking or to usual walking? Elucidating the gaps between gait performance in the lab and during 24/7 monitoring," *European Review of Aging and Physical Activity*, vol. 16, no. 1, pp. 1–12, 2019, ISSN: 18137253. DOI: 10.1186/s11556-019-0214-5.

[146] Y. Hutabarat, D. Owaki, and M. Hayashibe, "Recent Advances in Quantitative Gait Analysis using Wearable Sensors: A Review," *IEEE Sensors Journal*, vol. 21, no. 23, pp. 26 470–26 487, 2021, ISSN: 15581748. DOI: 10.1109/JSEN.2021.3119658.

[147] W. Pitt and L.-S. Chou, "Reliability and practical clinical application of an accelerometer-based dual-task gait balance control assessment.," eng, *Gait posture*, vol. 71, pp. 279–283, Jun. 2019, ISSN: 1879-2219 (Electronic). DOI: 10.1016/j.gaitpost.2019.05.014.

[148] J. T. Coulthard, T. T. Treen, A. R. Oates, and J. L. Lanovaz, "Evaluation of an inertial sensor system for analysis of timed-up-and-go under dual-task demands.," eng, *Gait posture*, vol. 41, no. 4, pp. 882–887, May 2015, ISSN: 1879-2219 (Electronic). DOI: 10.1016/j.gaitpost.2015.03.009.

[149] J. Howcroft, J. Kofman, E. D. Lemaire, and W. E. McIlroy, "Analysis of dual-task elderly gait in fallers and non-fallers using wearable sensors.," eng, *Journal of biomechanics*, vol. 49, no. 7, pp. 992–1001, May 2016, ISSN: 1873-2380 (Electronic). DOI: 10.1016/j.jbiomech.2016.01.015.

[150] Y. Freund and R. E. Schapire, "A Decision-Theoretic Generalization of On-Line Learning and an Application to Boosting," *Journal of Computer and System Sciences*, vol. 55, no. 1, pp. 119–139, 1997, ISSN: 00220000. DOI: 10.1006/jcss.1997.1504.

[151] T. Chen and C. Guestrin, "XGBoost: A Scalable Tree Boosting System," pp. 785–794, Aug. 2016. DOI: 10.1145/2939672.2939785. arXiv: 1603.02754.

[152] A. Althnian, D. AlSaeed, H. Al-Baity, *et al.*, "Impact of Dataset Size on Classification Performance: An Empirical Evaluation in the Medical Domain," *Applied Sciences*, vol. 11, no. 2, p. 796, Jan. 2021, ISSN: 2076-3417. DOI: 10.3390/app11020796.

[153] S. Bai, J. Z. Kolter, and V. Koltun, "An empirical evaluation of generic convolutional and recurrent networks for sequence modeling," *arXiv*, 2018, ISSN: 23318422. arXiv: 1803.01271.

[154] J. Yan, L. Mu, L. Wang, R. Ranjan, and A. Y. Zomaya, "Temporal Convolutional Networks for the Advance Prediction of ENSO," *Scientific Reports*, vol. 10, no. 1, p. 8055, Dec. 2020, ISSN: 2045-2322. DOI: 10.1038/s41598-020-65070-5.

[155] L. A. Gemein, R. T. Schirrmeister, P. Chrabaszcz, *et al.*, "Machine-learning-based diagnostics of EEG pathology," *NeuroImage*, vol. 220, no. December 2019, p. 117 021, Oct. 2020, ISSN: 10538119. DOI: 10.1016/j.neuroimage.2020.117021. eprint: 2002.05115.

[156] J. Chen, D. Chen, and G. Liu, "Using temporal convolution network for remaining useful lifetime prediction," *Engineering Reports*, vol. 3, no. 3, pp. 1–17, 2021, ISSN: 2577-8196. DOI: 10.1002/eng2.12305.

[157] P. Zhang, X. Wang, J. Chen, W. You, and W. Zhang, "Spectral and Temporal Feature Learning with Two-Stream Neural Networks for Mental Workload Assessment," *IEEE Transactions on Neural Systems and Rehabilitation Engineering*, vol. 27, no. 6, pp. 1149–1159, 2019, ISSN: 15580210. DOI: 10.1109/TNSRE.2019.2913400.

[158] Y. Hutabarat, K. Ekkachai, M. Hayashibe, and W. Kongprawechnon, "Reinforcement q-learning control with reward shaping function for swing phase control in a semi-active prosthetic knee," *Frontiers in Neurorobotics*, vol. 14, pp. 1–10, November Nov. 2020, ISSN: 1662-5218. DOI: 10.3389/fnbot.2020.565702.

[159] H. Herr and A. Wilkenfeld, "User-adaptive control of a magnetorheological prosthetic knee," *Industrial Robot: An International Journal*, vol. 30, no. 1, pp. 42–55, Feb. 2003, ISSN: 0143-991X. DOI: 10.1108/01439910310457706.

[160] K. Ekkachai and I. Nilkhamhang, "Swing Phase Control of Semi-Active Prosthetic Knee Using Neural Network Predictive Control With Particle Swarm Optimization," *IEEE Transactions on Neural Systems and Rehabilitation Engineering*, vol. 24, no. 11, pp. 1169–1178, Nov. 2016, ISSN: 1534-4320. DOI: 10.1109/TNSRE.2016.2521686.

[161] Y. Wen, J. Si, A. Brandt, X. Gao, and H. H. Huang, "Online Reinforcement Learning Control for the Personalization of a Robotic Knee Prosthesis," *IEEE Transactions on Cybernetics*, vol. 50, no. 6, pp. 2346–2356, Jun. 2020, ISSN: 2168-2267. DOI: 10.1109/TCYB.2019.2890974.

[162] L. Rochester, C. Mazzà, A. Mueller, *et al.*, "A Roadmap to Inform Development, Validation and Approval of Digital Mobility Outcomes: The Mobilise-D Approach," *Digital Biomarkers*, vol. 4, no. 1, pp. 13–27, 2020, ISSN: 2504-110X. DOI: 10.1159/000512513.

# Acknowledgements

The completion of this dissertation was not by a single effort, but attainable with the tremendous supports from many people throughout my journey. First, I would like to express my sincerest gratitude to Professor Mitsuhiro Hayashibe for giving me chance to conduct my Ph.D. study at the Neuro-Robotics laboratory of Tohoku University. Thank you for giving me enough space for exploring research ideas while also giving me a push when needed to keep me on track. Your kind support in both professional and personal development has helped me through this doctoral journey. I am equally grateful to Professor Dai Owaki for his insights in both practical and technical areas during my doctoral research. Thank you for your kind help in buying and sending me sensors to Indonesia during the early travel ban due to Covid-19, it really helped me keep up research progress.

Next, I would like to thank my thesis committee members, Professor Ryoichi Nagatomi and Professor Takashi Watanabe, for asking interesting questions and giving constructive comments to improve my doctoral work. I truly enjoyed and highly value your comments and discussions we had during the pre-defense. A special acknowledgment to the Ministry of Education, Culture, Sports, Science, and Technology (MEXT), Government of Japan for providing me a full scholarship for this Ph.D. study through the Data Science Program II (DSP II) of Tohoku University.

I would also like to thank my colleagues and members of the Neuro-Robotics laboratory for their support during my lab days, friends and people that have helped my days in Sendai, and everyone who has helped participate in my experiments. I wish each and every one of you will succeed and be happy in life.

Further, I would like to thank my mother and my father for their never-ending support to this very day. Thank you for you have done it good and right in raising us three, your children. To my sister and my brother, and my in-laws, thank you also for your support.

Finally, I would like to thank my wife, Fani, for her understanding, patience, and relentless support for me to finish this degree. Moreover, to our daughter, our little loved one, Brielle, for her presence in this tough time that have filled me with joy and elevated my mental power to overcome challenges during my doctoral study. You both are the greatest blessing, so I thank God, and I thank you both for making me the happiest.